$\delta^{56}Fe$

In-plant Fe translocation

Strategy I
Fe^{2+}
Root-uptake
Fe^{3+}

Strategy II
Fe^{3+}- PS
Root-uptake
Fe^{3+}- PS

H+
H+
H+

phytosiderophores (PSs)

Iron isotope fractionation in arable soil and graminaceous crops

Ying Xing

JÜLICH
Forschungszentrum

Iron isotope fractionation in arable soil and graminaceous crops

Ying Xing

ABSTRACT

Soils contain large quantities of Fe, however, the Fe-solubility is very low. Plants have developed two efficient strategies to secure Fe uptake from soil under Fe-deficient conditions: (i) the sequential acidification-reduction-transport strategy (strategy I) and (ii) the chelation-based strategy (strategy II). All processes involved in the Fe cycle in soil-plant systems can fractionate stable Fe isotopes. Hence, I (i) conducted a systematic review about the state of Fe isotope research in plant studies and highlighted the research gaps. Then I supplemented this theoretical study by two experiments: I (ii) examined the effect of different Fe availabilities on Fe isotope fractionation in wheat plants under controlled conditions and I (ii) investigated the effect of 50 years of irrigation on Fe isotope fractionation in soils and cereals in a long-term field experiment.

My review suggested that strategy I plants especially take up light Fe isotopes, while strategy II plants fractionate less towards light isotopes. Aboveground tissues usually show even lighter Fe isotope signatures than the roots, with flowers (δ^{56}Fe: -2.15 to -0.23‰) being isotopically the lightest. I found that all reported strategy I plants consistently enriched light Fe isotopes under all growth conditions. Strategy II plants, however, could be enriched with either light or heavy Fe isotopes, depending on the growth conditions. Depending on the Fe speciation and concentration present in the growth medium, some strategy II plants like rice are able to adapt their uptake strategy as they also possess ferrous transporters and are hence also able to take up Fe(II) ions.

In a greenhouse study, I cultivated summer wheat (*Triticum aestivum* L.) under Fe-sufficient (control, 0.0896 mM Fe-EDTA) and deficient (Fe-deficient, 0.0022 mM Fe-EDTA) conditions. Plants were sampled at different growth stages (vegetative and reproductive growth stages) and separated into different plant organs (root, stem, leaf, spike/grain). All samples were analyzed for their Fe concentrations and δ^{56}Fe isotope compositions. The results showed that Fe-deficiency reduced the whole plant Fe mass by 59% at vegetative growth. During reproductive growth, Fe mass fluxes indicated different preferential Fe translocation pathways under different Fe supply. Under Fe-deficient conditions, Fe uptake from growth substrate increased whereas under Fe-sufficient conditions Fe was preferentially redistributed within the plant. Under Fe-sufficient conditions increasingly lighter δ^{56}Fe values from older to younger plant parts were found, but no indications that the chelation-based uptake strategy was activated. However, with serious shortage of Fe, the shift towards lighter δ^{56}Fe values was reduced. This suggested that Fe isotope ratios can reflect both wheat growth conditions and ages.

In a field study, I sampled wheat plants and Retisol soil cores down to a depth of 100 cm from a long-term irrigation treatment at Berlin-Thyrow. The irrigated plots had higher Fe_{avail} concentrations than the non-irrigated plots in the top 40 cm of soil, but there were no changes in δ^{56}Fe values. Due to the research site being one of the driest areas in Germany with hardly a meaningful water percolation, the maximum difference of $\delta^{56}Fe_{avail}$ values between 40 to 50 cm and 70 to 100 cm was explained soil pedogenesis rather than irrigation treatment. The wheat plants grown in both irrigated and non-irrigated plots were slightly enriched in light Fe isotopes, exhibiting similar δ^{56}Fe values to those of the respective topsoil. I concluded that the overall δ^{56}Fe signature of wheat was regulated by plant-homeostasis and specific on-site soil characteristics, whereas irrigation had little if any significant effect on the Fe isotopes in the crops.

Overall, my study showed that the Fe isotope compositions of wheat plants were not affected by Fe availabilities in substrate until the anthesis stage. However, during the reproductive growth phase with sufficient Fe supply, δ^{56}Fe values of different plant organs showed significant Fe fractionation. The former processes were hardly affected by irrigation.

ZUSAMMENFASSUNG

In Böden sind große Mengen an Fe vorhanden, jedoch ist die Fe-Löslichkeit sehr gering. Alle Prozesse, die am Fe-Kreislauf in Boden-Pflanzen-Systemen beteiligt sind, können stabile Fe-Isotope fraktionieren. Um diese Prozesse besser zu verstehen habe ich (i) ein Literaturreview zum Stand der Fe-Isotopenforschung in Pflanzenstudien erstellt und anschließend diese Studie durch zwei Experimente ergänzt: Ich (ii) untersuchte den Effekt verschiedener Fe Verfügbarkeiten auf die Fe Isotopenfraktionierung in Weizenpflanzen unter kontrollierten Bedingungen und ich (ii) untersuchte den Effekt von 50 Jahren Bewässerung auf die Fe Isotopenfraktionierung in Böden und Getreide in einem Langzeit-Feldversuch.

Die Literaturstudie zeigte, dass Strategie-I-Pflanzen durchweg vor allem leichte Fe-Isotope aufnehmen, während Strategie-II-Pflanzen weniger in Richtung leichter Isotope fraktionieren. Oberirdische Gewebe weisen in der Regel leichtere Fe-Isotopenverhältnisse auf als die Wurzeln, wobei Blüten (δ^{56}Fe: -2.15 bis -0.23‰) isotopisch am leichtesten sind. Anders als bei Strategie-I-Pflanzen könnten Strategie-II-Pflanzen je nach Wachstumsbedingungen mit leichten oder schweren Fe-Isotopen angereichert sein. Einige Strategie-II-Pflanzen wie Reis können sogar ihre Aufnahmestrategie anpassen, wenn sie über Fe(II)-Transporter zusätzlich Fe(II)-Ionen aufnehmen. Im Gewächshaus wurde Sommerweizen (*Triticum aestivum* L.) unter ausreichender Fe-Versorgung (0,0896 mM Fe-EDTA) sowie unter Fe-Mangel-Bedingungen (0,0022 mM Fe-EDTA) angezogen. Die Pflanzen wurden während verschiedener Wachstumsphasen beprobt und in verschiedene Pflanzenorgane (Wurzel, Stamm, Blatt, Spieß/Korn) unterteilt. Alle Proben wurden auf ihre Fe-Konzentrationen und δ^{56}Fe Isotopenzusammensetzungen hin analysiert. Die Ergebnisse zeigten, dass Fe-Mangel die Fe-Aufnahme zum Zeitpunkt des vegetativen Wachstums um 59% reduzierte. Während des reproduktiven Wachstums fand eine unterschiedliche Fe-Anreicherung in den einzelnen Organen statt. Unter Fe-Mangel-Bedingungen wurde Fe besonders effizient aus der Nährlösung aufgenommen und innerhalb der Pflanze umverteilt, die δ^{56}Fe Werte nahmen von den älteren zu den jüngeren Pflanzenteilen hin ab. Es fanden sich keine anfänglichen Hinweise auf chelatbasierte Aufnahmewege. Erst zur Anthesis fand diese vermutlich statt, was die Verschiebung zu niedrigen Isotopenwerten verringerte. Die Fe-Isotopenverhältnisse im Weizen sind somit sowohl eine Funktion der Wachstumsbedingungen als auch des Alters.

Im Freiland habe ich Weizenpflanzen und Bodenproben (Retisol) bis in 100 cm Tiefe aus dem Langzeitbewässerungsversuch in Berlin-Thyrow entnommen. Die bewässerten Parzellen zeigten höhere Fe-Konzentrationen im verfügbaren Fe-Pool an als die nicht bewässerten Parzellen in den oberen 40 cm des Bodens, aber keine Veränderungen der δ^{56}Fe Werte. Veränderungen der Fe-Isotopenverhältnisse im Bodenprofil erklären sich damit überwiegend durch Pedogenese und nicht über die Bewässerungsbehandlung. Die Pflanzen waren geringfügig mit leichten Fe-Isotopen angereichert. Die gesamte δ^{56}Fe-Signatur des Weizens wird damit vermutlich durch homöostatische Reaktionen in der Pflanze und spezifische Bodenmerkmale vor Ort reguliert, während die Bewässerung keinen signifikanten Einfluss auf die Fe-Isotope in den Kulturen hatte. Insgesamt zeigt meine Arbeit, dass die Fe-Isotopenzusammensetzungen von Weizen bis zum Anthesis-Stadium nicht von der Fe-Verfügbarkeit im Substrat beeinflusst wird. Erst in der reproduktiven Wachstumsphase mit ausreichender Fe-Anreicherung zeigten δ^{56}Fe Werte verschiedener Pflanzenorgane signifikante Fe-Fraktionierungen. Letztere scheinen dann vom Bewässerungsmanagement weitgehend unbeeinflusst zu sein.

CONTENT

CONTENT

LIST OF FIGURES

LIST OF TABLES

LIST OF ABBREVIATIONS

a.s.l.	Above sea level
ATP	Adenosine triphosphate
CO_2	Carbon dioxide
$CaCO_3$	Calcium carbonate
DNA	Deoxyribonucleic acid
equil	Equilibrium
Fe	Iron
Fe(II)	Ferrous iron
Fe(III)	Ferric iron
Fe_{avail}	Plant-available iron
Fe_{bulk}	Iron in bulk soil
$FeCO_3$	Ferrous carbonate
$FeSO_4$	Iron sulfate
H_2O_2	Hydrogen peroxide
HCl	Hydrochloric aid
HNO_3	Nitric acid
ICP-MS	Inductively Coupled Plasma - Mass Spectrometry
kin	Kinetic
MC-ICP-MS	Multicollector - Inductively Coupled Plasma - Mass Spectrometry
NH_4^+	Ammounium ion
NO_3^-	Nitrate ion
–OH	Hydroxyl group
S	Sulphur
SD	Standard deviation
SE	Standard error
SRM	Standard reference material

I

GENERAL INTRODUCTION

1. RATIONAL

Among the essential micronutrients in plants, Fe represents one of the most important nutrients for plant growth. It is required for plant photosynthesis and mitochondrial respiration, where it participates in electron transfer reactions through reversible redox reactions between Fe(II) and Fe(III) forms (Marschner, 1995; Weber et al., 2006). In particular, Fe is an important component of heme and Fe-S enzymes, which support electron transport in photosynthesis and energy metabolism (Briat et al., 2007a; Nikolic and Römheld, 2007). To sustain these basic functions, plants acquire Fe from the soil.

Although Fe is the fourth most abundant element in the Earth's crust (Murad and Fischer, 1988), Fe-solubility is very low in well aerated soils at physiological optimal pH (Lindsay and Schwab, 1982). As response to this problem, plants have developed two efficient strategies (strategy I and II, respectively) to secure Fe uptake from the soil (Marschner et al., 1986), thereby securing the Fe uptake and translocation processes within soil-plant system. Uptake and translocation are continuously accompanied by a variety of biochemical reactions, including reduction, oxidation and complexing. All these processes have the potential to generate Fe isotope fractionations in different extent (Wiederhold, 2015).

A number of studies have investigated Fe isotope compositions in higher plants and demonstrated that plants of strategy I type consistently take up light iron isotopes, while strategy II plants fractionate less towards light isotopes and even enrich heavy Fe isotopes under certain circumstances (Guelke and Von Blanckenburg, 2007). Aboveground plant organs usually display lighter Fe isotope signatures than the roots, with flowers (δ^{56}Fe: -2.15 to -0.23‰) being isotopically the lightest (Wu et al., 2019). Furthermore, the authors hypothesize Fe isotope

fractionation among higher plants is influenced by both plant species and Fe availabilities in soils (Kiczka et al., 2010), which needs to be confirmed with more advanced studies.

In Germany, the predominant crop is wheat, covering nearly one third of the arable lands (Macholdt and Honermeier, 2017). Wheat belongs to the strategy II type plants. Measuring the stable Fe isotope fractionation may provide a new tool that holds promise to be useful for studying Fe uptake and translocation in soil-crop system. In addition, assessing the δ^{56}Fe signatures of different wheat organs as well as the substrate for wheat growth may be an indicator for wheat response to different Fe supply in different growth stages. Apart from plant growth and harvest, changes in soil properties, e.g. induced by agricultural management, may potentially alter the Fe isotope compositions of soil and thus of the plants. In this case, stable Fe isotopes may also reflect the dynamic of soil Fe fluxes. Hence, there is an urgent need for research on how Fe isotopes might be utilized under in-house or field conditions as a tracer to study Fe uptake and translocation processes in soil-crop system.

2. STATE OF THE ART

2.1   Iron in arable soil

Iron (Fe) is the fourth most abundant element and the second most abundant metal (after aluminium) in the Earth's crust. The upper layer of the Earth's crust where plants grow, a black or dark brown material which is the product of a long-lasting interaction between atmosphere, biosphere hydrosphere and lithosphere, is known as soil . Fe is released from the lithosphere into the soils by weathering and microorganism activities of primary Fe-containing clay silicates and sulphide minerals which mainly contain Fe in its ferrous Fe(II) state (Cornell and Schwertmann, 2003). As a redox sensitive element, the released Fe(II) subsequently forms a series of Fe(hydro)oxides compounds in the presence of oxygen and hydroxyls during pedogenetic

processes (Cornell et al., 1989; Stumm, 1987). In most compounds, Fe is present in the form of crystalline Fe(hydro)oxides including the most abundant minerals goethite (α-FeOOH) and hematite (α-Fe$_2$O$_3$) in well-drained soils. In poorly drained soils Fe exists as either poorly crystalline Fe(hydro)oxides (lepidocrocite, maghemite, and magnetite) or short-range ordered crystalline minerals (ferrihydrite and feroxyhyte) (Cornell and Schwertmann, 2003; Schwertmann, 1958). The redox potential (Eh) and pH are considered as the most important factors governing the Fe behavior in soil, where under most common Eh–pH soil conditions goethite and hematite are highly stable. Only at extremely low Eh and pH soil conditions crystalline Fe(hydro)oxides of goethite and hematite can produce the same Fe concentration in solution. While the poorly crystalline Fe(hydro)oxides of lepidocrocite and short-range ordered crystalline minerals of ferrihydrite are preferentially found in younger soils characterized by the non-equilibrium state in the cold climate and acidic soils. Small amounts of Fe reduced pyrite (FeS$_2$) and siderite (FeCO$_3$) can be found in acid and alkaline soils, respectively (Schwertmann, 1988). It should be noted that many crystalline Fe, poorly crystalline Fe and reduced form of Fe could interact with inorganic and organic collides thus forming complex aggregates with new surfaces (Colombo and Torrent, 1991). Accordingly, it can be concluded that Fe species in soil environment may have the following forms (Colombo et al., 2014): (1) Fe(II) in primary minerals; (2) Fe(III) in both crystalline minerals and poorly ordered crystalline (hydro)oxides; (3) exchangeable and soluble Fe; (4) Fe bound with organic matter in soluble or insoluble forms.

Generally, the average Fe concentration in soil is 20-40 g kg^{-1} (Cornell and Schwertmann, 2003). However, due to agricultural practices e.g. fertilization, irrigation of agricultural fields, soil properties can be changed and thus influence the Fe availability in soil. This is mainly due to redox changes of Fe(II) and Fe(III) by soil management with Fe(II) forms having high solubility under

reduced or strongly acidic conditions, whereas Fe(III) compounds are characterized by a low solubility (Cornell and Schwertmann, 2003). There is hence a need to clarify how soil management practices influence Fe dynamics in soil. The latter mainly applies to management techniques that alter Fe mobility, such as irrigation. As irrigation management could influence the diffusion of O_2 in soil, and thus Fe availability (Skopp et al., 1990). It is reasonable to assume that elevated water contents enhances the reductive dissolution of Fe minerals. This released Fe(II) can be transported through adjective and diffusive processed until it is re-precipitated as secondary Fe(III) (hydr)oxides or be taken up by plants (Wiederhold et al., 2006).

2.2 Iron uptake by plant

Fe is an essential micronutrient in many cellular functions for plants growth, such as respiration, photosynthesis and chlorophyll biosynthesis (Marschner, 1995). Its functions are generally based on 1) the reversible redox reaction of Fe(II) and Fe(III), 2) the ability to form octahedral complexes with various organic ligands and, 3) its redox potential varying in response to different ligand environments (Hell and Stephan, 2003). As a redox sensitive element, Fe(II) is rapidly oxidized to Fe(III)-(hydr)oxides in the presence of oxygen and thus be insoluble in soil decreasing Fe availability, which particularly happens at calcareous sites with high pH (Mengel, 1994). The solubility of Fe(III) in soil decreases dramatically with increasing pH values, where the concentration of Fe(III) decreases from 10^{-6} M at pH of 3.3 to 10^{-17} M at pH of 7 (Neilands, 1987). Plants require Fe(III) between 10^{-4} and 10^{-8} M much higher than the Fe solubility range for plant growth in well-aerated soils with pH values mostly above 7 and thus caused Fe deficiency in plants. Fe deficiency is a worldwide agricultural problem in both dicotyledonous and monocotyledonous species, which results in chlorosis and thus reduces plant productivity (Wallace and Lunt, 1960). As plants are the primary source of Fe for humans, it is crucial to guarantee efficient Fe uptake by

plants to avoid the risk of human anemia caused by plant Fe deficiency (Nogueira Arcanjo et al., 2012). Fe-containing fertilizers can be used to cure Fe deficiency to some extent. However, this treatment is costly and cannot be precisely targeted to the Fe-deficient plant organs. In response to Fe-deficiency, plants induce a series of processes e.g. 1) significantly enhancing the secretion of mugineic acid family phytosiderophores (MAs) from their roots into the rhizosphere (Kobayashi et al., 2019), 2) triggering the expression of many Fe uptake associated gens including AtAHA2 and AtAHA7 (Zhang et al., 2019), 3) remodeling of the electron transfer chain in both photosystem I (PSI) and II (PSII) processes and, 4) modifying post-translationally proteins particularly in the PSII oxygen-evolving complex (Briat et al., 2015). It is noteworthy that plant Fe deficiency is a problem of Fe solubility and not of abundance (Guerinot, 2001).

Plants have developed two efficient strategies to secure Fe uptake from the soil (Fig. I-1a) (Marschner et al., 1986). The sequential acidification-reduction-transport strategy (strategy I) is carried out by all higher plants, except for the graminaceous plants, which use the chelation-based strategy (strategy II) for Fe uptake (Hell and Stephan, 2003). Strategy I plants excrete protons via a plasmalemma AHA H^+-ATPases to acidify the rhizosphere, and then the NADPH-dependent ferric chelate reductase AtFRO2 reduces Fe(III) to Fe(II) which is then available to plants and can be transported through a plasmalemma by Fe transporter proteins (IRT1) (Hell and Stephan, 2003; Robinson et al., 1999). Strategy II plants release phytosiderophores (PS) that chelate Fe(III) in the rhizosphere. The Fe(III)-PS complexes are then channeled into the root by specific plasmalemma transporter proteins (YS1/YSL) (Curie et al., 2001; Schaaf et al., 2004; Takagi et al., 1984). However, rice is a strategy II plant which contains the previously identified Fe(II) transporter of OsIRT1 which enables rice to absorb Fe(II) forms. This strategy is well adapted for rice growing under submerged conditions where Fe(II) is more abundant than Fe(III) in paddy fields (Ishimaru

et al., 2006). Under Fe deficiency condition, OsYSL15 expression was dominant in root epidermis thus elevating the Fe(III)- PS uptake processes (Inoue et al., 2009). Hence, rice displays aspects of both strategy I and strategy II Fe-uptake mechanisms. It is generally assumed that the chelation-based strategy (Strategy II) is more efficient than the sequential acidification-reduction-transport strategy (Strategy I) and allows graminaceous plants to survive under more drastic Fe-deficient conditions (Mori, 1999). All reported Strategy I plants (Arabidopsis, cumber, tomato etc.,) (Eide et al., 1996; Li et al., 2004; Zocchi and Cocucci, 1990) consistently take up Fe in their specific way with FRO2 and IRT1 transporters either under Fe deficiency or sufficiency growing conditions. However, Strategy II plants, especially wheat, might absorb Fe using both strategies similar as rice depending on Fe availability in growth media. However, the mechanisms remain unclear and it needs to be shown whether and to what degree Fe isotope fractionation assessment provides insights into the Fe uptake processes.

Fig. I-1: a) Scheme of Fe uptake from rhizosphere (Strategy I, Strategy II) and translocation in plant. b) Scheme of Fe translocation in plant cell. Red arrows indicate the dominant Fe pathways and transfers between different Fe pools (different colors), with blue ellipses indicating specific transporters which adjust Fe loading and unloading from plasma membrane.

Apart from Fe deficiency, plants also face the problem of Fe toxicity, which is mostly associated with plant growth in highly acidic soil conditions such as growth in waterlogged soil, where the diffusion of oxygen into the soil is limited and thus promotes the growth of anaerobic microbes, decreasing the pH of soil solution due to high CO_2 accumulation. The highly accumulated CO_2 generates reduction conditions for Fe(III) with Fe(II) concentrations between 10 and 2000 mg L^{-1}, which is in the range of Fe-toxic soil types and can affect lowland-rice yields (Becker and Asch, 2005). The amount of Fe(II) increases with temperature, decomposable organic matter and the

redox buffers as reported by Ponnamperuma et al. (1967). Fe toxicity can result in visual symptoms of leaves bronzing and reduced crop production. Fe is a transition metal with high redox reactivity, which can act as an efficient cofactor and catalyst and thus generate the extremely reactive hydroxyl radical, which can react with almost all the molecules in the living cells and hence cause severe damage on membranes, proteins and DNA, even plant death (Halliwell and Gutteridge, 1984; Sahrawat, 2000). To deal with Fe toxicity, rice plants have developed morphological and physiological avoidance or tolerance mechanisms, which includes 1) Fe(II) oxidation at the root surface, 2) root membrane selectivity of Fe(II), 3) Fe(II) retention in root and stem tissues, 4) Fe(II) retention in the apoplast of the leaf and, 5) symplastic tissue tolerance to Fe(II) (Becker and Asch, 2005). Therefore, plants have to finely regulate the Fe concentration within a narrow range to avoid both Fe-deficiency and Fe-toxicity problems.

2.3 Fe translocation in plant

Plants acquire Fe from the rhizosphere by their roots. Subsequently, the absorbed Fe has to be distributed between different plant parts through translocation. Fig. I-1 summarized the Fe uptake, translocation in different plant parts as well as in plant cell. As particularly free Fe ions produce reactive oxygen species, like superoxide and hydroxyl radicals, Fe needs to be bound with chelators or incorporated into structures to prevent oxidative cell damage (Marschner, 2011). Therefore short- and long-distance Fe transport in plants happens through different chelators, such as phytosiderophores (PS), citrate and nicotianamine (NA) (Zhang et al., 2019). Plants have developed two types of vessel for nutrient transport: xylem and phloem. Xylem vessels consist of dead cells which result in passive Fe transportation. The phloem, on the other hand, consists of living cells. Thus Fe transportation in the phloem is active. Fe, once taken up by the roots, is then accumulated in the discrimination center (DC) at the basal part of the shoot, from which Fe is

translocated to the aboveground plant parts through both xylem and phloem to older and youngest leaves driven by the transpiration stream and root pressure (Mori, 1998; Tsukamoto et al., 2008; Zhang et al., 1995a). Subsequently, Fe is remobilized and translocated to the seeds through phloem loading (Walker and Waters, 2011). Fe transport in the xylem mostly occurs as Fe(III)-citrate complex (Durrett et al., 2007; Rellán-Álvarez et al., 2009). The citrate transporters of FRD3 in Arabidopsis or OsFRDL1 in rice are localized in the plasma membrane surrounding the xylem loading citrate into the xylem. Unlike the xylem, phloem cells use YS1 or YSL transporters to pump Fe into the phloem which is then chelated by NA and 2'-deoxymugineic acid (DMA) in rice phloem exudates (Nishiyama et al., 2012). Although NA can chelate both Fe(II) and Fe(III), capillary electrophoresis results indicated that Fe(II)-NA complexes are kinetically more stable than Fe(III)-NA (von Wirén et al., 1999). Hence, NA complexes in the phloem are assumed to be predominantly Fe(II)-NA complexes. Meanwhile, AtYSL1, AtYSL3 and OPT3 are found to take part in Fe redistribution from senescent leaves to younger leaves or developing tissues via the phloem (Jean et al., 2005; Mendoza-Cózatl et al., 2014; Waters et al., 2006; Zhai et al., 2014). Moreover, in Arabidopsis FPN1 is localized in the plasma membrane and regulates Fe homeostasis in vascular loading (Morrissey et al., 2009). In rice, the OsYSL2 and OsYSL9 are the transporters which have been suggested to be responsible for Fe(II)-NA or Fe(III)–DMA transport into developing seeds (Ishimaru et al., 2010; Senoura et al., 2017).

In the subcellular Fe transport, chloroplasts and mitochondria consume the largest amounts of Fe as they are the main sites for plant photosynthesis and respiration (Jain and Connolly, 2013; López-Millán et al., 2016). The vacuole is the major iron storage organelle in cell and plays a key role in intracellular Fe homeostasis especially for the seeds (Lanquar et al., 2005). Therefore, it is worth to focus Fe translocation at subcellular level more on these three organelles. VIT1 is proposed to

efflux Fe from the cytosol into the vacuole (Kim et al., 2006). In Arabidopsis, six members of the NRAMP family have been identified, the AtNRAMP3 AtNRAMP4 double mutant species cannot mobilize Fe from the vacuolar to cytoplast, which suggests that NRAMP3 and NRAMP4 are responsible for Fe retrieval from the vacuole into the cytosol during germination (Lanquar et al., 2005). With the presence of vacuolar membrane-localized transporter ZIF1, NA can be transported into the vacuole and mostly bound with vacuolar Fe (Haydon et al., 2012). Similar to vacuolar, Fe in chloroplasts also exists as Fe-NA complex but with AtYSL4 and AtYSL6 transporters (Divol et al., 2013). Jeong et al. (2008) reported the Arabidopsis ferric reductase oxidase FRO7 has 75% more Fe(III) chelate reductase activity than the FRO7 loss-of-function mutants and further promote Fe acquisition into chloroplasts. Meanwhile, an ancient permease in chloroplasts PIC1 is proposed to take up Fe into chloroplasts (Duy et al., 2007). Mitochondrion as a crucial organelle for plant respiration, which accompany Fe(III) reduction reaction by FRO3 and FRO3 in the mitochondrial membrane. The reduction reaction product of Fe(II) can later be transported to mitochondria by MITs transporters, which was verified in rice (Jain and Connolly, 2013). In any case, both Fe uptake into and translocation within plants regulated by kinds of transporters could result in Fe isotope fractionation.

2.4 Iron isotopes

Iron consists of four stable isotopes in nature (abundancies are given in the brackets), ^{54}Fe (5.845%), ^{56}Fe (91.754%), ^{57}Fe (2.119%) and of ^{58}Fe (0.282%) (Lide, 1995). Every Fe compound has all of these four Fe isotopes regardless of its form, be it mantle rock, soil minerals or heme proteins. However, the relative distribution of the four isotopes slightly varies caused by isotope fractionation during geochemical and biological processes in the natural environment (Bigeleisen and Mayer, 1947; Schauble, 2004).

Natural Fe isotope fractionation between reactant and product are mostly due to mass dependent isotope fractionation effects, which can be divided into kinetic and equilibrium (thermodynamic) effects (Criss, 1999; Schauble, 2004). The kinetic isotope effect is caused by different reaction rates between light and heavy isotope and is being used to describe unidirectional incomplete chemical reactions, like diffusion, adsorption, precipitation or biological processes. The equilibrium isotope effect occurs in the situation of two phases reacting with forward and backward reactions proceeding at equal rates, where heavy isotopes are enriched in the compounds with more stable bonds (Fig. I-2) (Wiederhold, 2015).
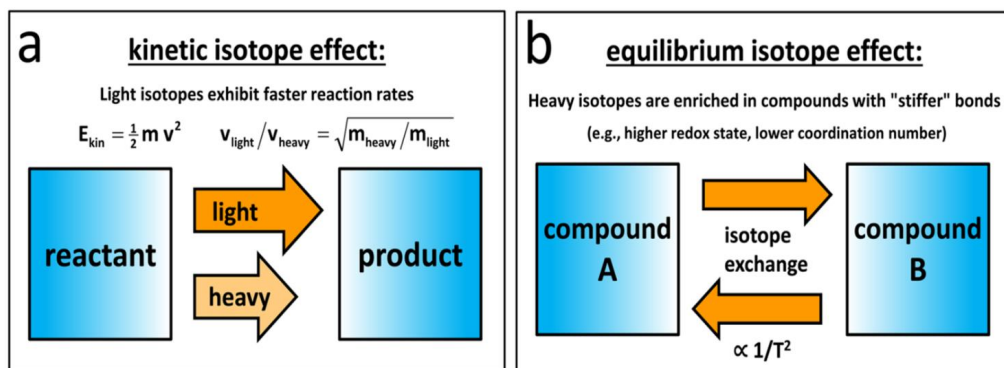
Fig. I-2: a) Schematic illustration of kinetic and b) equilibrium stable isotope fractionation, adapted from Wiederhold (2015).

To express the Fe isotope ratios and better relate isotope data of different laboratories, the delta-notation (δ) in per mil (‰) unit is defined by the measured $^{56}Fe/^{54}Fe$ or $^{57}Fe/^{54}Fe$ ratios in unknown samples relative to those in the international reference material. The international Fe isotope standard is IRMM-014 of which isotopic composition is close to that of rocks at the earth surface.

The Fe isotope composition of a given sample is therefore expressed following the equation Dauphas et al. (2017):

$$\delta^{56}Fe(‰) = \left[\frac{\left({}^{56}Fe / {}^{54}Fe \right)_{Sample}}{\left({}^{56}Fe / {}^{54}Fe \right)_{IRMM-014}} - 1 \right] \times 1000 \quad (1.1)$$

Or
$$\delta^{57}Fe(‰) = \left[\frac{\left({}^{57} / {}^{54}Fe \right)_{Sample}}{\left({}^{57}Fe / {}^{54}Fe \right)_{IRMM-014}} - 1 \right] \times 1000 \quad (1.2)$$

For mass-dependent isotope fractionation, these two values can be easily converted into each other by using $\delta^{57}Fe = 1.5 \times \delta^{56}Fe$.

To better describe the isotope fractionation between the reactant and the product in a certain reaction, the fractionation factor (α) is commonly used with the following equation:

$$\alpha_{A-B} = \frac{R_A}{R_B} \quad (1.3)$$

Where R is the isotope ratio of ${}^{56}Fe/{}^{54}Fe$ or ${}^{57}Fe/{}^{54}Fe$ for compounds A and B in a kinetically controlled process. In an equilibrium process, A and B represent the two phases.

To compare the isotope composition of A and B, the apparent difference of δ values between A and B is describe by the following equation:

$$\Delta_{A-B} = \delta_A - \delta_B \quad (1.4)$$

Where the α_{A-B} and the Δ_{A-B} can be converted by using:

$$\Delta_{A-B} \approx 1000 \ln \alpha_{A-B} \quad (1.5)$$

For element with three or more stable isotopes, an exponential law can be used to describe the relationship between the fractionation factors (α) and the isotope ratios ($^{56}Fe/^{54}Fe$ or $^{57}Fe/^{54}Fe$) in a mass-dependent isotope fractionation:

$$\alpha_{^{56}Fe/^{54}Fe} = \left(\alpha_{^{57}Fe/^{54}Fe}\right)^{\beta} \qquad (1.6)$$

Where the scaling factors β for kinetic and equilibrium fractionation are, respectively:

$$\beta_{kin} = ln(\tfrac{54}{56})/ln(\tfrac{54}{57}) \qquad (1.7)$$

$$\beta_{equil} = (\tfrac{1}{54} - \tfrac{1}{56})/(\tfrac{1}{54} - \tfrac{1}{57}) \qquad (1.8)$$

2.5 Iron isotope fractionation in soil-plant system

In the last two decades, studies of tracing stable Fe isotope variations in environment have markedly increased and the analysis of stable Fe isotope fractionation has been established as a new tool to study Fe cycling in the biogeochemical process (Beard et al., 1999; Liu et al., 2014; Poitrasson and Freydier, 2005). As we mentioned above, a series of abiotic and biotic processes have been identified to induce Fe redox reactions like reductive dissolution of Fe minerals, adsorption and precipitation to uptake and translocation within plants. All of these processes are accompanied by Fe isotope fractionation which is largely related to the transformation between Fe(II) and Fe(III) (Brantley et al., 2001; Guelke-Stelling and von Blanckenburg, 2012; Teutsch et al., 2005; von Blanckenburg et al., 2009). It is generally assumed that processes of plant Fe uptake, straw deposition and decomposition could leave behind a fingerprint on the soil's Fe isotope compositions. Changes in soil properties like pH and Eh can affect Fe solubility thus having effects on plant Fe isotope signatures. A number of controlled and field studies have investigated Fe isotope compositions in higher plants (Guelke-Stelling and von Blanckenburg, 2012; Guelke and

Von Blanckenburg, 2007; Kiczka et al., 2010) and demonstrated that Fe isotope fractionation among higher plants is influenced by both plant species and Fe availability in soils. The processes, however, are complex, so that it seemed useful to do a brief overview of the state of Fe isotope research in soil-plant systems, with special focus on plant Fe uptake and translocation processes (Wu et al., 2019). My contributions to this joint review will be outlined in detail in chapter two of this theses, so that I am not going more into detail in this part of the introduction section.

3. OBJECTIVES

The present study aims to use stable Fe isotopes as tracers to investigate Fe biogeochemical processes in soil-plant systems especially in the system of arable soil and wheat. Specifically, my thesis addressed the following questions:

➢ Can stable Fe isotopes be a valid tool to track Fe cycling in soil-plant systems?

A number of research studies have investigated the Fe isotope distributions in soil as well as in plants. The state of Fe isotope research in plant studies was systematically reviewed and research gaps highlighted.

➢ Do different Fe availabilities affect Fe isotope signatures in wheat?

All reported Strategy I plants consistently enriched light Fe isotopes under all growth conditions. In Strategy II plants, however, fractionation of Fe isotopes is supposed to depend on the growth conditions. To clarify this, a pot experiment in greenhouse was performed growing wheat plants under both Fe sufficient and deficient conditions.

➢ Can δ^{56}Fe values of soil and plant samples shed light on the effect of agricultural soil management like irrigation on Fe uptake in wheat plants?

How do anthropogenic practices affect Fe uptake of crops? In this section I analyzed how irrigation affects different Fe pools (bulk Fe pool and plant-availability pool) and used stable Fe isotopes to track associated processes. Furthermore, soil management could change δ^{56}Fe values on the growing plants.

To answer these questions, I first conducted a detailed literature review as indicated above, and then supplemented this theoretical study by two experiments. On the one and, I examined the effect of different Fe availabilities on Fe isotope fractionation of wheat plants under controlled conditions. On the other hand, I considered the effect of long-term irrigation management on Fe isotope fractionation in soils and cereals. In the latter case I got access to a long-term agricultural experimental field site, which was located in an agricultural area near Thyrow (52°15 N, 13°23 E, 44 m a.s.l.), 20 km southwest of Berlin (Germany). A detailed description of microcosm experiments and the study sites as well as the methods applied will be provided in each of the following chapters separately.

II

IRON ISOTOPE FRACTIONATION IN PLANTS

Modified on the basis of

Wu, B., Amelung, W., Xing, Y., Bol, R., & Berns, A. E. (2019). Iron cycling and isotope fractionation in terrestrial ecosystems. Earth-Science Reviews, 190, 323-352.

1. Introduction

Although Fe is the fourth most abundant element in the Earth's crust, Fe-solubility is very low in well aerated soils at physiological optimal pH (Lindsay and Schwab, 1982). As response to this problem, plants have developed two efficient strategies to secure Fe uptake from soil (Marschner et al., 1986). The sequential acidification-reduction-transport strategy (strategy I) is carried out by all higher plants, except for the graminaceous plants, which use the chelation-based strategy (strategy II) for Fe uptake (Hell and Stephan, 2003). Strategy I plants excrete protons via a plasmalemma AHA H+-ATPases to acidify the rhizosphere, and then the NADPH-dependent ferric chelate reductase AtFRO2 reduces Fe(III) to Fe(II) which is then available to plants and can be transported through a plasmalemma by Fe transporter proteins (Hell and Stephan, 2003; Robinson et al., 1999). Strategy II plants release phytosiderophores (PSs) that chelate Fe(III) in the rhizosphere. The Fe(III)–PS complexes are then channeled into the root by specific plasmalemma transporter proteins (Curie et al., 2001; Schaaf et al., 2004; Takagi et al., 1984). It is generally assumed that the chelation-based strategy is more efficient than the sequential acidification-reduction-transport strategy and allows graminaceous plants to survive under more drastic Fe-deficient conditions (Mori, 1999). Both strategies can induce Fe isotope fractionation between the soil and the plant root, as they basically rely on reductive dissolution and organic compound complexation of Fe. Once Fe is taken up into the plant roots, it is cycled through a variety of biochemical reactions moving from roots to stems, then to leaves and seeds, also leading to fractionation of Fe isotopes within the plant.

2. Iron isotopic fractionation in plants

2.1 Iron isotope fractionation during root uptake

Iron isotope fractionation during root uptake was first proposed by (Guelke and Von Blanckenburg, 2007), based on that all seven strategy I plants they analyzed were enriched in lighter Fe isotopes and the δ^{56}Fe values decreased from soils to shoots, while strategy II plants had slightly heavier Fe isotope compositions compared with the plant available Fe in the soil. Even though the Fe isotope composition in roots was not analyzed, the difference in δ^{56}Fe values in the growth medium and the aboveground tissues indicated a clear Fe isotope fractionation. Kiczka et al. (2010) later found a significant fractionation towards negative δ^{56}Fe values within the strategy II plant *Agrostis*. The authors suggested that the Fe isotopic signature of plant biomass depended not only on the Fe uptake strategy, but also on the nutrient availability in the substrate. When Fe is sufficiently available in the growth medium, mechanisms of Fe mobilization are similar for both plant groups, resulting in an isotopically light signature in the plants, whereas when Fe is deficient, the strategy II plants mobilize Fe with Fe-PS complexes leading to no apparent Fe isotope fractionation during uptake (Kiczka et al., 2010). The statement is further consolidated by (Guelke-Stelling and von Blanckenburg, 2012), who subsequently showed that there was a preferential uptake of lighter Fe isotopes by strategy II plants when growing in non-limiting Fe(III)-EDTA nutrient solution. Furthermore, previous observations showed that the root exudation of siderophores was suppressed under Fe sufficient conditions (Charlson and Shoemaker, 2006; Marschner, 1995), which was probably also the case in the field trials studied by (Kiczka et al., 2010).

Charlson and Shoemaker (2006) pointed out that both strategy I and II plant species could possess either all or some genes to acidify and reduce Fe, possibly enabling strategy II plants to also take up Fe through reduction reactions similar to strategy I plants when Fe is sufficient in soils. The strategy II plant rice (*Oryza sativa*) is an example of such a plant that possesses the ferrous

transporter OsIRT1, allowing the crop to directly absorb Fe(II) from the soil (Arnold et al., 2015; Kobayashi and Nishizawa, 2012), in addition to a PS-mediated Fe(III) transport system (Bughio et al., 2002). This suggests that rice takes up Fe both as Fe(III)-phytosiderophores and Fe(II) ions (Ishimaru et al., 2006), which may result in different extents of Fe isotope fractionation.

Using pot experiments, Arnold et al. (2015) showed that rice shoot and grain contained isotopically light Fe compared with the bulk soil or the leachate of the soil, suggesting possible changes in the redox state of Fe occurring during the uptake and translocation processes. In a paddy soil feld study, rice roots were found to be enriched in heavy Fe isotopes with $\delta^{56}Fe$ values similar to those of the Fe plaques on its root surface (Garnier et al., 2017). In contrast, the soil pore water had extreme negative δ values, and the plant available soil Fe (0.5 M HCl extracted) was also depleted in heavy Fe isotopes. These Fe isotope composition data indicated that the Fe in the root originated mainly from the Fe plaques, which could not be identified by simply analyzing Fe concentrations or Fe speciation. However, under Fe-rich conditions such as in the studied paddy soils, the mechanisms of how rice roots utilize Fe from the plaques still warrant further attention. Nevertheless, the study of Garnier et al. (2017) clearly indicates that for an understanding of Fe isotope signature in rice plants it is decisive to consider not only the plant and the soil, but also Fe plaques specifically.

Apart from Fe uptake strategies and Fe availability in growth media, Fe isotope compositions in plants may also vary among plant species and within the growing season (Akerman et al., 2014; Kiczka et al., 2010). In addition, plant growth promoting bacteria (PGPR) were found to release lighter Fe isotopes into the living medium indicating that PGPR may have an influence on Fe isotope fractionation during plant uptake in pot experiments (Rodríguez et al., 2014).

2.2 Iron isotope fractionation during translocation

Iron acquisition in plants starts from the apoplast of the root epidermal cells (Sattelmacher, 2001), followed by Fe diffusion through the root apoplast across the plasma membrane to the root symplast. Subsequently, Fe will pass through both xylem and phloem sap bound by chelating compounds (Kim and Guerinot, 2007). To cross the membrane and enter the cells, Fe is mediated by several transporter proteins and ligands (Álvarez-Fernández et al., 2014), such as PSs, nicotianamine (NA) and citrate (Hell and Stephan, 2003).

Moynier et al. (2013) computed the orbital geometries and vibrational frequencies of aqueous Fe(II) and Fe(III) species that are relevant to plants and calculated the corresponding isotope composition. By using such quantum chemical calculations, they estimated the magnitude of equilibrium Fe isotope fractionation among different Fe species [Fe(II)-citrate, Fe(III)-citrate, Fe(II)-NA and Fe(III)-PSs] relevant to Fe transport in higher plants, thereby showing that Fe(II)-NA was by ~3‰ (δ^{56}Fe) isotopically lighter than Fe(III)-PSs. The isotopic variation is due to differences in both Fe redox state and speciation: Fe(III)-PSs are up to 1.5‰ heavier than Fe(III)-citrate and Fe(II)-NA up to 1‰ heavier than Fe(II)-citrate (Moynier et al., 2013). As Fe is stored as Fe(II)-NA in plant seeds (Hell and Stephan, 2003) and likely present as Fe(III)-PSs in the roots, especially for strategy II plants (Becker et al., 1995; Bienfait et al., 1985), the calculated δ^{56}Fe values for these Fe species may partially explain the often reported isotopically heavier Fe in root than in aboveground tissues.

The translocation of Fe from roots to shoots is similar for plants of both strategies. In the xylem sap, Fe is transported as Fe(III)-citrate (Pich et al., 1994), while in the phloem sap Fe is preferentially transported as Fe(II)-NA (von Wirén et al., 1999). Moreover, processes including xylem loading, transport and unloading, xylem to phloem transfer, phloem loading, transport and unloading (Kim and Guerinot, 2007) are involved in Fe translocation in the aboveground tissues,

which may potentially lead to further Fe isotope fractionation in favor of light Fe isotopes in younger leaves (Guelke-Stelling and von Blanckenburg, 2012).

The translocation mechanism of Fe within the aboveground tissues and its relation with Fe isotope fractionation is still uncertain. Younger leaves primarily receive Fe from the phloem where Fe is mostly chelated as Fe(II)-NA, while older leaves acquire Fe from the xylem where Fe is transported as Fe(III)-citrate complexes (Tsukamoto et al., 2008). However, the isotopic difference of Fe(II)-NA and Fe(III)-PSs in the roots of strategy II plants of −3‰ in δ^{56}Fe (Moynier et al., 2013) is much larger than the observed isotopic variations between leaves and roots (Fig. II-1). Therefore, a mixing between Fe transported by the phloem and the xylem likely controls the extent of Fe isotope fractionation during translocation from roots to shoots (Moynier et al., 2013). It is worth noting that the calculated extent in Fe isotope fractionation by Moynier et al. (2013) was due to an equilibrium effect, while processes in plant uptake and translocation are more likely kinetically controlled. Therefore, the values given above should be carefully examined when comparing them with the observed Fe isotope variation in plants.

It is also possible that "dilution effects" during the maturation of the leaves can alter Fe isotopic composition. Besides, plants can also remobilize Fe from older leaves prior to litter fall to avoid Fe losses. This process can also lead to changes in the final Fe isotope ratio determined in the leaves. In addition, other types of ligands such as Fe transport protein (ITP) may be involved in isotope fractionation during translocation into younger leaves. At the cellular level, chloroplast and mitochondria use the largest amount of Fe in plant cells and represent crucial sites for Fe biosynthesis. However, their contribution to Fe isotope fractionation still remains unexplored and deserves further investigation in order to understand the mechanisms of Fe translocation and transformation in plants.
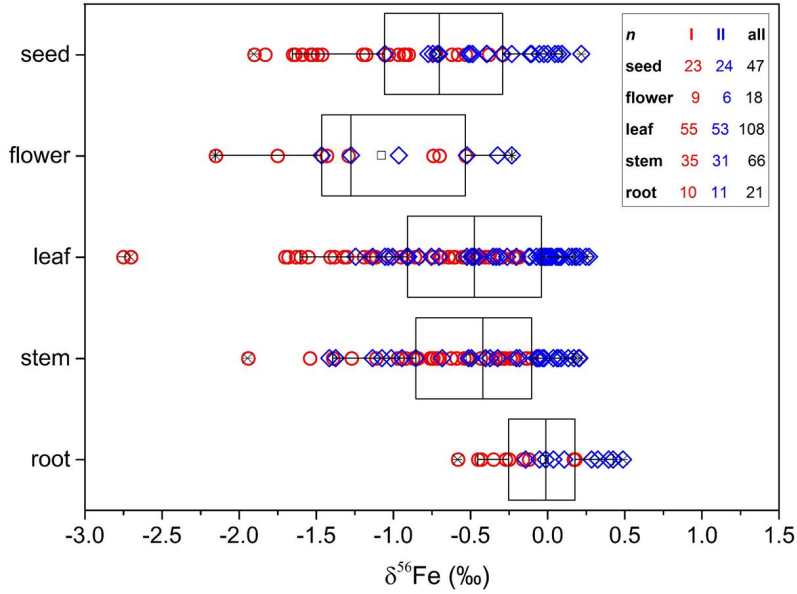
Fig. II-1: Iron isotope variation in different tissues of plants with Fe uptake strategy I (red circles) and strategy II (blue diamonds). The black boxplots show the δ^{56}Fe value distribution of all plants that have to date been studied. The number of the data n is given with respective colors (Wu et al., 2019).

2.3 Fe isotope composition in different plant tissues

Fig. II-1 shows the range of δ^{56}Fe values in different plant tissues that have to date been studied for Fe isotopes, including 12 species of strategy I plants [bean (*Phaseolus vulgaris* L.), lettuce (*Valerianella locusta* L.), spinach (*Spinaci oleracea* L.), rape (*Brassica napus* L.), pea (*Pisum sativum* L.), amaranth (*Amaranthus hybridus* L.), soybean (*Glycine max* L.), lentil (*Lens culinaris*), mountain sorrel (*Oxyria digyna*), French sorrel (*Rumex scutatus*), umbrella tree (*Musanga cecropioides*), and West African piassava palm (*Raphia vinifera*)] and 10 species of strategy II plants [black bent (*Agrostis gigantea*), oat (*Avena sativa* L.), maize (*Zea mays* L. convar.

Sacharata), wheat (*Triticum aestivum* L.), wild rye (*Elymus virginicus*), Johnsongrass (*Sorghum halepense*), Kentucky bluegrass (*Poa pratensis*), river oat (*Uniola latifolia*), Indian goosegrass (*Eleusine indica*) and rice (*Oryza sativa* L. cv. Oochikara)]. It clearly indicates that Fe in plants is isotopically lighter than in soils (Fig. II-1) (Wu et al., 2019). Compared with strategy II plants, strategy I plants are enriched in light Fe isotopes with median δ^{56}Fe of −0.72‰ vs. −0.10‰ (strategy II) for the whole plants (including root and aboveground tissues). For both types of plants, aboveground tissues possess lighter Fe isotopes compared with that in the roots, with the lightest Fe being found in flowers with mean δ^{56}Fe of −1.26 ± 0.53‰ and − 0.96 ± 0.63‰, respectively. It is hypothesized that roots may be enriched in relatively heavy Fe isotopes, as light Fe isotopes are transported into younger plant (aboveground) parts (Guelke-Stelling and von Blanckenburg, 2012). However, it is worth noting that Fe isotope fractionation due to plant uptake should be interpreted relative to Fe isotope composition of the Fe source (e.g. nutrient solution, plant available Fe in soil), which has not been carried out in every study. Nevertheless, we can summarize that Fe isotopic data in soils and plants demonstrate that the processes of uptake and translocation of Fe can lead to significant isotope fractionation, which is controlled by changes of redox state and the binding ligands for Fe (von Blanckenburg et al., 2009).

III

IRON ISOTOPE FRACTIONATION DURING WHEAT GROWTH UNDER DIFFERENT FE SUPPLY

Modified on the basis of the manuscript

Ying Xing, Wulf Amelung, Bei Wu, Yi Wang, Arnd Kuhn, Anne E. Berns

Manuscript finalizing

1. Introduction

In the last decade the analysis of stable isotope fractionation has been established as a new tool to study metal uptake and translocation in plants as a number of processes in the biogeochemical cycling of metals (e.g., Mg, Ca, Cu, Zn, Fe) in plants and soil-plant systems often discriminate isotopes of differing masses (Arnold et al., 2010; Bolou-Bi et al., 2010; Caldelas et al., 2011; Guelke and Von Blanckenburg, 2007; Schmitt et al., 2013; Wiggenhauser et al., 2018).

Iron (Fe) is an essential nutrient for plants. It is required as cofactor for enzymes and directly mediates electron transport processes (Briat et al., 2007b; Kappler and Straub, 2005; von Wirén and Bennett, 2016). A number of controlled studies have investigated Fe isotope compositions in higher plants (Guelke-Stelling and von Blanckenburg, 2012; Guelke and Von Blanckenburg, 2007) and demonstrated that Fe isotope fractionation among higher plants is influenced by both plant species and Fe availability in soils. Guelke and Von Blanckenburg (2007) found that the reduction transport strategy (strategy I) plants, where Fe enters the plant as Fe(II), resulted in plants enriched in light Fe isotopes. The chelation-based strategy (strategy II) plants maize (*Zea mays* L. *convar. Saccharata*) and wheat (*Triticum aestivum* L.), consisting of complexation of Fe(III) by organic phytosiderophores (PS) and subsequent uptake of the PS–Fe(III) complex, exhibited enrichment of heavy Fe isotopes during plant growth. Subsequent work done by Guelke-Stelling and von Blanckenburg (2012) revealed that some strategy II plants like oat (*Avena sativa* L.), growing in non-limiting Fe(III)-EDTA nutrient solution, also have the ability to create reducing conditions in the rhizosphere and take up Fe(II), resulting in enrichment of light Fe isotopes similar to strategy I plants. However, the study contained no oat plants growing under Fe deficient conditions to verify whether Fe isotope fractionation also occurs under sub-optimal Fe supply. In a greenhouse

pot experiment study, Arnold et al. (2015) found that the strategy II plant rice (*Oryza sativa* L. *cv. Oochikara*) growth in both aerobic and anaerobic soils enriched isotopically light Fe to similar extent in both cases, which demonstrated that different physicochemical soil conditions in soils do not necessarily affect the Fe isotope signatures in the plants. Studying the influence of environmental factors on Fe uptake and isotope fractionation in plants under field conditions is less straight forward. In an alpine glacier forefield, Kiczka et al. (2010) found that the strategy II plant *Agrostis gigantean* was enriched in light Fe isotopes. The authors explained this by selective Fe isotope uptake by the plants induced by processes preceeding active transport such as mineral dissolution, which preferentially releases light isotopes into soil solutions.

Compared to Fe uptake, the influence of Fe translocation within plants on Fe isotope ratios in plant organs is less studied. A number of authors hypothesized that the translocation of Fe from roots to shoots is similar for plants of both strategies (Kim and Guerinot, 2007; Pich et al., 1994; von Wirén et al., 1999). Moynier et al. (2013) investigated the effects of ligand exchange reactions on Fe isotope compositions during translocation by computing the orbital geometries and vibrational frequencies of Fe(II)- and Fe(III)-complexes, which included 4 different Fe ligands: Fe(II)-citrate, Fe(III)-citrate, Fe(II)-nicotianamine (NA) and Fe(III)-phytosiderophore (PS) complexes. Fe(III)-PS complexes are up to 1.5‰ (δ^{56}Fe) heavier than Fe(III)-citrate complexes and Fe(II)-NA complexes are up to 1‰ heavier than Fe(II)-citrate complexes. However, Fe(III)-PS complexes were by ~3‰ isotopically heavier than Fe(II)-NA complexes.

In any case, it is found that all reported strategy I plants consistently enriched light Fe isotopes in all growth conditions. Strategy II plants, however, could exhibit enrichments in either light or heavy Fe isotopes depending on the growth conditions. Furthermore, it should be kept in mind that Fe isotopic signatures in plants can be the combined results from plant growth conditions as well

as plant Fe uptake and translocation processes. The current working hypothesis is that strategy II plant species also possess ferrous transporters (Arnold et al., 2015; Cheng et al., 2007; Kim and Guerinot, 2007; Kobayashi and Nishizawa, 2012), which enable them to utilize the reduction strategy I under non-Fe-deficient conditions, thereby enriching light Fe isotopes. Our aim was to test how Fe isotope fractionation in wheat plants is influenced by different Fe availabilities in the growth medium under controlled greenhouse conditions. Moreover, we set up several different harvesting time points to observe the Fe isotope fractionation in wheat plants from vegetative growth (seeding to anthesis) to reproductive growth (anthesis to full maturity) (Sharma, 1992; Wiggenhauser et al., 2018).

2. Material and methods

2.1 Plant material and growth conditions

Summer wheat (*Triticum aestivum* L.) was chosen as experimental plant. All seeds were germinated in petri dishes for 48 h with distilled water at room temperature in the dark. Subsequently, all germinated seeds were transferred to 40×25 cm nursery seedling plates for 3 days. Plants were then grown in washed silica sand (grain size 0.7–1.4 mm) with two plants per pot (pot height: 13 cm, pot volume: 2 L). The use of sand permitted to grow all plants at similar substrate density (1.65 g cm^{-3}) and water content (10.4 weight-%) (Füllner et al., 2012). The experiment was conducted in a greenhouse of the Plant Sciences Institute (IBG-2, Forschungszentrum Jülich GmbH) at 250 µmol m^{-2} s^{-1} light intensity, with a 16 h/8 h and 24 °C/18 °C light/dark schedule, and 50-60% relative humidity. A filter tissue of 250 µm mesh size, which prevented roots from growing out of the pots but enabled free drainage of nutrient solution at the same time, closed the bottom of the pots. Modified Hoagland solutions were used with two different Fe concentrations for the Fe-deficient (0.0022 mM Fe-EDTA) and the control (0.0896

mM Fe-EDTA) treatments (Appendix A, Table A1). The plants were irrigated through a percolating drip irrigation system 3 times a day (at 9 am, 1 pm, 5 pm, respectively) for 1 min at a rate of 30 mL min^{-1}. Fourty-five days after seeding, drip irrigation was increased to 4 times (at 9 am, 1 pm, 5 pm, 8 pm, respectively) a day to meet higher water demand of the plants. To study Fe isotope fractionation changes along with the wheat growth, plants were sampled at 3 time points when they were in anthesis, post-anthesis and fully maturity (52, 74 and 87 days after seeding, respectively) with 4 pots per harvest. The plants were washed with deionized water to remove possible aerial depositions and then separated into roots, stems, leaves, and spikes on anthesis and post-anthesis stage or husks and grains at maturity. All plant samples were freeze-dried (CHRIST® Beta1-8 LDplus, Germany) and milled to powder in a custom-made ball mill (Collomix Viba 330, Collomix GmbH, Germany) using metal-free tungsten carbide milling balls.

2.2 Plant sample digestion, Fe purification and isotope measurements

Plant samples were precisely weighed into Teflon digestion tubes and digested in a pressurized microwave single reaction chamber (turboWAVE®1500, MLS GmbH, Germany) with distilled ultrapure HNO$_3$ (68%) and H$_2$O$_2$ (30%). Iron concentrations in the digests were then determined by inductively coupled plasma mass spectrometry (ICP-MS, Agilent 7900, Germany). A certified reference material (NIST SRM 1575a Pine Needles) and acid blanks were used as standard and control samples.

The Fe purification procedures were carried out in a custom-made laminar flow hoods with particle filters (High-Efficiency Particulate Air H14, AS Luftfilter, Germany). Aliquots of the acid digests were evaporated to dryness in acid-cleaned Teflon beakers (Savillex® beakers, USA) on a hotplate at 85 °C. Subsequently, the dried samples were redissolved in 2.0 ml of 6 M distilled ultrapure HCl. Iron purification was performed using anion exchange chromatography resins (Bio-Rad

AG1-X4, 200-400 mesh) (Dauphas et al., 2004). Matrix elements were washed out stepwise with 6 M HCl. Fe isotopes were eluted stepwise from the columns with 0.05 M HCl. Complete separation of Fe from Zn was obtained in a second column clean-up by eluting Fe with 1.5 M HCl and Zn with 0.05 M HCl. All eluates (matrix elements, Fe and Zn) were dried down in acid-cleaned Savillex® beakers on a hotplate at 85 °C and redissolved in 2.0 ml 0.3 M ultrapure HNO_3. Quantitative recovery of Fe(recovery >95%) and the absence of matrix elements were controlled by ICP-MS to ensure no artificial isotope fractionation and matrix effects during isotope measurement (Anbar et al., 2000). Additionally, solution blanks and Fe isotope standard IRMM-524a samples were also processed through the purification procedure.

The Fe isotope ratios of all samples and the nutrient solution were determined on multi-collector ICP-MS (MC-ICP-MS, Nu Plasma II, Nu Instruments, UK). High-mass resolution mode with a mass resolving power (Rp 5, 95%) of > 8000 at ion beam transmission of 10% were used. A membrane desolvating nebulizer (Aridus II, Cetac technologies, USA) coupled to the MC-ICP-MS was used to minimize argide interferences (ArN^+, ArO^+, $ArOH^+$) by reducing the solvent loading to the plasma. To correct instrumental mass bias, a standard-sample-standard bracketing strategy was applied during the measurements using Fe isotope standard (IRMM-524a) solutions with matched Fe concentrations with the samples (Dauphas et al., 2009). Although IRMM-524a was used during the measurement in the present study, the results of Fe isotope analysis in samples were expressed using IRMM-014 as the standard (recommended by Dauphas et al. (2017)) (Eq.III-1):

$$\delta^{56}Fe(‰) = \left[\frac{\left(^{56}Fe/_{54}Fe\right)_{Sample}}{\left(^{56}Fe/_{54}Fe\right)_{IRMM-014}} - 1 \right] \times 1000 \quad \text{(Eq. III-1)}$$

We achieved a precision of $\pm$ 0.08 ‰ (2SD) for δ^{56}Fe and $\pm$ 0.12 ‰ for δ^{57}Fe, respectively, obtained from repeated measurements of the standard IRMM-524a during the analytical sessions. The three-isotope-plot using measured δ^{56}Fe and δ^{57}Fe values confirmed the absence of mass-independent isotope fractionation during the analyses (Appendix A, Fig. A1). For each sample, the isotopic composition was measured at least three times with some measurements being repeated in different sessions showing good reproducibility.

A mass balance approach was used to determine the Fe isotope composition of the whole plant and aboveground organs (shoot) with the following equation (Kiczka et al., 2010):

$$\delta^{56}Fe_{\,Shoot\;or\;Plant} = \frac{\sum_i m_i c_i \delta^{56} Fe_i}{\sum_i m_i c_i} \qquad \text{(Eq. III-2)}$$

Where i symbolizes the different plant organs (root, stem, leaves, spike/husk and grain), m the plant dry biomass (g), c the Fe concentration ($\mu g\ kg^{-1}$), and $\delta^{56}Fe_i$ the isotope composition of plant organ i.

2.3 Statistical analyses

Statistical analyses were performed in SigmaPlot 14.0 (Systat software Inc., USA). Two-way analysis of variance was performed for the data on plant dry biomass, Fe concentration values and Fe isotope compositions to compare different Fe supplies. Based on the ANOVA output, all pairwise multiple comparison procedures were done by Duncan's multiple-range test (Duncan, 1955). Level at 0.05 was used to test the significant differences.

3. Results

3.1 Plant dry biomass and Fe concentrations under different Fe supply

The Fe-deficient treatment significantly ($P < 0.05$) decreased the whole plant dry biomass compared to the control plants at both anthesis and maturity stages during plant growth (Fig. III-

1; Appendix A, Table A2). Specifically, Fe-deficiency significantly decreased the dry biomass of roots, stems and leaves at the anthesis stage. At maturity, Fe-deficiency reduced the dry biomass of the husks. However, at the post-anthesis stage, the root dry biomass significantly increased from 1.7 g to 2.9 g in the Fe-deficient treatment. At anthesis, stems had the largest dry biomass with 3.7 g and 5.2 g for Fe-deficient and control treatments, respectively. At both post-anthesis and maturity, the spikes were the plant organs with the largest dry biomass in both variants.
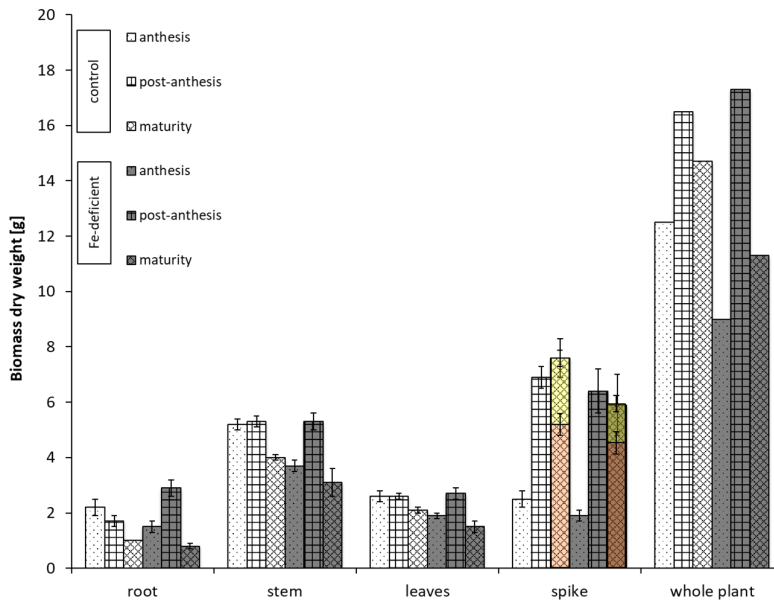
Fig. III-1: Dry biomass of the organs and the whole plant of summer wheat grown under different Fe supplies on different growth stages. The yellow and orange rectangles represent plant husks and grains, respectively. Each column represents the mean values of three replicates and their standard error.

Except for the roots the different plant organs exhibited Fe concentrations within the expected range for wheat organs (Çakmak et al., 2004; Marschner, 2011). The plant roots consistently had

the highest Fe concentrations for all three harvest time points. The leaves contained the second largest Fe concentrations across all growth stages and the stems displayed the lowest Fe concentrations. Fe-deficiency significantly ($P < 0.05$) decreased the Fe concentrations of the whole plants at the anthesis and post-anthesis stages (Fig. III-2; Appendix A, Table A2). At the anthesis and post-anthesis stages, the Fe-deficient treatment decreased Fe concentrations in plant roots and leaves. At wheat maturity, significant differences in Fe concentrations between both variants only occurred in plant leaves, which showed much lower Fe concentrations in the Fe-deficient variant. Conversely, the Fe-concentrations in roots increased noticeably at maturity, though statistical significance was likely obscured by the large sample variation. Over the complete growth period, Fe concentrations of the stems decreased from anthesis to post-anthesis then increased at maturity stage. In the plant sink organs (e.g., spikes, husks and grains) the Fe concentrations increased from anthesis to maturity under control treatment and remained unchanged in the Fe-deficient variant, but in the same range than the control (Fig. III-2; Appendix A, Table A2).
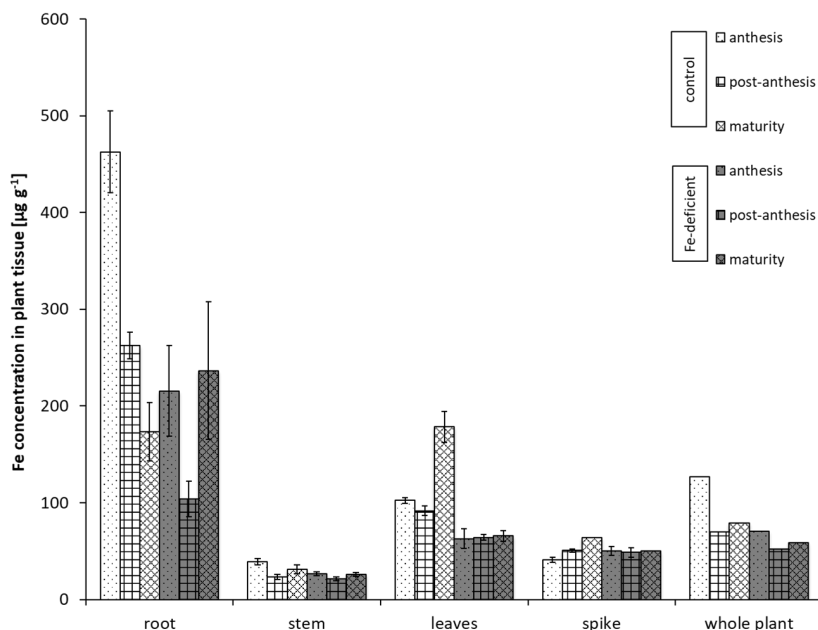
Figure III-2: Iron concentrations of the organs and the whole plant of summer wheat grown under different Fe supplies on different growth stages. Each column represents three replicates and their standard error.

3.2 Iron isotope composition in wheat

The Fe isotope composition of the nutrient solution was 0.38 ± 0.09 ‰ shown by the dotted line in Fig. III-3. Mass balance calculations (Eq. III-2) showed that total wheat plants were preferentially enriched in lighter Fe isotopes for all three harvest time points compared to the nutrient solution (range of $\Delta^{56}Fe_{\text{plant–nutrient solution}} = -0.24$ to -0.11 ‰) for both Fe-deficient and control treatments (Fig. III-3; Appendix A, Table A2). Compared with the nutrient solution, the calculated $\delta^{56}Fe$ values for the shoots (Eq. III-2) also exhibited lighter Fe isotope compositions (range of $\Delta^{56}Fe_{\text{shoot–nutrient solution}} = -0.30$ to -0.18 ‰) in both Fe-deficient and control treatments (Fig. III-3; Appendix A, Table A2). At all three growth stages there was no significant difference in the calculated Fe isotope compositions, neither in whole plants nor in shoots, between both Fe-

supplies (Fig. III-3; Appendix A, Table A2). However, during growth, the difference between both variants in the Fe isotope compositions of the whole plant increased from -0.04 ‰ to 0.13 ‰ (Fig. III- 3). Furthermore, on all three growth stages the variations of δ^{56}Fe values among the different plant organs of one treatment was always larger in the control treatment. The Fe-deficient variant displayed the smallest variation at post-anthesis (Δ^{56}Fe$_{\text{root-spike}}$ = 0.17 ‰), while the control variant already nearly reached its maximum variation at this stage (Δ^{56}Fe$_{\text{leaf-spike}}$ = 1.21 ‰). At maturity Δ^{56}Fe$_{\text{leaf-spike}}$ of the control reached 1.22 ‰ and was even as high as 1.43 ‰ for Δ^{56}Fe$_{\text{leaf-grain}}$.

The control treatment showed consistent behavior along the three growth stages, where roots and stems did not show significant Fe isotopic differences neither among stages nor at a specific growth stage among different plant organs and were slightly enriched in lighter isotopes compared to the nutrient solution. On all growth stages the leaves were enriched in heavier Fe isotopes compared with all other plant organs. The largest shift towards more positive δ^{56}Fe values for the leaves took place between the anthesis and post-anthesis stages. The spikes, respectively the grain, always displayed the most negative δ^{56}Fe values on all three growth stages. If the δ^{56}Fe values of spikes are compared then the shift towards negative δ^{56}Fe values was relatively even paced (Fig. III-3; Appendix A, Table A2).

The behavior of the Fe-deficient variant was much less consistent along the growth stages than the control. At the anthesis stage, even though roots, stems and spikes showed Fe isotopic differences between the Fe-deficient and the control treatments, none of them were statistically significant. The overall δ^{56}Fe pattern at this stage, however, was comparable to the control variant with the leaves being slightly enriched in heavier isotopes and the spike displaying the most negative δ^{56}Fe value of the plant organs. At the post-anthesis stage, the δ^{56}Fe values of all plant organs converged around a mean δ^{56}Fe of 0.19 ‰ with no significant differences among the δ^{56}Fe values of the plant

organs. At maturity, the δ^{56}Fe pattern of the Fe-deficient variant was partly consistent with the control except for the roots, which enriched heavier isotopes and had a comparable δ^{56}Fe value to the leaves, and the grains, which were significantly heavier than the control and had a δ^{56}Fe value which was not significantly different from the δ^{56}Fe value of the stems (Fig. III-3).
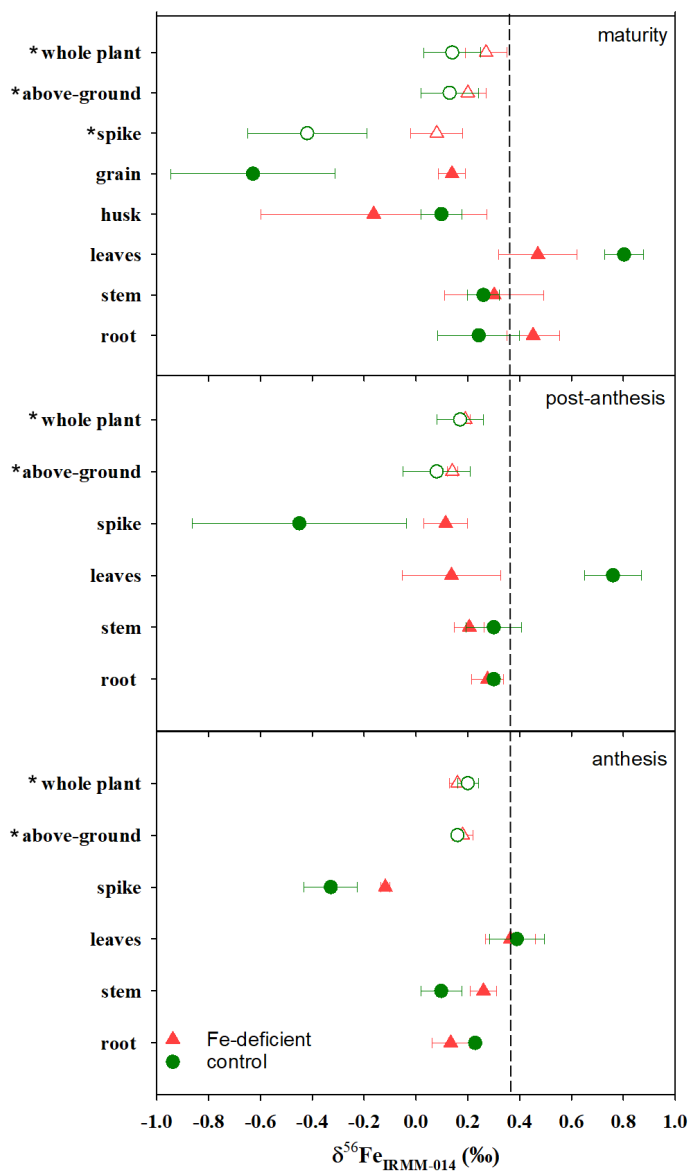
Fig. III-3: Iron isotope compositions in plant organs during anthesis, post-anthesis and maturity. *
Fe isotope compositions of the above-ground, the whole plant and the mature spike were calculated
based on Eq. III-2, which were indicated by hollow symbols. The dotted line indicates the Fe

isotopic composition of the nutrient solution. Each data point represents three plant replicates and their standard error.

4. Discussion

4.1 Effects of Fe-deficiency on wheat growth

The plant dry biomass of the control variant developed as expected with the maximum at the post-anthesis stage and a subsequent decline during ripening (Fig. III-1). This biomass development was mainly driven by the shoot parts of the plants which made up over 80% of the dry biomass at all stages (Fig. III-1). Among the above-ground plant organs, the spike displayed the largest mass gain as the cellular division was rapid after floret fertilization and the grains start to fill (Acevedo et al., 2006). The growth of the spike requires extensive nutrient supply, for which nutrients are remobilized from the primary storage reservoirs of leaves and stems via the phloem to the developing seeds (Borg et al., 2009). Even though the dry biomass of these stems and leaves remained stable between anthesis and post-anthesis, their Fe concentrations decreased due to the internal redistribution of nutrients. During grain ripening these organs lost dry biomass may due to that plant respiration was no longer counteracted by photosynthesis.

The overall development of plant dry biomass in the Fe-deficient variant was similar to the control with respect to the largest plant dry biomass being found at the post-anthesis stage. The whole plant dry biomass was, however, higher than the control variant at this stage, which was due to an unusual increase of the root dry biomass. As all plant organs displayed lower dry biomass than the control at anthesis, the nutrient amounts accumulated during initial vegetative growth were likely not sufficient to ensure grain filling which triggered an increase in root mass to increase nutrient uptake from the growth medium. The subsequent dry biomass loss during ripening, however,

caused the spike to lose mass between post-anthesis and maturity. The Fe concentration in the grains was reduced by 21% in the Fe-deficient variant though the difference was statistically not significant at the 0.05 level (Appendix A, Table A2). Unlike the control, in the Fe-deficient variant the Fe concentration in the leaves did not change between anthesis and post-anthesis and the Fe concentration in the stems showed only a small decrease. As Fe-deficiency affected both plant dry biomass and Fe concentration of the plant organs the total Fe masses contained in the plant organs had to be considered in order to get the true picture of Fe fluxes among them (Fig. III-4).
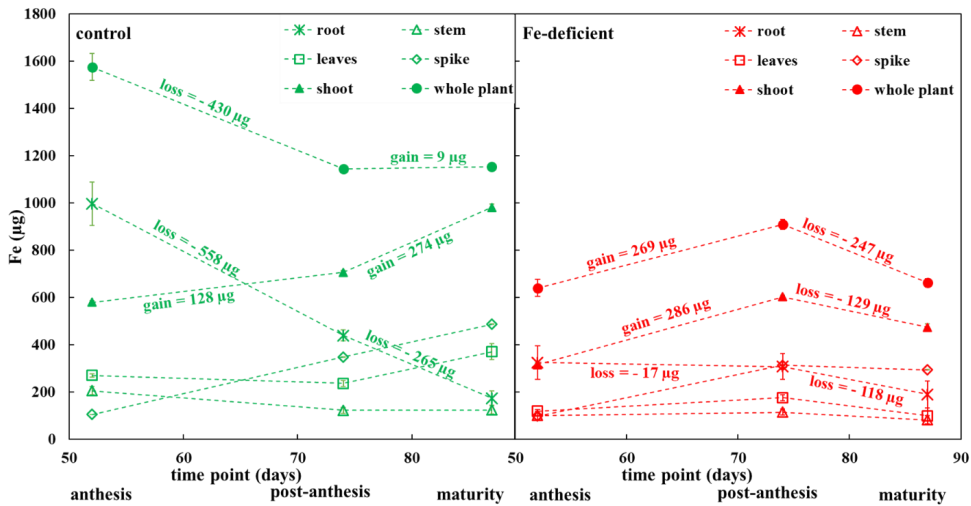
Fig. III-4: Fe mass in plant organs. Each data point represents three replicates and their standard error. The values given show mean net losses or gains per pot (= 2 plants).

The largest amount of whole plant Fe mass in the control was found at the anthesis stage. Subsequently, between anthesis and post-anthesis a net loss of 430 µg Fe in the whole plant Fe mass occurred. During ripening the overall Fe mass in the plant then remained basically unchanged. This large net loss in Fe mass between anthesis and post-anthesis stages was due to a massive Fe mass loss in the root (558 µg) in this period of which only 128 µg Fe were translocated

to the shoot. The translocated Fe from the root was most likely directly transferred to the spike as both leaf and stem also displayed a decline in Fe mass, indicating an additional translocation of Fe from leaf and stem to the spike within this period. The recorded decline in root dry mass between anthesis and post-anthesis was due to remobilization of assimilates and nutrients from vegetative plant parts to the developing grain (Belford and Henderson, 1985) and simultaneous root decay, which also caused the release of Fe from the root tissue back into the substrate. This decline in root mass continued at the same rate after post-anthesis and concurred with an equally unchanged Fe mass loss rate in the root. However, the overall Fe mass in the plant did not change during ripening as the Fe mass gain rate in the shoot increased. This increase was due to an increase in Fe mass in the leaves while the Fe mass gain in the spike continued at the same pace. Furthermore, the stems no longer showed a loss in Fe mass indicating that translocation of Fe from leaves and stems to spikes had stopped and that Fe was mainly translocated from the root (also see Appendix A, Fig. A2).

The Fe mass of the whole plant at anthesis in the Fe-deficient variant was reduced by 59 % compared to the control variant. The subsequent Fe mass gain in the shoot due to grain filling was increased by a factor of 3.2 and unlike the control variant there was only minor loss of Fe in the root. Furthermore, the Fe masses contained in the leaves and stems did not decrease between anthesis and post-anthesis, which lead us to conclude that under Fe-deficient conditions no Fe was redistributed from the plant organs, but the increase in the spike was solely due to an increased uptake from the nutrient solution. This is supported by the recorded increase of root dry mass during that period (Fig. III-1). We attribute this difference to plants counteracting their nutrient deficient stress by changing root morphology which included swelling of root tips, enhanced lateral root development, and a boost increase of the number and length of root hairs (Moog, 1995;

Müller and Schmidt, 2004; Schmidt et al., 2000). Conversely to the control variant, between post-anthesis and maturity the overall Fe mass decreased. Whereas in the control the Fe gain in the spike continued at a comparable rate during ripening, in the Fe-deficient variant the Fe content of the spike remained at a status quo and all other organs showed a loss of Fe.

4.2 Fe isotope fractionation during vegetative growth

Iron in plants primarily moves to photosynthetically active organs like leaves, where chloroplasts and mitochondria consume the largest amounts of Fe (Jain and Connolly, 2013; López-Millán et al., 2016) as they are the crucial sites for plant photosynthesis and respiration. As particularly free Fe ions produce reactive oxygen species, like superoxide and hydroxyl radicals, Fe needs to be bound to chelators or incorporated into structures to prevent oxidative cell damage (Broadley et al., 2012). Storage and transport of Fe in plants happens by different chelators, such as phytosiderophores (PS), citrate and nicotianamine (NA) (Zhang et al., 2019). As strategy II plant wheat releases PS that chelate $Fe(III)$ in the rhizosphere. The $Fe(III)$-PS complexes are then imported into the plant root epidermis cells by specific transporter proteins (Curie et al., 2001; Schaaf et al., 2004; Takagi et al., 1984). Rellán-Álvarez et al. (2009) suggested that $Fe(III)$-citrate complexes are the dominant Fe transporters from root xylem to shoots, whereas NA is restricted to phloem transport of Fe (Curie et al., 2008). Although NA can chelate both $Fe(II)$ and $Fe(III)$, capillary electrophoresis results indicated that $Fe(II)$-NA complexes are kinetically more stable than $Fe(III)$-NA (von Wirén et al., 1999). Hence, NA complexes in the phloem are assumed to be predominantly $Fe(II)$-NA complexes (von Wirén et al., 1999). These changes in ligands during Fe translocation within plants induce Fe isotope fractionation. Different plant organs thus may present various Fe isotope compositions.

Indeed, we found that the newly formed spikes were enriched in light Fe isotopes at anthesis for both Fe-deficient and control variants (Fig. III-3). After root uptake, Fe can be accumulated in the discrimination center (DC) at the basal part of the shoot, from which Fe is translocated to the aboveground plant parts through both xylem and phloem to older and youngest leaves (Kobayashi et al., 2019; Tsukamoto et al., 2008). Subsequently, Fe is remobilized and translocated to the seeds through phloem loading. At anthesis, the spike has hence been fed by phloem loading with Fe(II)-NA. Moynier et al. (2013) confirmed that Fe isotope changes go along with changes in Fe chelating ligands where Fe(II)-NA (in the spike) was isotopically lighter than Fe(III)-citrate (in the stem) and Fe(III)-PS (in the roots).

It is possible that the wheat plants in the control variant used the reduction strategy in which case the reduction of Fe happened by the reductase in the plasma membrane of the root, followed by the translocation of Fe to shoots through the DC area along with valence and ligand changes. Possible evidence for reductive uptake of light Fe isotopes was provided by the δ^{56}Fe value of the whole plant, which showed a depletion in heavy Fe isotopes compared to the nutrient solution at anthesis (Fig. III-3). The leaves displayed heavier δ^{56}Fe values than those of the other plant organs at anthesis (Fig. III-3). This was on the one hand due to the fact that we mixed all leaves together and did not discriminate between younger, lighter leaves and older leaves, which are heavier due to prolonged translocation of isotopic lighter Fe from leaves to spikes. On the other hand, the δ^{56}Fe values in leaves could generally be heavier as a result of Fe isotope fractionation during Fe transport from DC to leaves through both xylem and phloem ways. Guelke et al. published two studies on bean (*Phaseolus vulgaris*) which confirmed that Fe in new young leaves evolved towards lighter and Fe in older leaves towards heavier compositions (Guelke-Stelling and von Blanckenburg, 2012; Guelke and Von Blanckenburg, 2007). At anthesis, wheat plants are still in

vegetative growth where the newly formed younger leaves could contribute disproportionally to the total amount of leaves and Fe translocation to younger leaves through Fe(II)-NA should be more active than the Fe(III)-citrate translocation in older leaves. With ongoing wheat growth, no new leaves are formed and the proportion of older and younger leaves changes. In the aging leaves Fe(III)-citrate played an increasingly dominating role and thus may have caused heavier Fe isotope signatures in leaves after anthesis. This was confirmed in the control variant by the δ^{56}Fe values in the leaves at post-anthesis and maturity, which were heavier than those at anthesis (Fig. III-3). Hence, the relative proportion of old and new leaves as well as the proportion of xylem and phloem Fe translocation will decide the final δ^{56}Fe values in leaves.

At anthesis, the wheat plants under Fe-deficient condition showed no significant differences compared to the control variant with the wheat roots being isotopically lighter than the nutrient solution, the spikes being enriched in the lightest Fe isotopic signature and the leaves displaying heavier δ^{56}Fe values. These results suggested that at anthesis wheat plant in both variants could prompt the acidification-reduction transport strategy (strategy I) resulting in a whole plant Fe isotope composition depleted in heavy isotopes. Moreover, considering the extreme difference of the Fe masses taken up at anthesis (1574 µg per pot in control vs. 640 µg per pot in Fe-deficient), which indicated the Fe concentration of plant organs appears to hardly influence on Fe isotope compositions.

4.3 Fe isotope fractionation during reproductive growth

Both at post-anthesis and full maturity, the newly-formed plant organs like grains were significantly enriched in lighter Fe isotopes compared to other plant organs (root, stem, leaf and husk) under the control condition, which was consistent with the result of wheat growth at anthesis (Fig. III-3). Conversely, under Fe-deficient condition, all plant organs showed a narrow range of

δ^{56}Fe values without significant difference at post-anthesis, while the spread in δ^{56}Fe values became larger at maturity, albeit not statistically significant due to the high variability of the samples (Fig. III-3). We therefore concluded that wheat plants under optimal nutrient supply may behave like strategy I plants and fractionate Fe either through reduction or ligand exchanges during Fe uptake and translocation. Conversely, after anthesis the Fe-deficiency triggered strategy-specific Fe uptake processes during the reproductive growth. This caused a change in the Fe-chelators distribution during Fe translocation, finally resulting in limited Fe isotope fractionation within different plant organs. The oligopeptide transporters (OPT) which take part in Fe transport in different plant tissues and were likely upregulated in response to Fe deficiency (Lubkowitz, 2011). Our results were in agreement with the recent research of Liu et al. (2019), who demonstrated that rice grown with sufficient Fe supply significantly fractionated Fe isotopes, while under Fe-deficiency the Fe isotope fractionation across of all rice plant organs after plant matured was limited. It should be noted that changes in the Fe isotope fractionation due to different Fe supplies only became evident at reproductive growth.

At post-anthesis and full maturity the δ^{56}Fe values of leaves and grains under control condition were significantly different compared to those growing under Fe-deficiency. The leaves in the control were enriched in heavier Fe isotopes at both stages. This was likely due to enhanced loading of isotopically lighter Fe(II)-NA to the spikes leaving behind heavier Fe in the leaves. Additionally, with aging leaves enriched in isotopically heavier Fe(III)-citrate through xylem loading (Kobayashi et al., 2019; Rellán-Álvarez et al., 2009). However, in response to Fe-deficiency, plants induce a series of processes including 1) a significant enhancement of secreted mugineic acid family phytosiderophores (MAs) into the rhizosphere, which chelated Fe and other divalent metals like Cu and Zn (Chaignon et al., 2002; Flemming and Trevors, 1989; Kobayashi

and Nishizawa, 2012; Ryan et al., 2013) and 2) a decreasing photosynthetic rate which damages chloroplast structures and modifies electron transport in both photosystem I and II processes (Briat et al., 2015). It is clear that MAs are strongly associated with Cu and Zn, as well as Fe (Ryan et al., 2013). The mechanism of their mobilization within plants could also have a strong overlap as the reported divalent metal transporters like IRT1 can transport various divalent metals, including Fe, Zn, Cu, Mn, Cd, Ni and Co (Guerinot, 2000; Korshunova et al., 1999; Nakanishi et al., 2006; Pedas et al., 2008). Although the relationship between Fe-chelating complexes and other metal translocation in plants under Fe-deficient condition is not totally understand (Briat et al., 2007b), it is possible that all metals can bond with chelators and compete with each other, which could cause poor mobility of Fe and even Fe retention. As lighter Fe isotopes diffuse faster than heavy isotopes (Rodushkin et al., 2004). Thus isotopically lighter Fe were preferential translocated to photosynthetically active organs like leaves. Furthermore, it is also worth noting that electron transport changes in photosystem I and II processes induced by Fe-deficiency in chloroplast definitely alter Fe oxidation state thus of isotope compositions (von Blanckenburg et al., 2009).

We further noticed that the significant discrepancies of Fe isotope ratios in grains under different Fe supplies. The grains under control condition displayed the lightest δ^{56}Fe value of all plant organs, which may be due to most Fe in the grain being translocated by lighter Fe(II)-NA through phloem loading from flag leaves and upper leaves as Fe is immobile in older and lower leaves at full maturity (Yoneyama et al., 2010). Correspondingly, the δ^{56}Fe values in leaves displayed the heaviest values (Fig. III-3). Whereas, plants kept taking up Fe from nutrient solution under Fe-deficiency (Fig. III-3), where Fe-PS complexarion may be expected to contributed more than Fe(II)-NA to wheat grains. Therefore, the grains under Fe-deficient condition displayed heavier δ^{56}Fe value than wheat growth under control condition.

In summary, Fe-deficiency reduced the whole plant Fe mass by 59% at vegetative growth. At reproductive growth, Fe mass fluxes map indicated different preferential Fe translocated ways under different Fe supply, where Fe-deficiency increased Fe uptake from the soil. Whereas, more Fe redistributed from roots to the shoots under control condition. Across of all wheat growth period, wheat (strategy II) under control condition continually utilized acidification-reduction transport strategy (strategy I) thus displaying strategy I like activities with increasingly lighter δ^{56}Fe values from older to younger plant parts. However, with serious shortage of Fe after anthesis, Fe-deficiency promote strategy-specific (strategy II) Fe uptake process during wheat reproductive growth, thus resulting in limited Fe isotope fractionation. This suggests that Fe isotope ratios can reflect both wheat growth conditions and ages.

Acknowledgements

IV

IRRIGATION EFFECTS ON IRON ISOTOPE FRACTIONATION AND MOBILIZATION IN LONG-TERM AGRICULTURAL RESEARCH TRIAL (THYROW, GERMANY)

Modified on the basis of the manuscript

Ying Xing, Bei Wu, Wulf Amelung, Kathlin Schweitzer, Anne E. Berns

Manuscript finalizing

1. Introduction

Water and nutrient availability are key environmental controls for plant growth and crop yields (Mon et al., 2016; Rathore et al., 2017; Wang et al., 2014). As an essential nutrient, iron (Fe) is required for plant respiration and photosynthesis, where it participates in electron transfer reactions through reversible redox reactions between Fe(II) and Fe(III) forms (Marschner, 1995; Weber et al., 2006). In particular, Fe is an important component of heme and Fe-S enzymes, which support electron transport in photosynthesis and energy metabolism (Briat et al., 2007a). Plants take up Fe from soil solution, into which Fe is released from the lithosphere by weathering of primary Fe-containing silicates and sulphide minerals (Cornell and Schwertmann, 2003) or from different secondary inorganic and organic pools, accumulated through pedogenesis and management (Colombo et al., 2014). In general, Fe-solubility is very low in well aerated soils at physiological optimal pH. There are two type of strategies by which plants may utilize Fe from soil (Kim and Guerinot, 2007). Strategy I plants acidify the rhizosphere and induce the production iron chelate reductase, which reduces chelated Fe(III) from soil solution to the more soluble Fe^{2+}, which is then taken up by transporter proteins through root plasmalemma. Strategy II plants like graminaceous crops of maize, barley and wheat, excrete high-affinity complexing agents, so-called phytosiderophores (PS), which form organic Fe(III)-PS complexes that are taken up by specific transporters (Curie et al., 2001; Hell and Stephan, 2003; Römheld and Marschner, 1986; Schaaf et al., 2004). As variations of valence states of Fe within the soil-plant system can induce Fe isotope fractionations between the reactants and the products, these plants often exhibit differed Fe isotope compositions from the soil where they grow, thus also leaving behind a fingerprint on the soil's Fe isotope composition. In addition, Fe isotope compositions of plants may also depend on the

growth conditions and their growing stages (Guelke-Stelling and von Blanckenburg, 2012; Kiczka et al., 2010).

Apart from plant growth and harvest, changes in soil properties, e.g. induced by agricultural management, may potentially alter the Fe isotope composition of soil and thus of the plants. Particularly irrigation management could affect soil Fe dynamics significantly, as it influences the diffusion of O_2 in soil (Skopp et al., 1990), and thus Fe availability. It seems reasonable to assume that enhanced water contents enhances the reductive dissolution of Fe minerals. This released Fe(II) can be transported through advective and diffusive processed until it is re-precipitated as secondary Fe(III) (hydr)oxides (Wiederhold et al., 2006). However, any Fe dissolution and leaching processes frequently go along with Fe isotope fractionation, releasing light Fe isotopes first and leaving behind the relative heavier Fe isotopic counterparts (Wiederhold et al., 2006; Wu et al., 2019; Wu et al., 2010).

Over the last two decades, studies of tracing stable Fe isotope variations in environment have markedly increased (Beard et al., 1999; Garnier et al., 2017; Kavner et al., 2005; Liu et al., 2014). Most studies showed that oxidized Fe species were isotopically heavier than their reduced counterparts in soil (Anbar et al., 2005; Dideriksen et al., 2008; Wu et al., 2019). Also, Fe uptake and transformation within plants can generate Fe isotope fractionation, with strategy I plants tending to enrich light Fe isotopes and strategy II plants either enriching light or heavy Fe isotopes depending on growth condition (Guelke-Stelling and von Blanckenburg, 2012; Guelke and Von Blanckenburg, 2007; Kiczka et al., 2010).

Despite these potentials of using the Fe isotope signatures for tracking the fate of Fe in soil-plant systems, there are currently only two studies we are aware of that related to the fate of Fe in

agricultural soils, and both refer to rice. By using pot experiments, Arnold et al. (2015) concluded that the aboveground organs of rice were isotopically lighter than in bulk soil and soil leachates, suggesting possible changes in the redox state of Fe during uptake and translocation processes. Garnier et al. (2017) finally demonstrated for a paddy soil that Fe uptake by roots more likely originated from Fe plaques on the root surface rather than from direct uptake of the plant available Fe in soil (0.5 M HCl extracted). We could not find any information, to what extend different soil moisture regimes influence redox reactions and the Fe dynamics in other cropping systems, which renders it difficult to transfer the above-mentioned findings to other ecosystems. To answer this question, we investigated the $\delta^{56}Fe$ signatures in soils and plants from the long-term "Static Irrigation and Fertilization agricultural Experiment" station in Thyrow, Germany, where graminaceous strategy II plants have been grown in a Retisol soil with and without irrigation for 50 years.

2. Material and Methods

2.1 Field site

The field site is located in an agricultural area near Thyrow (52°15 N, 13°23 E, 44 m a.s.l), 20 km southwest of Berlin (Germany). The site has a mean annual precipitation of 510 mm and a mean annual temperature of 9.2 °C (standard reference period 1981 – 2010). The dominant soil is a Retisol (IUSS Working Group WRB, 2015) (Deckers and Nachtergaele, 1998; Schweitzer and Hierath, 2010). The investigated field trial was established in 1969, as a long-term two factorial "Static Irrigation and Fertilization Experiment" (Thy_D1) (Ellmer et al., 2000; Trost et al., 2014), where the two irrigation treatments ("No irrigation" (a1), "Irrigation" (a2)) are combined with four treatments with mineral N and straw application ("N0 + Straw" (b1), "Low N + straw" (b2), "Medium N + straw" (b3), "Medium N, without straw" (b4)). Straw has been incorporated after

cereal crops in two years of the five year crop rotation. The eight treatments are arranged in a non-randomized standard control design. The three plots within one treatment are considered as field replicates (Appendix B, Fig.B1). The irrigation occurred by a controlled sprinkler system (BEREST) by which the irrigation is calculated according to the plant growth stage, the actual soil water content in the rooted zone and the potential evapotranspiration (Schirach et al., 1988). On average, the irrigated plots received a yearly irrigation of 98.6 mm, i.e. almost 20% more than the mean annual rainfall of 510 mm, applied during the main growing season from March to August (Trost et al., 2014). The experiment runs with a regular crop rotation of cooksfood *(Dactylis glomerata* L*.),* potatoes *(Solanum tuberosum* L*.),* winter wheat *(Triticum aestivum* L*),* rapeseed *(Brassica napus* L*),* and winter rye *(Secale cereale* L*.).* Every crop is grown every year. More detailed information about this field site can be found in the work of Ellmer et al. (2000).

In the present study we only investigated plots of "No irrigation Medium N + straw" and "irrigation Medium N + straw" in the field where winter wheat was grown in 2017 (Appendix B, Fig. B1).

2.2 Soil and plant sampling

Soil cores were sampled in April 2016 with a soil auger of 6-cm inner diameter according to the current standard for the German Inventory of Agriculture, allowing for simultaneous determination of bulk density (Bauke et al., 2018; Walter et al., 2016). Each core was drilled to a depth of 100 cm and divided into seven depth intervals: 0-24 cm, 24-30 cm, 30-40 cm, 40-50 cm, 50-59 cm, 59-70 cm, and 70-100 cm. Three soil cores were taken in each plot and the respective intervals of the same depth were pooled on-site. All soil samples were freeze-dried (CHRIST® Beta1-8 LDplus, Germany) and sieved to 2 mm. More details on soil sampling, pH analysis, P, C and N contents, water content and bulk density can be found in Bauke et al. (2018).

Plants of winter wheat were sampled at three different locations of each monitoring plot in mid-June 2017 at growth stage of anthesis. Samples were combined into one composite sample per plot and immediately stored in a box with dry ice. In the laboratory, plant samples were washed with Milli-Q water (18.2 MΩ cm, Millipore, Germany), separated into roots, stems, leaves and spikes, then freeze-dried. The plant organs were ground in a custom-made ball mill (Collomix Viba 330, Collomix GmbH, Germany) using metal-free tungsten carbide milling balls.

2.3 Sample digestion and Fe concentration determination

Soil and plant samples were precisely weighed and digested in a pressurized microwave assisted digestion system (turboWAVE®1500, MLS GmbH, Germany) with ultrapure HNO_3 (68%) and H_2O_2 (30%). The reaction chamber was pressurized with N_2-atmosphere and then heated stepwise up to 220 °C and held for 30 to 40 min. After digestion, all digests were transferred to 15 mL centrifuge tubes and then centrifuged at $5000 \times g$ for 10 min (Heraeus Primo, Thermo Scientific, USA). Fe concentrations in the clear supernatants were determined by inductively coupled plasma mass spectrometry (ICP-MS, Agilent 7900, Agilent, Germany).

2.4 Extraction of plant-available Fe

The extraction method with 0.5 M HCl for the plant-available Fe pool in soil was adapted from Guelke et al. (2010), which avoids extraction-induced isotope fractionation. Thus, 300 mg of each soil sample were accurately weighed into 50 mL falcon tubes with 30 mL 0.5 M HCl. The mixture samples were placed into an end-over-end shaker (at a rotation ratio of 11 rpm) (REAX 20, Heidolph, Germany) at room temperature for 24h before being centrifuged at $5000 \times g$, for 15 min. The supernatant was then filtered through a 0.45 μm PTFE membrane filter, followed by adding 2 mL H_2O_2 (30%) to oxidize organic matter (Emmanuel et al., 2005).

2.5 Fe purification

The separation of the Fe from the matrix elements was carried out in a custom-made laminar flow fume hood with particle filters (High-Efficiency Particulate Air H14, AS Luftfilter, Germany). The supernatant of the digests and the 0.5 M HCl extracts were evaporated to dryness in acid-cleaned Teflon beakers (Savillex, Eden Prairie, USA) on a hotplate at 85 °C. Subsequently, the dried materials were re-dissolved in 2.0 mL of 6 M distilled ultrapure HCl and the Fe concentrations were analyzed by ICP-MS to verify that there was no Fe loss during evaporation. Iron purification was performed using anion exchange chromatography resins (Bio-Rad AG1-X4, 200-400 mesh) (Dauphas et al., 2004). Aliquots of the samples containing around 10 µg Fe were loaded onto the resin. Matrix elements were stepwise eluted with 6 M HCl. Followed by elution of Fe with 0.05 M HCl, complete separation of Fe from Zn was obtained by eluting Fe with 1.5 M HCl and Zn with 0.05 M HCl for plant samples. The matrix and Fe eluates were dried down in Savillex® beakers on a hotplate at 85 °C, and then re-dissolved in 2.0 mL 0.3 M ultrapure HNO_3. Quantitative Fe recovery (>95%) and removal of matrix elements during Fe separation was validated by Fe concentration measurements by ICP-MS. This is important to avoid artificial isotope fractionation and matrix effects during isotope measurement (Anbar et al., 2000). A solution blank and a dissolved sample of Fe isotope standard IRMM-524a were also processed through the columns together with the samples. The results of Fe isotope analysis in samples were expressed using IRMM-014 as recommended by (Dauphas et al., 2017).

2.6 **Fe isotope composition measurements**

The isotopic composition was determined by multi-collector inductively coupled plasma mass spectrometry (MC-ICP-MS, Nu Plasma II, Nu Instruments Ltd, UK) by means of a high-mass resolution mode with a mass resolving power (Rp $_{5,\ 95\%}$) of > 8000 at an ion beam transmission of 10%. A membrane desolvating nebulizer (Aridus II, Teledyne Cetac, USA) was used to minimize

argide interferences (ArN^+, ArO^+, $ArOH^+$) by reducing the solvent loading to the plasma and achieving better resolved Fe isotope peaks. To correct instrumental mass bias, a standard-sample-standard bracketing method was applied by using the Fe isotopic reference material IRMM-524a with a matched Fe concentration to the samples (Dauphas et al., 2009; Schoenberg and von Blanckenburg, 2005). The results of Fe isotope analysis in samples were expressed using IRMM-014 as the standard:

$$\delta^{56}Fe(‰) = \left[\frac{\left({}^{56}Fe \big/ {}^{54}Fe \right)_{\text{Sample}}}{\left({}^{56}Fe \big/ {}^{54}Fe \right)_{\text{IRMM}-014}} - 1 \right] \times 1000$$

We achieved a precision of $\pm$ 0.08 ‰ (2SD) for the δ^{56}Fe and $\pm$ 0.12 ‰ for δ^{57}Fe, respectively, obtained from long term repeated measurements of the standard IRMM-524a during the analytical sessions. The measured δ^{56}Fe and δ^{57}Fe values of each measurement session for all samples were plotted against each other and were found to follow the theoretical mass-dependent fractionation law (Appendix B; Fig. B2), indicating the absence of mass-independent isotope fractionation during the analytical sessions. For each sample, the isotopic composition was measured at least three times with some measurements being repeated in different sessions.

A mass balance approach was used to determine the Fe isotope compositions in the total plant and aboveground plant organs (without the roots) that was calculated with the following equation (Kiczka et al., 2010):

$$\delta^{56}Fe_{plant} = \frac{\sum_i m_i c_i \delta^{56}Fe_i}{\sum_i m_i c_i}$$

Where i symbolizes the different plant parts (root, stem, leaf, spike/husk and grain), m the plant dry mass, c the Fe concentration, and $\delta^{56}Fe_i$ the isotoratiopic composition of plant organs i.

2.7 Statistical analyses

Statistical analyses were performed in SigmaPlot 14.0 (Systat software Inc., San José, USA). A paired t-test was performed for the data on Fe concentration values and Fe isotope signatures for the two irrigation treatments within soil profiles. Normality test was confirmed by Shapiro-Wilk's test (P<0.05). If significant differences occurred, we used a Fisher's LSD test for post-hoc separation of means (P < 0.05).

3. Results and Discussions

3.1 Fe concentrations and stocks in the bulk soil

The Fe concentrations in bulk soil (Fe_{bulk}) over the soil depth of 0-59 were relatively uniform and ranged from 3223 to 4438 mg kg^{-1} without pronounced differences between soil horizons (Table IV-1; Appendix B, Fig. B3). In the deeper soil below 59 cm, the Fe_{bulk} concentrations increased with maxima of 12084 mg kg^{-1} and 13082 mg kg^{-1} at 70-100 cm depth in irrigated and non-irrigated plots, respectively.

Due to both the higher Fe concentrations and bulk densities, the Fe stocks per 10 cm depth interval were significantly larger below 59 cm soil depth than in the upper soil horizons. Largest Fe stocks were found at the depth of 70-100 cm with 67.0 t ha^{-1} and 72.6 t ha^{-1} in irrigated and non-irrigated plots, respectively (Table IV-1).

The irrigated plots had consistently lower Fe concentrations and stocks than the non-irrigated plots, especially in the soil layers between 59-70 cm and 70-100 cm. The maximum difference in Fe concentration between the irrigation and non-irrigation treatment was found in the soil layer of 59 to 70 cm, with a mean difference of 2664 mg kg^{-1} soil. In this depth interval, the Fe stocks were lower by 31% compared with non-irrigation treatment. In total, after 50 years of irrigation, the

irrigated plots contained 15.4 t ha^{-1} less Fe over the investigated depth of 100 cm, which corresponds to a yearly loss of 308 kg Fe ha^{-1} (Table IV-1). It is noteworthy that the calculated Fe loss of 15.4 t ha^{-1} representing >10% of the total Fe stock. This implied that irrigation would remove all Fe from the soil within 50 years, which seems unlikely. In addition, it was visible that some redoximorphic features were in the E/Btg and Btg/E horizon. As the study site being of the driest areas in Germany with hardly a meaningful water percolation into the subsoil. Therefore, it was conclude that soil pedogenesis would play a major role, which changed Fe concentrations and stocks in the subsoil layers for both irrigated and non-irrigated plots rather than irrigation treatment.
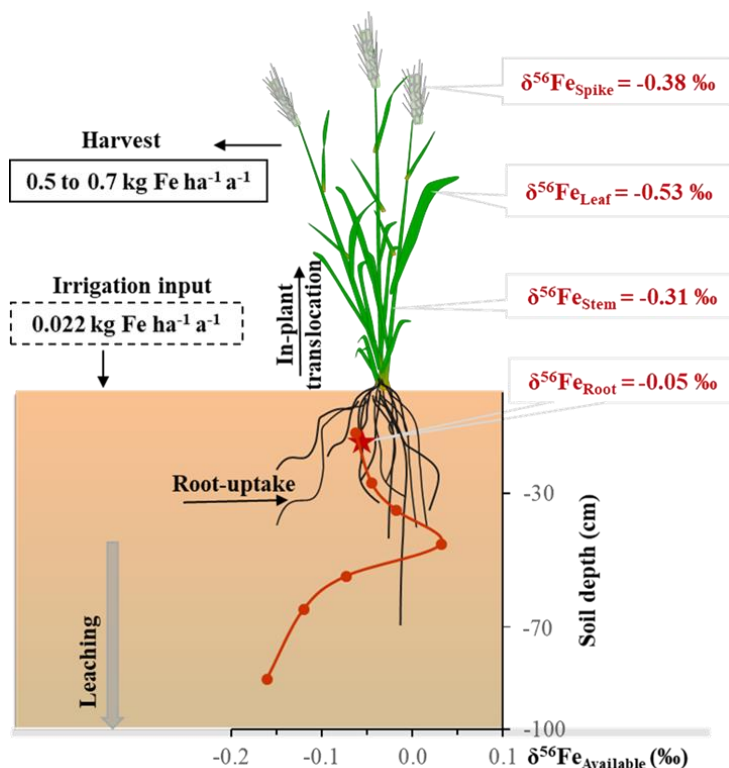
Fig. IV-1: Scheme of annual irrigation effect on Fe cycle in sandy Retisol in Thyrow. Values in box with black dashed lines are Fe input (irrigation input), with full lines are Fe losses (plant harvest and leaching). Fe isotope compositions of the plant available Fe pool ($\delta^{56}Fe_{avail}$) are indicated by a red line along the soil profile. The Fe isotope composition of different plant organs (Fe$_{plant organss}$, red font) is shown in the grey boxes.

The Fe concentrations in the bulk soil at this long-term experiment trial in Thyrow were relatively low compared to average Fe concentrations of 20000 to 40000 mg kg^{-1} found in other cultivated soils (Colombo et al., 2014; Cornell and Schwertmann, 2003). We attribute this difference to the low contents of clay and silt as well as of soil organic matter of the sandy soil in Thyrow (Kiem and Kögel-Knabner, 2002). The coarse texture suggests that this soil lacks silicates as a primary source of Fe, and that it has a low capacity for Fe to accumulate in the soil organic pool, both explaining the small metal (Fe) stocks in general (Bauke et al., 2018; Buol et al., 2011).

The higher Fe concentrations below a soil depth of 59 cm are likely due to two reasons. On the one hand the E/Btg horizon likely indicates a shift in parent material from a periglacial sand to a loam derived from glacial till which characterized by higher Fe contents compared with the overlaying younger sands (Evans and Benn, 2014). On the other hand, as also indicated by Bauke et al. (2018), the soil layers corresponding to a Bt horizons received illuvial clay and thus also Fe inputs from the A and E horizons above.

The lower Fe stocks in the topsoil of the irrigated plots compared with that of the non-irrigated plots can be explained by mass balance in some extent, which is influenced by vertical Fe transport and/or by higher plant Fe uptake due to higher crop yields with the better water supply (Appendix B, Table B1). Fe input with the irrigation water has only marginal impact. It amounts to 1.1 kg ha^{-1} Fe only, taking the measured, extremely low Fe concentration of 23 ug L^{-1} in the irrigation water

and the average amounts of irrigation water over 50 years, which accounts for 0.022 kg ha^{-1} Fe input per year (Fig. IV-1; Appendix B, Table B3).

Fe export by harvested biomass was calculated using mean Fe concentration in plant organs of 50-70 mg kg^{-1} and an average biomass of straw and yields (Appendix B, Table B1) in our field, which is similar with the data calculated by Shenker and Chen (2005) of 10,000 kg per hectare. Fe loss via harvest thus accounts for only $25 - 35$ kg ha^{-1} over 50 years (Fig. IV-1). Sandy soils with low sorption and water holding capacity also easily leach nutrients from topsoil to subsoil. Ellmer and Baumecker (2005) reported that nutrients like nitrogen, phosphorus, potassium, and magnesium and soil organic carbon were more depleted in the irrigated plots. While a significant soluble transport of Fe is unlikely at the given amount of irrigation of 98.6 mm and pH (H_2O) values of $6.1 - 7.2$ in the irrigated plots. It is assumed that a small portion of Fe loss in the topsoil may due to Fe lost in (nano) particulate form (Hartemink, 2016). Gottselig et al. (2017) gave the evidence, that similarly surface waters contained more than half of its Fe in (nano) particulate form. Although we calculated 15.4 t ha^{-1} less Fe over the investigated depth of 100 cm in the irrigated plots, the significant reduction in Fe stocks mainly indicated soil pedogenesis rather than irrigation treatment.

Table IV-1: Chemical soil properties, Fe concentrations and δ^{56}Fe values in the bulk soil of the long-term "Irrigation and fertilization experiment" in Thyrow; represented as means of three field replicates.

Soil management	Depth cm	Horizon [KA5]	Horizon [WRB]	Bulk density[b] [g cm^{-3}]	Gravimetric water content[b] [%]	pH[b] (H$_2$O)	pH[b] (CaCl$_2$)	Fe$_{bulk}$[a] [mg kg^{-1}]	Fe stock[a] [t ha^{-1}]	δ^{56}Fe[a] ‰
with irrigation	0-24	Ap1	Ap1	1.5	6.6	7.2	6.2	3345 ± 25	11.9 ± 0.1	-0.10 ± 0.04
	24-30	Ap2	Ap2	1.7	6.8	7.4	6.5	3257 ± 158	3.4 ± 0.2	-0.11 ± 0.11
	30-40	Bv-Ael1[1]	EBw1[1]	1.7	7.7	7.3	6.4	3223 ± 149	5.5 ± 0.1	-0.01 ± 0.02
	40-50	Bv-Ael2[2]	EBw2[2]	1.8	8.7	7.3	6.3	3496 ± 165	6.2 ± 0.3	-0.02 ± 0.07
	50-59	Bv-Ael2	EBw2[3]	1.9	9.0	7.0	6.0	4066 ± 318	6.8 ± 0.8	-0.04 ± 0.06
	59-70	Bt+Ael[4]	E/Btg[3]	1.9	10.1	6.3	5.4	6098 ± 984	12.9 ± 2.4	-0.02 ± 0.03
	70-100	Ael+Bt	Btg/E	1.9	12.2	6.1	5.0	12084 ± 256	67.0 ± 2.3	-0.06 ± 0.04
without irrigation	0-24	Ap1	Ap1	1.4	6.4	6.7	5.9	3791 ± 186	13.1 ± 0.7	-0.03 ± 0.03
	24-30	Ap2	Ap2	1.7	7.2	6.6	5.7	3472 ± 113	3.5 ± 0.1	0.01 ± 0.03
	30-40	Bv-Ael1[1]	EBw1[1]	1.8	8.3	6.5	5.4	3635 ± 186	6.5 ± 0.5	0.01 ± 0.08
	40-50	Bv-Ael2[2]	EBw2[2]	1.9	8.6	6.1	4.8	3734 ± 283	7.0 ± 0.6	0.06 ± 0.04
	50-59	Bv-Ael2	EBw2[1]	2.0	9.1	5.8	4.5	4438 ± 492	7.8 ± 0.8	0.01 ± 0.03
	59-70	Bt+Ael	E/Bt	1.9	10.5	5.9	4.7	8762 ±1399	18.6 ± 4.6	0.00 ± 0.02
	70-100	Ael+Bt	Bt/E	1.9	12.1	6.5	5.5	13082 ± 174	72.6 ± 1.1	-0.07 ± 0.02

[a] Given as the mean ± standard error ; [b] cited from (Bauke et al., 2018). [1] Ael (=E) horizon had been developed before secondary weathering and formation of Bw horizon has taken place; [2] separated by depth increment only; [3] presence of few Mn concretions; [4] interfingering of Ael into Bt, annotated with + sign in the German soil classification system (KA5).

3.2 Fe isotope compositions in the bulk soil

Despite the large range of Fe concentrations in bulk soil, all bulk soil samples exhibited relatively uniform range of isotopic compositions, with δ^{56}Fe-values from -0.11 to +0.06 ‰ relative to IRMM-014 (Table IV-1), and with a tendency of lowest values in the topsoil of the irrigated plots and in the Btg/E horizons at 70-100 cm depth.

The narrow range of isotope compositions are in agreement with (Guelke et al., 2010) who found only small variations in bulk Fe isotope compositions of -0.04 ± 0.06 ‰ for Luvisol soils in the Ap horizon. We therefore conclude that clay illuviation during the formation of the Retisol did not go along with significant Fe isotope fractionation, reflecting that clay particles rather than dissolved Fe ions or secondary precipitated iron oxides were translocated during pedogenesis, and/or that the translocated clay minerals contained relatively little structural Fe compared to the overall Fe reservoir in the bulk soil. Hence, the Fe isotope values in the investigated soils of our current study rather reflect the parent material of periglacial sand than changes through pedogenesis and management.

In addition, irrigation induced limited water transport in the soil profiles did also not result in significant Fe isotope fractionation. This is likely due to the fact that dissolved Fe, which is usually isotopically light (Wu et al., 2019), is not occurring in significant amounts at ambient pH values, further supporting our hypothesis that Fe transport was mainly in particulate forms in the topsoil profiles.

Nevertheless, in our current case of a well-drained sandy soil, the E_h typically lies in the range of +300 to +500 mV under aerobic conditions (Macías and Arbestain, 2010). With the prevailing pH range of 6.1 to 7.2 (Table IV-1), the dominant Fe-species in the soil is most likely $Fe(OH)_3$ across

the whole investigated 100 cm depth in the both irrigated and non-irrigated treatment, thus lacking major redox transformations between Fe(II) and Fe(III), and not producing pronounced vertical δ^{56}Fe changes. Only in the case of irrigation, reduced E_h values below +150 mV might occur at temporary pH of 6, in this case $Fe(II)_{aq}$ can become the dominant species in soils with low organic carbon content, which then have possibilities to change the Fe isotope compositions during the short time of elevated soil moisture (Macías and Arbestain, 2010). Yet, the mass fraction of available Fe that might be influenced temporarily by such processes is not large enough to leave a fingerprint on the total Fe isotope composition of the bulk soil. Hence, we determined plant-available Fe contents.

3.3 Fe concentrations in the soil-plant system

The concentrations of 0.5 M HCl-extractable, plant-available Fe (Fe_{avail}) in soil significantly varied with soil depth (Fig. IV-2): Fe_{avail} decreased from the Ap horizon down to a depth of 50 cm and increased again up to 1504 mg kg^{-1} and 1473 mg kg^{-1} in the depth of 59 to 70 cm and of 70 to 100 cm for the irrigated and non-irrigated plots, respectively. This gain in Fe_{avail} followed the overall increase in bulk soil Fe contents in that depths (Fe_{bulk}, Table IV-1).

Comparing "Irrigation" with "No Irrigation", the irrigated plots had, on average, higher Fe_{avail} concentrations than the non-irrigated plots in the top 40 cm of soil, but lower Fe_{avail} concentrations at 59 to 70 cm soil depth (Fig. IV-2). In the lowermost soil horizons, Fe_{avail} did not differ significantly between irrigated and non-irrigated plots.
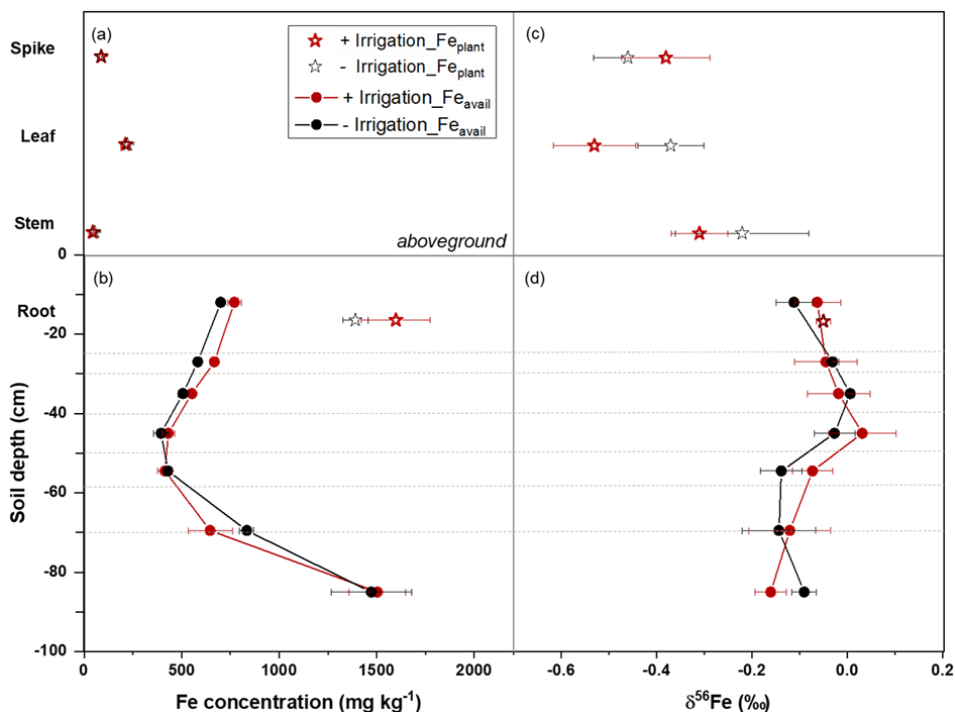
Fig. IV-2: (a) Fe concentration in plant organs (star), (b) Fe concentration in plant available pool (circle), (c) Fe isotope signatures in plant organs (star), (d) Fe isotope signatures in plant available pool (circle). The dotted lines visualize the sampled soil layers. Each data point represents three field replicates and their standard error. Note that the plant organs are not positioned on their heights.

Within the sampled soil profiles, the Fe_{avail} concentrations contributed between 10 to 23% to the bulk soil Fe concentration (Fe_{bulk}), with clear differences between soil layers and irrigation treatments (Fig. IV-3). In the topsoil at 0-24 cm depth, the highest Fe_{avail} / Fe_{bulk} ratios were found with values of 0.23 and 0.19 in irrigated and non-irrigated plots, respectively. Downwards along the soil profile, the ratios declined significantly in both treatments to a value of 0.10 to 59 cm soil depth. This trend was caused by decreasing Fe_{avail} concentrations with the depth, while those of

Fe_{bulk} remained fairly constant. Below the depth of 59 cm, in the E/Btg and Btg/E-horizons, the Fe_{avail} / Fe_{bulk} ratio increased again.
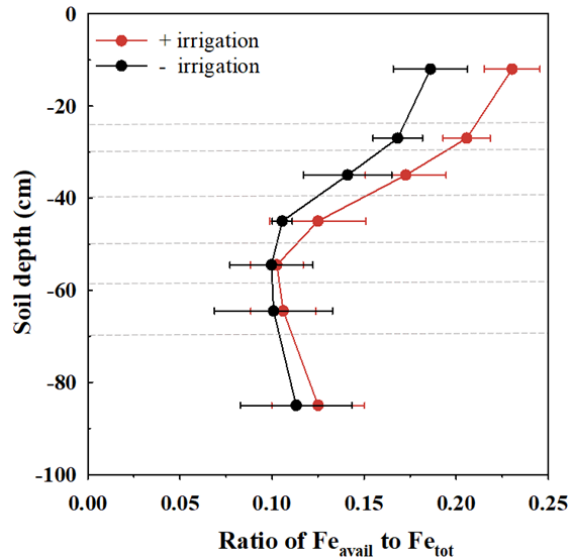
Fig. IV-3: Ratio of Fe_{avail} to bulk soil Fe concentration (Fe_{bulk}) in plots with and without irrigation in Thyrow. The dotted lines visualize the sampled soil layers. Each data point represents three field replicates and their standard error.

It is noteworthy that irrigated plots contained significantly higher portions of Fe_{avail} than their non-irrigated counterparts in the topsoil, additionally reflecting that irrigation mobilized plant-available Fe. One possible reason is that the biomass of the plant roots, which remains in the soil after crop harvest, was considerable larger in the irrigated plots than that in non-irrigated plots (Asseng et al., 1998). Fe in the roots continuously recycled as a source of plant-available Fe, contributing to a higher Fe concentration and a higher ratios of Fe_{avail} / Fe_{bulk} in the irrigated plots in the topsoil where the roots accumulate after 50 years.

The plant-available Fe concentration together with the Fe_{avail} / Fe_{bulk} ratios clearly displayed an effect of the soil horizon and irrigation on the plant-available Fe mobility. Apparently, the continuous supply of water combined with higher biological activity mobilized plant-available Fe in the Ap horizon under irrigation, despite the increase in pH (Table IV-1), while soil pedogenesis controlled both Fe_{avail} and Fe_{bulk} in the horizon below. At the depth below 59 cm in the E/Btg and Btg/E horizons, the absolutely highest concentrations of plant-available Fe together with increasing Fe_{avail} / Fe_{bulk} ratios were likely a result of the combination of higher Fe stocks and a prolonged period of elevated moisture in subsoil reflected also by some stagnic properties of the Bt horizon (Table IV-1).

Irrigation had no effect on the Fe concentrations in the analyzed wheat organs (Fig. IV-2), despite clear differences in Fe_{avail} concentrations and in Fe_{avail}/Fe_{bulkl} ratios in the topsoil (Fig. IV-2, Fig. IV-3). However, irrigation significantly increased crop yields by 38% from 3.27 t ha^{-1} to 4.51 t ha^{-1}, and increased straw biomass by 37% from 3.64 t ha^{-1} to 4.99 t ha^{-1} (Appendix B, Table B1). As a result, there was a higher Fe export by plants from irrigated plots, although the exact Fe concentrations of harvested biomass remain unknown for the duration of the long-term irrigation experiment.

Notably, there were significant differences in Fe concentrations between the plant organs (Fig. IV-2). In the aboveground plant organs, the leaves contained the highest Fe concentrations, followed by spikes and stems. Fe concentrations of the roots exceeded that of the aboveground organs by a factor of two or three. Maximum Fe concentrations were found in the wheat roots, even those of Fe_{avail} in the topsoil.

All plant organs except roots exhibited Fe concentrations within the range of 5 to 109 mg kg^{-1} typical for wheat (Çakmak et al., 2004). The very large Fe concentrations in roots exceeded those found in a former study of Silva et al. (2010) by a factor of four to eight. This was probably due to the presence of apoplastic iron accumulated as extracellular root Fe which can be mobilized to shoot as the plant became Fe deficient. In the aboveground organs Fe accumulated primarily in the leaves, because they are responsible for plant photosynthesis in which Fe is involved. Adamski et al. (2011) concluded that approximately 80% of Fe in plants is found in photosynthetic cells, where it is contained in Fe-bearing proteins like cytochromes and other heme molecules and is essential for the biosynthesis of chlorophyll and the construction of Fe-S clusters. Considering that our sampling time point was anthesis, the developing spikes are the sink for all nutrients until the maturity and show therefore elevated Fe concentrations.

On the basis of determined Fe concentrations in the plant organs, especially the high Fe concentrations in the root probably accumulated in the apoplast. In addition, less variations of Fe concentrations in both root and aboveground plant organs were found between the irrigation treatments, which was likely due to the fact that the pool size of the plant-available Fe in soil was considerably larger than that of the annual crop, thus providing sufficient Fe to the plants to conceal the difference in Fe_{avail} between the irrigation treatments. We conclude, therefore, that the wheat plants did not suffer from Fe deficit, but rather prevented the Fe uptake to a degree exceeding their needs. Halliwell and Gutteridge (1992) reported that plants generally tend to avoid high Fe concentrations in their cells in order to limit toxic effects due to the formation of hydroxyl radicals. Nevertheless, with larger plant biomass also Fe export by the plant was enhanced, and the increase in the available Fe content supports the hypothesis that plant-available Fe mobilization in the

topsoil occurred. This mobilization of plant-available Fe was enhanced by irrigation despite the pH (H_2O) increased to values ≥ 7.0.

3.4 Fe isotope compositions in the soil-plant system

All aboveground organs of wheat were enriched with lighter Fe isotopes by up to 0.48‰ compared with the isotope composition of Fe_{avail} in the topsoil (Fig. IV-2; Appendix B, Table B2). In contrast, the roots exhibited a Fe isotope composition similar to the average $\delta^{56}Fe$ values of Fe_{avail} in topsoil, showing values of -0.05‰ and -0.07‰ in irrigated and non-irrigated plots, respectively. Within the plant, the $\delta^{56}Fe$ values decreased from the roots via the stems and leaves, and partly even to the spikes, except for the spikes from the irrigated plots, which contained comparatively heavier Fe isotopes than the leaves (Fig. IV-2). Using mass balance calculations, we obtained an overall $\delta^{56}Fe$ value of -0.09‰ for the whole plant, indicating Fe isotope fractionation due to uptake of light Fe from the rhizosphere and Fe translocation within the wheat plants.

Wheat is a strategy II plant, which exudes the mugineic acid phytosiderophores (MAs) to acquire Fe from rhizosphere (Schaaf et al., 2004). Within the plant, Fe is transport from root epidermal cells to the xylem and then to the aboveground organs. Upon developing production organs, Fe is recirculated from leaves via phloem to flowers and seeds. During these processes, Fe is always in and varies its chelating forms. In the xylem of wheat Fe is present as Fe(III)-citrate, while in phloem as Fe-(NA) and Fe(III)-PS likely presenting in roots (Hell and Stephan, 2003; Kobayashi and Nishizawa, 2012). As changing chelating ligands may induce Fe isotope fractionation (Moynier et al., 2013), these organs thus present differed Fe isotope compositions. Indeed, in our study, we found that the wheat roots exhibited similar $\delta^{56}Fe$ values to the plant-available pool in the soil, while the aboveground organs were isotopically significantly lighter. The differences in

δ^{56}Fe values between roots and aboveground organs hinted at Fe isotope fractionation during Fe translocation within the plant. The δ values of the roots here with reflected the combined effect of both uptake into roots and export into the shoots. On the one hand, the δ^{56}Fe values in plant roots are the integrated result of Fe uptake, which includes adsorption, precipitation of enriching heavier Fe isotopes on root cortex, and reduction and transfer through plasma membrane into the root symplasm, which may then enrich the light Fe isotopes (Kiczka et al., 2010). On the other hand, however, lighter Fe was enriched in above-ground organs, so that overall the plant primarily acquired light Fe. Heavier δ^{56}Fe signatures in the roots must thus be a secondary effect of an increased preferred transport of light Fe from shoot to roots, thus leaving behind heavy Fe in the roots to a degree, which finally was not different from that found in soil (Fig. IV-1, Fig. IV-2). Nevertheless, here we were not able to differentiate between equilibrium effects and kinetically controlled fractionation processes of plant uptake and translocation, i.e., the assignment of different δ^{56}Fe values in plant organs to specific transporter systems may still warrant attention.

It is found that there were larger δ^{56}Fe$_{avail}$ values in the depth interval of 40 to 50 cm, but smaller δ^{56}Fe$_{avail}$ values at 70-100cm soil depth (Fig. IV-2; Appendix B, Table B3). The maximum difference among soil horizons was 0.2 delta units (Fig. IV-1, Fig. IV-2). This could lead us to conclude the wrong information of 15.4 t ha^{-1} Fe loss from the irrigated field, with isotopically light Fe preferentially leached into subsoil (Fekiacova et al., 2013; Wiederhold et al., 2007). Indeed, the Bt horizon at lower depth, was clearly enriched in light Fe isotopes, thus leaving behind the relative heavier δ^{56}Fe values at 40-50 cm soil depth. However, considering the research site being of the driest areas in Germany and limited water can be percolated to subsoil, the maximum difference of δ^{56}Fe values between 40 to 50 cm and 70 to 100 cm can not from irrigation treatment. The thousand years of soil pedogenesis should mainly take into considerstion.

As the Fe acquisition by crops hardly affected the overall mass balance of soil, even the preferred acquisition of light Fe by the crops did hardly alter the δ^{56}Fe signature of bulk soil. In this regard, the δ^{56}Fe depth profiles result from long-term pedogenesis with some influence on the δ^{56}Fe$_{avail}$ pool by irrigation management but not from crop selection and Fe removal with harvest. As lessivation during soil genesis mainly affects colloidal particles and less ion transport, we failed detecting significant changes in δ^{56}Fe$_{bulk}$ signals with depth, as outlined before. However, changes in the δ^{56}Fe$_{avail}$ values may be influenced by both altered redox-regimes upon irrigation practice and soil pedogenesis.

In summary, irrigation of the sandy arable soil for 50 years led to higher Fe$_{avail}$ concentrations than the non-irrigated plots in the top 40 cm of soil, but there were no changes in δ^{56}Fe values. Due to the research site being of the driest areas in Germany with hardly a meaningful water percolation, the maximum difference of δ^{56}Fe$_{avail}$ values between 40 to 50 cm and 70 to 100 cm was explained by the soil pedogenesis rather than irrigation treatment. Also the crops primarily utilized light Fe, though not to an extent that it effected overall Fe mass balances. Fe isotope fractionation inside the plants, however, re-increased the δ^{56}Fe isotope signatures of the roots, which finally exhibited a similar Fe isotope composition to the topsoil. Any loss of surface soil materials by wind or water erosion, for instance, may thus lead to a defined input of δ^{56}Fe values into other ecosystems, irrespectively whether this Fe is bound to minerals or left as rot debris in soil. Any loss of Fe with harvest or leaching, in contrast, will leave a lighter fingerprint in the food chain or hydrosphere, respectively.

Acknowledgements

V

FINAL DISCUSSION

1. SUMMARY OF THE RESEARCH OBJECTIVES

Iron (Fe) is the fourth most abundant element in the Earth's crust. As an essential nutrient, Fe is required for plant chloroplast photosynthesis and mitochondrial respiration, where it participates in electron transfer reactions through reversible redox reactions between Fe(II) and Fe(III) forms. Higher plants are known to develop at least two different strategies to acquire poorly bioavailable Fe from soil. Once Fe is absorbed by plant roots, it is translocated to the aboveground plant organs. Both Fe uptake and translocation within plants can generate Fe isotope fractionation (Arnold et al., 2015; Garnier et al., 2017; Liu et al., 2019). Thus, stable Fe isotope compositions in plant growing substrate as well as in different plant organs can be used to trace Fe mobilization processes.

In my work, I aimed at elucidating the role of Fe isotope signatures during plant Fe uptake and translocation. Firstly, I systematically reported the state of art on Fe isotope researches during Fe uptake and translocation in soil-plant system, following hypothesis that Fe availability is controlling plant growth, as many cropping systems in the world suffer from Fe-deficiency. Moreover, I tested the soil management of long-term irrigation effect on Fe dynamics in the soil-plant system, since irrigation changes soil moisture regimes, where redox conditions change and thus Fe speciation controls the degree of Fe isotope fractionation.

To achieve these aims, I adapted and applied a combination of different analytical methods for the characterization of Fe availability and cycling in soil-plant system. I used 0.5 M HCl extraction to determine the content of plant-available Fe pool containing water-soluble Fe, freely exchangeable Fe, organically sorbed/bound Fe and poorly crystalline Fe oxides. This method can avoid extraction-induced isotope fractionation (Guelke et al., 2010). In addition, I analyzed the stable Fe isotopic composition of the bulk soil Fe pool, the plant-available Fe pool and of different plant

organs by multi-collector ICP-MS. With respect to my research questions outlined in chapter I.3, I may now summarize the following results:

1) Can stable Fe isotopes be a valid tool to track Fe cycling in soil-plant system?

The cycling of Fe is often closely linked with that of carbon, nitrogen, phosphorus and manganese. Therefore, alterations in the Fe cycle may be indicative of concurrent overall changes in the biogeochemistry of terrestrial and aquatic ecosystems. Biogeochemical processes taking part in the Fe cycle frequently fractionate stable Fe isotopes, leaving soil, plant and other compartments of the ecosystems with varied Fe isotopic signatures. I performed a literature review to answer particularly the question of Fe isotopes as tracers to track Fe cycling in soil-plant system. The meta-analyses showed that depending on the Fe speciation and concentration present in the growth medium, plants can adapt their uptake strategy for Fe. Plants of the strategy I type especially take up light Fe isotopes, while strategy II plants fractionate less towards light isotopes. Above-ground tissues usually show even lighter Fe isotope signatures than the roots, with flowers (δ^{56}Fe: -2.15 to -0.23‰) being isotopically the lightest. I found that all reported strategy I plants consistently enriched in light Fe isotopes under all growth conditions. Strategy II plants, however, could be enriched in either light or heavy Fe isotopes, depending on the growth conditions. Depending on the Fe speciation and concentration present in the growth medium, some strategy II plants like rice are able to adapt their uptake strategy as they also possess ferrous transporters and are hence also able to take up Fe(II) ions. However, there is no systematic research on the influence of Fe deficiency on Fe isotope fractionation in plants. In addition, I found that researches are missing on how Fe isotope compositions changes are induced by agricultural management in the soil-plant system. Nevertheless, it is still unclear to what extent Fe availabilities and soil managements influence the Fe dynamics and thus of Fe isotope compositions in the soil-plant system.

2) Do different Fe availabilities affect Fe isotope signatures in wheat?

Iron (Fe) is an essential nutrient for plant growth and proliferation. Higher plants have developed two distinct strategies (strategy I and strategy II) to acquire Fe from the rhizosphere. However, the ongoing Fe uptake depends on the Fe uptake strategy as well as on the Fe availability in soils. Here, Fe isotopes have been used as indicators and I hypothesized that Fe-deficiency induces changes in the Fe specific uptake strategy, thus affecting Fe isotope compositions during uptake and subsequent translocation processes. To test this hypothesis, I cultivated summer wheat (*Triticum aestivum* L.) under Fe-sufficient (control, 0.0896 mM Fe-EDTA) and deficient (Fe-deficient, 0.0022 mM Fe-EDTA) conditions in a controlled greenhouse experiment, and analyzed Fe concentrations as well as δ^{56}Fe isotope compositions in roots, stems, leaves, and spikes at different growth stages (vegetative growth and reproductive growths). The results showed that Fe-deficiency reduced the whole plant Fe mass by 59% at vegetative growth. At reproductive growth, Fe mass fluxes map indicated different preferential Fe translocated ways under different Fe supply, where Fe-deficiency increased Fe uptake from the soil. Whereas, more Fe redistributed from roots to the shoots under control condition. Across of all wheat growth period, wheat (strategy II) under control condition continually utilized acidification-reduction transport strategy (strategy I), thus displaying strategy I like activities with increasingly lighter δ^{56}Fe values from older to younger plant parts. However, with serious shortage of Fe after anthesis, Fe-deficiency promote strategy-specific (strategy II) Fe uptake process during wheat reproductive growth, thus resulting in limited Fe isotope fractionation. This suggests that Fe isotope ratios can reflect both wheat growth conditions and ages.

3) Can δ^{56}Fe values of soil and plant provide information on agricultural soil management like irrigation?

The Fe isotopes signature can be used to track the biogeochemical cycling of Fe in terrestrial environments. I hypothesized that long-term irrigation in arable land results in a depletion of light Fe in soil-plant systems. I thus determined the Fe stocks and Fe isotopic compositions in soil profiles as well as in wheat plant organs in the long-term "Static Irrigation and Fertilization Experiment" at Thyrow, Germany. The results showed that fifty years of irrigation resulted in higher Fe_{avail} concentrations than the non-irrigated plots in the top 40 cm of soil, but there were no changes in $\delta^{56}Fe$ values. Due to the research site being of the driest areas in Germany with hardly a meaningful water percolation, the maximum difference of $\delta^{56}Fe_{avail}$ values between 40 to 50 cm and 70 to 100 cm was explained by the soil pedogenesis rather than irrigation treatment. The wheat plants grown in both irrigated and non-irrigated plots were slightly enriched in light Fe isotopes, exhibiting similar $\delta^{56}Fe$ values to those of the respective topsoil. I concluded that the overall $\delta^{56}Fe$ signature of wheat was regulated by plant-homeostasis and specific on-site soil characteristics, whereas irrigation had little if any significant effects on the Fe isotopes in the crops.

2. SYNTHESIS AND OUTLOOK

As the results outlined above indicate that Fe availabilities as well as soil managements have effects on Fe cycling in the soil-plant system, I will now conduct an evaluation to which extent both can be relevant for Fe acquisition from the growing substrates. As the range of conditions and field sites included in this work is rather limited, the final part of this discussion will be extended to $\delta^{56}Fe$ data provided in the literature.

2.1 Utilization of Fe resources from the soil

As mentioned in introduction, plant Fe deficiency is a problem of Fe solubility and not of abundance. Low Fe availability in soil especially happens in alkali and calcareous soil with high

pH and high bicarbonate concentrations (Manthey et al., 1994). It is considered that over one-third of soil in the world is Fe-deficient. To deal with the limited availability of Fe in soil, plants have evolved typical "Strategy I" and "Strategy II" to obtain Fe from the soil (Marschner, 1995). The efficiency of these two strategies widely varies among plant species, which give an explanation of the well-know phenomena of large variations in plants resistance to Fe-deficiency. Strategy I plants like many agronomic plants of apple, peach, soybean and grape, are sensitive to Fe deficiency. In contrast, strategy II species including barley, maize and wheat are more tolerant to Fe deficiency (Römheld, 1991; Römheld and Marschner, 1986; Welch and Shuman, 1995). It is generally assumed that the chelation-based strategy (Strategy II) is more efficient than the sequential acidification-reduction-transport strategy (Strategy I) and allows graminaceous plants to survive under more drastic Fe-deficient conditions (Mori, 1999). Except for plant itself, proper soil management strategies could also be used to secure sufficient Fe supply. Fe fertilization and water regulation can improve Fe use efficiency in Fe-deficient soils.

As reported in chapter IV, the pool size of the plant-available Fe in soil was considerably larger than that of the annual crop needs, thus it is supposed that the wheat plants did not suffered from Fe deficit at the moment. However, with the increasing of soil nutrient loss through plant harvest and the coupling soil erosion, the soil will face Fe deficiency someday. Therefore, the above mentioned soil management strategies can be adapted to improve Fe supply for plant needs. Nevertheless, it is difficult to apply inorganic Fe to the field as it can quickly convert to unavailable $Fe(III)$ forms and be inaccessible to plants. A typical example is that adding $FeSO_4$ to calcareous soil will quickly induce the reaction with $CaCO_3$ and with the presence of oxygen to form Fe oxides, which are less available for plant uptake (Vempati and Loeppert, 1988). In soil with low $CaCO_3$ content, plant Fe-chlorosis may be alleviated for a limited period of time by applying

inorganic Fe fertilizer. It is reported by Mathers (1970), who applied 560 kg/ha of $FeSO_4$ to sandy loam soil (2.4 - 4.0% $CaCO_3$, pH 8.4), which supports sorghum (*Sorghum bcolor* L. Moench) plants with sufficient Fe supply for only one growth period. Soil applied with organic Fe chelates such as Fe-EDTA has even shown better results than inorganic Fe salts. In chapter III of the pot experiment, two modified Hoagland solutions were used for the Fe-deficient (0.0022 mM Fe-EDTA) and the control (0.0896 mM in) treatments. During the whole plant growth period, plants with sufficient Fe supply continuously enriched in more Fe content than Fe-deficient treatment, which indicated organic Fe chelates of Fe-EDTA can be a practical way to rise Fe content in plants. Other organic chelators like Fe-EDDHA and Fe-HEDTA have also been found to be agricultural fertilizers for improving the Fe nutrition for plants since 1950s (Chen and Barak, 1982). However, all these organic Fe chelates are costly for most agronomic crops in the field (Shenker and Chen, 2005; Wallace and Wallace, 1992). It is noteworthy that except inorganic Fe fertilizer and organic Fe chelates, some natural organic materials such as manure, peat or composted organic residues may naturally enrich in Fe and therefore can act as Fe source for plants (Chen, 1996; Chen and Aviad, 1990).

As pH is highly important to determine Fe availability in soil, where Fe is 1000 times more available at the pH 6 compared to at pH 7 and there is another 1,000 fold decrease in Fe availability from pH 7 to pH 8 (Zuo and Zhang, 2011). Soil acidification could be a very efficient mechanism to increase soil Fe solubility. By using 9 tons of sulfur (S) per hectare, the pH decreased from 8.0 to 5.8 in low (1%) $CaCO_3$ content soil and further increased Fe content in sorghum leaves (Olson, 1950). In this case, soil acidification is needed to facilitate Fe uptake. The N fertilization thus plays a major role for crops in determining root cation-anion uptake ratio and subsequent rhizosphere pH values. For example, the rice flower (*Ozothamnus diosmifolius*, Astraceae) fertilized with 3:1

NH_4^+ to NO_3^- ratio was 2 units pH lower than that of the plants supplied with a 1:3 NH_4^+ to NO_3^- ratio. In addition, the Fe concentration in plant leaves in 3:1 NH_4^+ to NO_3^- ratio showed 32% higher than those of plants grown in a 1:3 NH_4^+ to NO_3^- ratio (Silber et al., 2004). In this regard, understanding the Fe uptake in field trials is likely linked to N dynamics. Particular soil acidification by NH_4^+/NO_3^- species alterations with redox cycles upon irrigation thus contributes to the findings of the long-term field experiment studied in chapter IV where both the irrigated and non-irrigated variants were fertilized with 120 kg N ha^{-1} via calcium ammonium nitrate.

Soil management with irrigation is an extreme example, as it is rice in paddy soil growing in flood condition and evolving a specific Fe(III) reduction strategy to secure Fe uptake from soil. While with the development of novel water-saving rice production systems, the Fe deficiency in rice due to the water content shifts from flooded to aerobic condition becomes more and more severe. The results from field experiments done by Zou et al. (2008) showed that Fe application did not improve the Fe nutrition of aerobic rice, while different genotypes had different Fe harvest index. Here, I did not study rice but wheat. This suggests that development of high-Fe harvest index wheat genotypes would be a more promising strategy to increase Fe availability for wheat. I noticed that water content shifts from flooded to aerobic condition closely related to pH increases, thus affecting Fe availability. Nevertheless, in chapter IV, there was no significant difference in water content between irrigated and non-irrigated soil. Fifty-year irrigation, however, decreased soil pH by 1 unit and significantly increased Fe availability as indicated by 0.5 M HCl extraction in the top 40 cm of soil. I can thus summarize that water regulation on Fe availability is mostly due to pH changes.

2.2 Fe mobilization in the soil-plant system

Fe is the most commonly deficient micronutrient in human diet and about 2 billion people worldwide are suffering from Fe deficiency (Bouis and Welch, 2010). Fe acquisition from soil by plants is thus attractive as plants especially crop grains and seeds are the main Fe source for plant-based diets. Wheat is the dominant staple crop in Germany and constitutes more than 50% of the diet (Cakmak, 2010), which makes it a major source for essential micronutrients. Wheat growth from vegetative to reproductive period is continuously accompanied with Fe mobilization process. Initial Fe requirements will be covered with Fe mobilized from the seed. Once it is exhausted, Fe requirements need to be supplemented by Fe uptake from the soil. At anthesis, all the plants are still in vegetation growth, where plant take up Fe mainly for photosynthesis. That explains the highest Fe concentration and Fe content in leaves for both pot experiment (chapter III) and field experiment (chapter IV). During grain filling, the amount of Fe in the grains depends on both Fe uptake by roots and the amount of Fe redistribution from vegetative tissue via phloem. it is notably that all nutrient transport into the grain must at some stage pass through the phloem due to xylem discontinuity in the grain stalk (O'Brien et al., 1985). In this case, the Fe mobility in phloem is greatly important to grain filling and thus for human healthy. A field study with semi-dwarf spring wheat showed that less than 20% of Fe can be redistributed to grain from stems and leaves, whereas redistribution of some other key nutrients such as N, P and K from vegetative organs could occupy over 70% in grains (Hocking, 1994). Even though under Fe-deficiency condition, the remobilization and subsequent retranslocation of Fe from mature green leaves to grains still remain small for the bean plant (*Phaseolus vulgaris* L.) (Zhang et al., 1995b), I could prove in chapter III of the pot experiment that Fe redistribution from roots to the shoots under Fe-sufficiency condition plays a major role during grain filling, which was consistent with results of a greenhouse study by Garnett and Graham (2005). In contrast, Fe uptake from soil rather than redistribution processes

dominated grain filling process under Fe-deficiency conditions. All these results indicate that Fe mobilization in phloem varies, likely depending on plant species and Fe availabilities in soil. More studies are now needed to get a better understanding of the mechanisms controlling Fe mobility in phloem. Anyhow, my data confirmed that grains are finally able to enrich the Fe at maturity stage, as expected, due to remobilization processes within the plant.

2.3 Extended analyses of δ^{56}Fe values analysis across soil-plant ecosystems

In addition to two chapters presenting wheat plant δ^{56}Fe values, a total of 10 species of strategy II plants report δ^{56}Fe values in different plant organs given in figures below (Fig. V-1, Fig. V-2), which include to-date available Fe isotopic data in both controlled greenhouse and field conditions. The plant mostly studied is rice, since it occurs at the border between the two Fe uptake strategies (Bashir et al., 2011; Fourcroy et al., 2014; Ishimaru et al., 2011; Ishimaru et al., 2006; Rodríguez-Celma et al., 2013). Overall, variations of Fe isotope composition of different strategy II plant species range from -1.80‰ to 0.80‰ (Fig. V-1, Fig. V-2). Even within the same plant species, differences in their Fe isotope composition to various degrees were found (Fig. V-1, Fig. V-2). The question now arises to which extent the Fe isotope composition can be changed, and which factors control Fe isotope fractionations in strategy II plants.

It is demonstrated that three individuals of *Agrostis gigantea* presented large Fe isotope compositions variations by up to 1.23‰ in flowers (Kiczka et al., 2010). In my work of both pot and field experiment, variations in δ^{56}Fe values among plant replicates can also be observed to different degree, but generally the variations in the greenhouse were smaller than under field conditions. To better understand the effect of growth substrates on plant Fe isotope compositions, my data can be compared to a greenhouse pot experiment by Arnold et al. (2015). This experiment

demonstrated that strategy II plant rice (*Oryza sativa* L. cv. *Oochikara*) that was grown in aerobic and anaerobic soils enriched isotopically light Fe to similar extent. Garnier et al. (2017) explained such phenomena by the fact that root Fe uptake in paddy fields is not from the plant-available pool but from Fe plaque in roots. It mainly consists of amorphous and short-range ordered Fe(III) precipitates such as ferrihydrite and further easily transforms to Fe(III) oxides (Liu et al., 2006). In this case, rice plant in both aerobic and anaerobic soils fractionate the uptaken Fe in similar extent. In addition, it is observed that a Fe isotope fractionation factor of -0.9‰ was found from rice roots to the seeds. As the δ^{56}Fe in the Fe plaque is significantly heavier than that in roots and above-ground plant organs (Garnier et al., 2017), the isotopically light Fe in rice (Arnold et al., 2015) could come from Fe fractionation during plant physiological process rather than growth substrates.

In chapter IV, using mass balance calculations, I obtained that the whole wheat plants in irrigated and non-irrigated plots were both slightly enriched in light Fe isotopes of -0.09‰, which is consistent with the assumption above that the overall δ^{56}Fe signature of wheat was regulated by plant-homeostasis and physiological process. Furthermore, it is clearly shown that the range of Fe isotope compositions in different organs for wheat is within the range reported in the literature of field experiment for strategy II plants (Fig. V-2).

For wheat growth from seed germination to full maturity, plant growth changes from vegetative growth to reproductive growth, where Fe distribution and uptake rate are subsequently altered in order to support the on-time plant physiological needs (Briat et al., 2015; Garnett and Graham, 2005). This supports the need for studying Fe isotope fractionation during the whole wheat cycle. In chapter III, depending on wheat growth stages, Fe-availabilities can play a role influencing Fe isotope compositions in different organs of wheat or not influencing at all. At anthesis, Fe-

availabilities played no significant role in Fe isotope compositions of wheat. This is consistent with chapter IV, where different plant-available pool showed no significant influence on δ^{56}Fe values for wheat at anthesis stage. However, in wheat reproductive growth different Fe-availabilities can affect δ^{56}Fe values on different plant organs, especially in leaves and seeds. Hence, it is conclude that Fe isotope ratios in plant should come from at least two factors (plant growth stages and conditions) from my current study, suggesting more researches needed to better understand the relationship between δ^{56}Fe values and plant growth. All the Fe isotope data in different plant organs along with wheat growth in chapter III extend our knowledge on variations of Fe isotope compositions for strategy II plant growth under controlled greenhouse experiment (Fig. V-1).
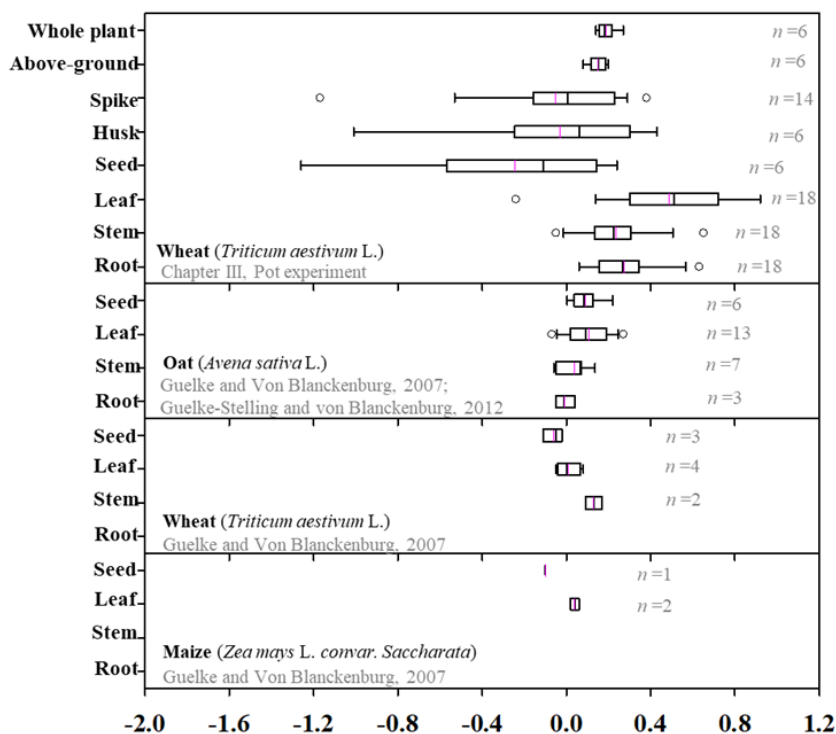
Fig. V-1: Summary of Fe isotope compositions in different organs of strategy II plants reported in the literatures of controlled greenhouse experiment. The numbers next to the boxes indicate the number of observations. The color lines indicate the mean value of δ^{56}Fe for each plant species and the dots represent outliers.
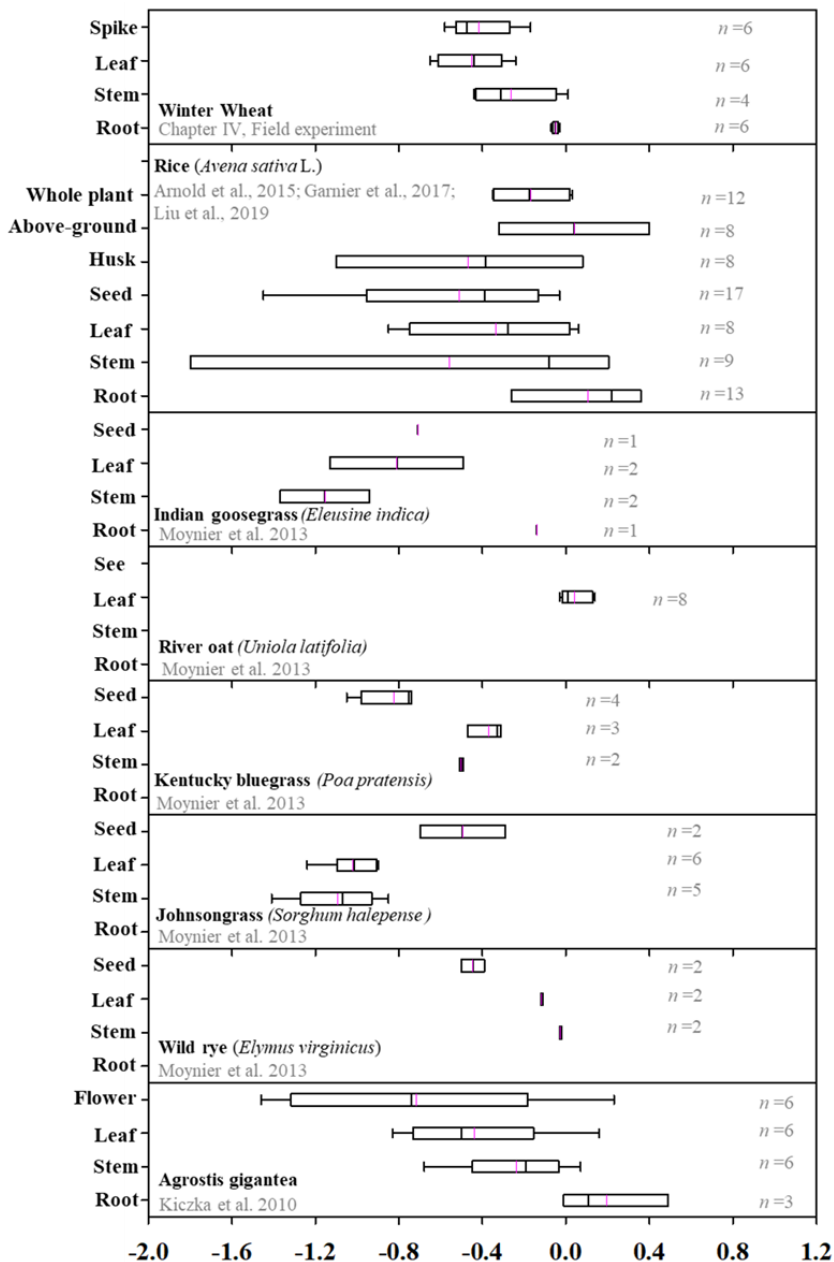
Fig. V-2: Summary of Fe isotope compositions in different organs of strategy II plants reported in the literatures of field experiment. The numbers next to the boxes indicate the number of observations. The color lines indicate the mean value of δ56Fe for each plant species and the dots represent outliers.
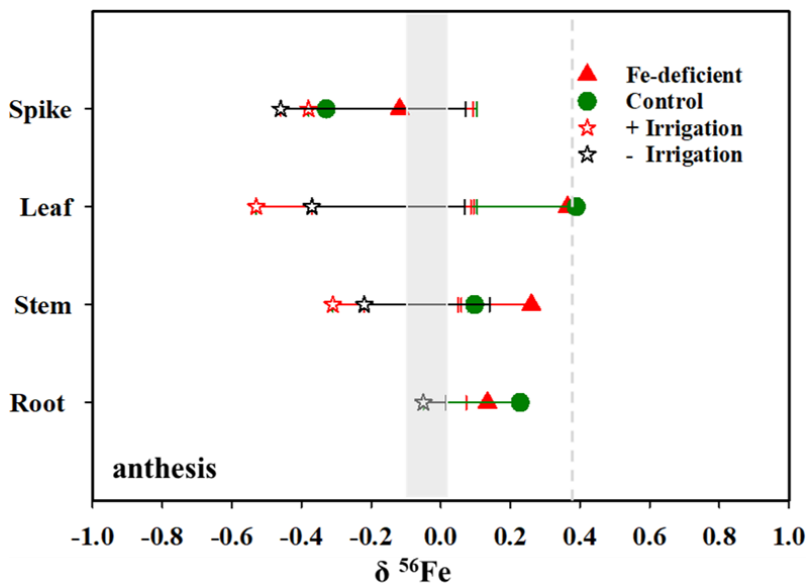

Fig. V-3: Fe isotope compositions of the different organs of wheat in greenhouse and field experiments in chapter III and IV. The solid circles and triangles indicate the data from chapter III and the hollow stars represent the data from chapter IV. The vertical grey line and bar indicate the Fe isotope compositions of plant-available Fe pools in controlled greenhouse and field conditions, respectively.

It should be noted that δ^{56}Fe values in different plant organs tended to indicate the Fe cycling process in the plants. However, as there were large variations in δ^{56}Fe values within the same plant species and organs, it will likely not easily be possible to perform an absolute comparison of δ^{56}Fe values among different studies, even if there is a rigorous control of the same certified standard measurements across all analyses in all studies. This is because slight differences in growth

conditions will likely contribute to differences in δ^{56}Fe values among different plant growth studies. Therefore, it is also difficult to explain why the wheat plant grown in the greenhouse condition enriched more isotopic heavier Fe than the wheat grown under field condition (Fig. V-3). Future studies should focus on the mechanisms of how Fe is cycled in individual plants under different environmental conditions.

Noteworthy, agricultural management like irrigation did not change Fe isotope compositions of the bulk soil Fe pool, it mainly reflected that of the original parent material, which lies within a narrow range (Poitrasson, 2006). Compared to several thousand years of rock weathering and pedogenesis at the sites under study, 50-year irrigation is likely too short to have an effect on the Fe isotope signatures in bulk soil. Hence, δ^{56}Fe values in bulk soil are unaffected by soil managements. However, this does not necessarily apply to the plant-available Fe-pool. Water soluble and freely exchangeable iron (Fe_{ex}), iron bound or adsorbed to organic complexes (Fe_{org}) and poorly crystalline Fe oxides ($Fe_{poorly-cry.-oxides}$) are generally considered as plant available Fe in soil proposed by Guelke et al. (2010). Therefore, when considering the plant-available Fe, redox-potential, organic matter content and water content should also be considered. Compared to bulk soil Fe pool, the plant-available Fe pool is quite small so that reservoir effects hardly play a role, offering more possibilities to be affected by agricultural management and thus being a useful research object to trace Fe cycling in soil. In my study, including the plant-available Fe pool into the analytical outline showed that the amount of plant-available Fe was increased by irrigation management. It also translated to a certain degree into the Fe isotope signatures of the plant roots, but not into those of the whole plant. The latter was rather determined by plant internal translocation processes, i.e., by plant homeostasis, and by the bulk δ^{56}value of the weathered parent rock. Assessing the Fe isotope composition of plants informs thus on nutrient conditions and

background Fe isotope values, whereas information on soil management can likely only be depicted from soil analyses.

3. CONCLUSIONS

My work shows that the general assumption that Fe-deficiency could reduce the whole Fe mass in wheat and induce different Fe translocation ways compared to wheat growth under sufficient Fe supply. Soil management like irrigation might increase Fe availability mainly in topsoil. I repeatedly showed that instead of Fe availability, the plant-homeostasis regulated the δ^{56}Fe signatures in different wheat organs at vegetative growth, where the newly formed plant organs like spike were continuously isotopic lighter than leaves, stems and roots. While with serious shortage of Fe after anthesis, Fe-deficiency promote strategy-specific (strategy II) Fe uptake process during wheat reproductive growth, thus resulting in limited Fe isotope fractionation throughout all plant organs. This suggests that Fe isotope ratios can reflect both wheat growth conditions and ages in some extent.

To verify this conclusion beyond the limited scope presented here, follow-up experiments should focus on extending the range of soil managements and crops, to allow for an up-scaling to other agricultural system across the world. Here, a special emphasis should be placed on the interaction of Fe supply and growth stages as Fe limitation of plants can induce different phenomenon along with plant growth. The field experiment in chapter IV only test the effect of irrigation treatment on δ^{56}Fe values changes during the anthesis stage. It remains unclear, whether the soil managements have influence on δ^{56}Fe values changes in plant reproductive growth. If any such effects could be observed in field trials, this could eventually provide a new way to trace Fe in soil-plant system.

VI

REFERENCES

Acevedo, E., Silva, P., Silva, H., 2006. Growth and wheat physiology, development. Laboratory of Soil-Plant-Water Relations. Faculty of Agronomy and Forestry Sciences. University of Chile. Casilla 1004.

Adamski, J.M., Peters, J.A., Danieloski, R., Bacarin, M.A., 2011. Excess iron-induced changes in the photosynthetic characteristics of sweet potato. Journal of plant physiology 168(17), 2056-2062.

Akerman, A., Poitrasson, F., Oliva, P., Audry, S., Prunier, J., Braun, J.-J., 2014. The isotopic fingerprint of Fe cycling in an equatorial soil–plant–water system: The Nsimi watershed, South Cameroon. Chemical Geology 385, 104-116.

Álvarez-Fernández, A., Díaz-Benito, P., Abadía, A., López-Millán, A.-F., Abadía, J., 2014. Metal species involved in long distance metal transport in plants. Frontiers in plant science 5, 105.

Anbar, A., Jarzecki, A., Spiro, T., 2005. Theoretical investigation of iron isotope fractionation between Fe (H 2 O) 6 3+ and Fe (H 2 O) 6 2+: implications for iron stable isotope geochemistry. Geochimica et Cosmochimica Acta 69(4), 825-837.

Anbar, A., Roe, J., Barling, J., Nealson, K., 2000. Nonbiological fractionation of iron isotopes. Science 288(5463), 126-128.

Arnold, T., Kirk, G.J., Wissuwa, M., Frei, M., ZHAO, F.J., Mason, T.F., Weiss, D.J., 2010. Evidence for the mechanisms of zinc uptake by rice using isotope fractionation. Plant, cell & environment 33(3), 370-381.

Arnold, T., Markovic, T., Kirk, G.J., Schönbächler, M., Rehkämper, M., Zhao, F.J., Weiss, D.J., 2015. Iron and zinc isotope fractionation during uptake and translocation in rice (Oryza sativa) grown in oxic and anoxic soils. Comptes Rendus Geoscience 347(7-8), 397-404.

Asseng, S., Ritchie, J., Smucker, A., Robertson, M., 1998. Root growth and water uptake during water deficit and recovering in wheat. Plant and Soil 201(2), 265-273.

Bashir, K., Ishimaru, Y., Shimo, H., Kakei, Y., Senoura, T., Takahashi, R., Sato, Y., Sato, Y., Uozumi, N., Nakanishi, H., 2011. Rice phenolics efflux transporter 2 (PEZ2) plays an important role in solubilizing apoplasmic iron. Soil Science and Plant Nutrition 57(6), 803-812.

Bauke, S.L., von Sperber, C., Tamburini, F., Gocke, M., Honermeier, B., Schweitzer, K., Baumecker, M., Don, A., Sandhage‐Hofmann, A., Amelung, W., 2018. Subsoil phosphorus is affected by fertilization regime in long‐term agricultural experimental trials. European Journal of Soil Science 69(1), 103-112.

Beard, B.L., Johnson, C.M., Cox, L., Sun, H., Nealson, K.H., Aguilar, C., 1999. Iron isotope biosignatures. Science 285(5435), 1889-1892.

Becker, M., Asch, F., 2005. Iron toxicity in rice—conditions and management concepts. Journal of Plant Nutrition and Soil Science 168(4), 558-573.

Becker, R., Fritz, E., Manteuffel, R., 1995. Subcellular localization and characterization of excessive iron in the nicotianamine-less tomato mutant chloronerva. Plant Physiology 108(1), 269-275.

Belford, R., Henderson, F., 1985. Measurement of the growth of wheat roots using a TV camera system in the field, Wheat growth and modelling. Springer, pp. 99-105.

Bienfait, H.F., van den Briel, W., Mesland-Mul, N.T., 1985. Free space iron pools in roots: generation and mobilization. Plant Physiology 78(3), 596-600.

Bigeleisen, J., Mayer, M.G., 1947. Calculation of equilibrium constants for isotopic exchange reactions. The Journal of Chemical Physics 15(5), 261-267.

Bolou-Bi, E.B., Poszwa, A., Leyval, C., Vigier, N., 2010. Experimental determination of magnesium isotope fractionation during higher plant growth. Geochimica et Cosmochimica Acta 74(9), 2523-2537.

Borg, S., Brinch-Pedersen, H., Tauris, B., Holm, P.B., 2009. Iron transport, deposition and bioavailability in the wheat and barley grain. Plant and Soil 325(1-2), 15-24.

Bouis, H.E., Welch, R.M., 2010. Biofortification—a sustainable agricultural strategy for reducing micronutrient malnutrition in the global south. Crop Science 50(Supplement_1), S-20-S-32.

Brantley, S.L., Liermann, L., Bullen, T.D., 2001. Fractionation of Fe isotopes by soil microbes and organic acids. Geology 29(6), 535-538.

Briat, J.-F., Curie, C., Gaymard, F., 2007a. Iron utilization and metabolism in plants. Current opinion in plant biology 10(3), 276-282.

Briat, J.-F., Dubos, C., Gaymard, F., 2015. Iron nutrition, biomass production, and plant product quality. Trends in Plant Science 20(1), 33-40.

Briat, J.F., Curie, C., Gaymard, F., 2007b. Iron utilization and metabolism in plants. Current Opinion in Plant Biology 10(3), 276-282.

Broadley, M., Brown, P., Cakmak, I., Rengel, Z., Zhao, F., 2012. Function of nutrients: micronutrients, Marschner's mineral nutrition of higher plants. Elsevier, pp. 191-248.

Bughio, N., Yamaguchi, H., Nishizawa, N.K., Nakanishi, H., Mori, S., 2002. Cloning an iron‐regulated metal transporter from rice. Journal of Experimental Botany 53(374), 1677-1682.

Buol, S.W., Southard, R.J., Graham, R.C., McDaniel, P.A., 2011. Soil genesis and classification. John Wiley & Sons.

Cakmak, I., 2010. Biofortification of cereals with zinc and iron through fertilization strategy, 19th World Congress of Soil Science, Brisbane.

Çakmak, İ., Torun, A., Millet, E., Feldman, M., Fahima, T., Korol, A., Nevo, E., Braun, H., Özkan, H., 2004. Triticum dicoccoides: an important genetic resource for increasing zinc and iron concentration in modern cultivated wheat. Soil Science and Plant Nutrition 50(7), 1047-1054.

Caldelas, C., Dong, S., Araus, J.L., Jakob Weiss, D., 2011. Zinc isotopic fractionation in Phragmites australis in response to toxic levels of zinc. Journal of experimental botany 62(6), 2169-2178.

Chaignon, V., Di Malta, D., Hinsinger, P., 2002. Fe‐deficiency increases Cu acquisition by wheat cropped in a Cu‐contaminated vineyard soil. New Phytologist 154(1), 121-130.

Charlson, D.V., Shoemaker, R.C., 2006. Evolution of iron acquisition in higher plants. Journal of plant nutrition 29(6), 1109-1125.

Chen, Y., 1996. Organic matter reactions involving micronutrients in soils and their effect on plants, Humic substances in terrestrial ecosystems. Elsevier, pp. 507-529.

Chen, Y., Aviad, T., 1990. Effects of humic substances on plant growth 1. Humic substances in soil and crop sciences: Selected readings (humicsubstances), 161-186.

Chen, Y., Barak, P., 1982. Iron nutrition of plants in calcareous soils, Advances in agronomy. Elsevier, pp. 217-240.

Cheng, L., Wang, F., Shou, H., Huang, F., Zheng, L., He, F., Li, J., Zhao, F.-J., Ueno, D., Ma, J.F., 2007. Mutation in nicotianamine aminotransferase stimulated the Fe (II) acquisition system and led to iron accumulation in rice. Plant Physiology 145(4), 1647-1657.

Colombo, C., Palumbo, G., He, J.-Z., Pinton, R., Cesco, S., 2014. Review on iron availability in soil: interaction of Fe minerals, plants, and microbes. Journal of Soils and Sediments 14(3), 538-548.

Colombo, C., Torrent, J., 1991. Relationships between aggregation and iron oxides in Terra Rossa soils from southern Italy. Catena 18(1), 51-59.

Cornell, R.M., Giovanoli, R., Schneider, W., 1989. Review of the hydrolysis of iron (III) and the crystallization of amorphous iron (III) hydroxide hydrate. Journal of Chemical Technology & Biotechnology 46(2), 115-134.

Cornell, R.M., Schwertmann, U., 2003. The iron oxides: structure, properties, reactions, occurrences and uses. 2nd edn ed. John Wiley & Sons, Weinheim.

Criss, R.E., 1999. Principles of stable isotope distribution. Oxford University Press on Demand.

Curie, C., Cassin, G., Couch, D., Divol, F., Higuchi, K., Le Jean, M., Misson, J., Schikora, A., Czernic, P., Mari, S., 2008. Metal movement within the plant: contribution of nicotianamine and yellow stripe 1-like transporters. Annals of botany 103(1), 1-11.

Curie, C., Panaviene, Z., Loulergue, C., Dellaporta, S.L., Briat, J.-F., Walker, E.L., 2001. Maize yellow stripe1 encodes a membrane protein directly involved in Fe (III) uptake. Nature 409(6818), 346.

Dauphas, N., Janney, P.E., Mendybaev, R.A., Wadhwa, M., Richter, F.M., Davis, A.M., Van Zuilen, M., Hines, R., Foley, C.N., 2004. Chromatographic separation and multicollection-ICPMS analysis of iron. Investigating mass-dependent and-independent isotope effects. Analytical Chemistry 76(19), 5855-5863.

Dauphas, N., John, S.G., Rouxel, O., 2017. Iron isotope systematics. Reviews in Mineralogy and Geochemistry 82(1), 415-510.

Dauphas, N., Pourmand, A., Teng, F.-Z., 2009. Routine isotopic analysis of iron by HR-MC-ICPMS: How precise and how accurate? Chemical Geology 267(3), 175-184.

Deckers, J.A., Nachtergaele, F., 1998. World reference base for soil resources: Introduction, 1. Acco.

Dideriksen, K., Baker, J.A., Stipp, S.L.S., 2008. Equilibrium Fe isotope fractionation between inorganic aqueous Fe (III) and the siderophore complex, Fe (III)-desferrioxamine B. Earth and Planetary Science Letters 269(1), 280-290.

Divol, F., Couch, D., Conéjéro, G., Roschzttardtz, H., Mari, S., Curie, C., 2013. The Arabidopsis YELLOW STRIPE LIKE4 and 6 transporters control iron release from the chloroplast. The Plant Cell 25(3), 1040-1055.

Duncan, D.B., 1955. Multiple range and multiple F tests. Biometrics 11(1), 1-42.

Durrett, T.P., Gassmann, W., Rogers, E.E., 2007. The FRD3-mediated efflux of citrate into the root vasculature is necessary for efficient iron translocation. Plant physiology 144(1), 197-205.

Duy, D., Wanner, G., Meda, A.R., von Wirén, N., Soll, J., Philippar, K., 2007. PIC1, an ancient permease in Arabidopsis chloroplasts, mediates iron transport. The Plant Cell 19(3), 986-1006.

Eide, D., Broderius, M., Fett, J., Guerinot, M.L., 1996. A novel iron-regulated metal transporter from plants identified by functional expression in yeast. Proceedings of the National Academy of Sciences 93(11), 5624-5628.

Ellmer, F., Baumecker, M., 2005. Static nutrient depletion experiment Thyrow. Results after 65 experimental years. Archives of Agronomy and Soil Science 51(2), 151-161.

Ellmer, F., Peschke, H., Köhn, W., Chmielewski, F.M., Baumecker, M., 2000. Tillage and fertilizing effects on sandy soils. Review and selected results of long‑term experiments at Humboldt‑University Berlin. Journal of Plant Nutrition and Soil Science 163(3), 267-272.

Emmanuel, S., Erel, Y., Matthews, A., Teutsch, N., 2005. A preliminary mixing model for Fe isotopes in soils. Chemical geology 222(1), 23-34.

Evans, D.J., Benn, D.I., 2014. A practical guide to the study of glacial sediments. Routledge.

Fekiacova, Z., Pichat, S., Cornu, S., Balesdent, J., 2013. Inferences from the vertical distribution of Fe isotopic compositions on pedogenetic processes in soils. Geoderma 209, 110-118.

Flemming, C., Trevors, J., 1989. Copper toxicity and chemistry in the environment: a review. Water, Air, and Soil Pollution 44(1-2), 143-158.

Fourcroy, P., Sisó‑Terraza, P., Sudre, D., Savirón, M., Reyt, G., Gaymard, F., Abadía, A., Abadia, J., Álvarez‑Fernández, A., Briat, J.F., 2014. Involvement of the ABCG 37 transporter in secretion of scopoletin and derivatives by Arabidopsis roots in response to iron deficiency. New Phytologist 201(1), 155-167.

Füllner, K., Temperton, V., Rascher, U., Jahnke, S., Rist, R., Schurr, U., Kuhn, A., 2012. Vertical gradient in soil temperature stimulates development and increases biomass accumulation in barley. Plant, Cell & Environment 35(5), 884-892.

Garnett, T.P., Graham, R.D., 2005. Distribution and remobilization of iron and copper in wheat. Annals of Botany 95(5), 817-826.

Garnier, J., Garnier, J., Vieira, C., Akerman, A., Chmeleff, J., Ruiz, R., Poitrasson, F., 2017. Iron isotope fingerprints of redox and biogeochemical cycling in the soil-water-rice plant system of a paddy field. Science of the Total Environment 574, 1622-1632.

Gottselig, N., Amelung, W., Kirchner, J.W., Bol, R., Eugster, W., Granger, S.J., Hernández‑Crespo, C., Herrmann, F., Keizer, J.J., Korkiakoski, M., 2017. Elemental composition of natural nanoparticles and fine colloids in European forest stream waters and their role as phosphorus carriers. Global Biogeochemical Cycles 31(10), 1592-1607.

Guelke-Stelling, M., von Blanckenburg, F., 2012. Fe isotope fractionation caused by translocation of iron during growth of bean and oat as models of strategy I and II plants. Plant and soil 352(1-2), 217-231.

Guelke, M., Von Blanckenburg, F., 2007. Fractionation of stable iron isotopes in higher plants. Environmental science & technology 41(6), 1896-1901.

Guelke, M., von Blanckenburg, F., Schoenberg, R., Staubwasser, M., Stuetzel, H., 2010. Determining the stable Fe isotope signature of plant-available iron in soils. Chemical Geology 277(3), 269-280.

Guerinot, M., 2001. Improving rice yields--ironing out the details. Nature biotechnology 19(5), 417.

Guerinot, M.L., 2000. The ZIP family of metal transporters. Biochimica et Biophysica Acta (BBA)-Biomembranes 1465(1-2), 190-198.

Halliwell, B., Gutteridge, J., 1984. Oxygen toxicity, oxygen radicals, transition metals and disease. The Biochemical journal 219(1), 1-14.

Halliwell, B., Gutteridge, J.M., 1992. Biologically relevant metal ion‑dependent hydroxyl radical generation An update. FEBS letters 307(1), 108-112.

Hartemink, A.E., 2016. Scheffer/Schachtschabel Soil Science. Soil Science Society of America Journal 80, 528.

Haydon, M.J., Kawachi, M., Wirtz, M., Hillmer, S., Hell, R., Krämer, U., 2012. Vacuolar nicotianamine has critical and distinct roles under iron deficiency and for zinc sequestration in Arabidopsis. The Plant Cell 24(2), 724-737.

Hell, R., Stephan, U.W., 2003. Iron uptake, trafficking and homeostasis in plants. Planta 216(4), 541-551.

Hocking, P., 1994. Dry‑matter production, mineral nutrient concentrations, and nutrient distribution and redistribution in irrigated spring wheat. Journal of Plant Nutrition 17(8), 1289-1308.

Inoue, H., Kobayashi, T., Nozoye, T., Takahashi, M., Kakei, Y., Suzuki, K., Nakazono, M., Nakanishi, H., Mori, S., Nishizawa, N.K., 2009. Rice OsYSL15 is an iron-regulated iron (III)-deoxymugineic acid transporter expressed in the roots and is essential for iron uptake in early growth of the seedlings. Journal of Biological Chemistry 284(6), 3470-3479.

Ishimaru, Y., Kakei, Y., Shimo, H., Bashir, K., Sato, Y., Sato, Y., Uozumi, N., Nakanishi, H., Nishizawa, N.K., 2011. A rice phenolic efflux transporter is essential for solubilizing precipitated apoplasmic iron in the plant stele. Journal of Biological Chemistry 286(28), 24649-24655.

Ishimaru, Y., Masuda, H., Bashir, K., Inoue, H., Tsukamoto, T., Takahashi, M., Nakanishi, H., Aoki, N., Hirose, T., Ohsugi, R., 2010. Rice metal‑nicotianamine transporter, OsYSL2, is required for the long‑distance transport of iron and manganese. The Plant Journal 62(3), 379-390.

Ishimaru, Y., Suzuki, M., Tsukamoto, T., Suzuki, K., Nakazono, M., Kobayashi, T., Wada, Y., Watanabe, S., Matsuhashi, S., Takahashi, M., 2006. Rice plants take up iron as an Fe3+‑phytosiderophore and as Fe2+. The Plant Journal 45(3), 335-346.

Jain, A., Connolly, E.L., 2013. Mitochondrial iron transport and homeostasis in plants. Frontiers in plant science 4, 348.

Jean, M.L., Schikora, A., Mari, S., Briat, J.F., Curie, C., 2005. A loss‑of‑function mutation in AtYSL1 reveals its role in iron and nicotianamine seed loading. The Plant Journal 44(5), 769-782.

Jeong, J., Cohu, C., Kerkeb, L., Pilon, M., Connolly, E.L., Guerinot, M.L., 2008. Chloroplast Fe (III) chelate reductase activity is essential for seedling viability under iron limiting conditions. Proceedings of the National Academy of Sciences 105(30), 10619-10624.

Kappler, A., Straub, K.L., 2005. Geomicrobiological cycling of iron. Reviews in Mineralogy and Geochemistry 59(1), 85-108.

Kavner, A., Bonet, F., Shahar, A., Simon, J., Young, E., 2005. The isotopic effects of electron transfer: An explanation for Fe isotope fractionation in nature. Geochimica et Cosmochimica Acta 69(12), 2971-2979.

Kiczka, M., Wiederhold, J.G., Kraemer, S.M., Bourdon, B., Kretzschmar, R., 2010. Iron isotope fractionation during Fe uptake and translocation in alpine plants. Environmental science & technology 44(16), 6144-6150.

Kiem, R., Kögel-Knabner, I., 2002. Refractory organic carbon in particle-size fractions of arable soils II: organic carbon in relation to mineral surface area and iron oxides in fractions< 6 μm. Organic Geochemistry 33(12), 1699-1713.

Kim, S.A., Guerinot, M.L., 2007. Mining iron: iron uptake and transport in plants. FEBS letters 581(12), 2273-2280.

Kim, S.A., Punshon, T., Lanzirotti, A., Li, L., Alonso, J.M., Ecker, J.R., Kaplan, J., Guerinot, M.L., 2006. Localization of iron in Arabidopsis seed requires the vacuolar membrane transporter VIT1. Science 314(5803), 1295-1298.

Kobayashi, T., Nishizawa, N.K., 2012. Iron uptake, translocation, and regulation in higher plants. Annual review of plant biology 63, 131-152.

Kobayashi, T., Nozoye, T., Nishizawa, N.K., 2019. Iron transport and its regulation in plants. Free Radical Biology and Medicine 133, 11-20.

Korshunova, Y.O., Eide, D., Clark, W.G., Guerinot, M.L., Pakrasi, H.B., 1999. The IRT1 protein from Arabidopsis thaliana is a metal transporter with a broad substrate range. Plant molecular biology 40(1), 37-44.

Lanquar, V., Lelièvre, F., Bolte, S., Hamès, C., Alcon, C., Neumann, D., Vansuyt, G., Curie, C., Schröder, A., Krämer, U., 2005. Mobilization of vacuolar iron by AtNRAMP3 and AtNRAMP4 is essential for seed germination on low iron. The EMBO journal 24(23), 4041-4051.

Li, L., Cheng, X., Ling, H.-Q., 2004. Isolation and characterization of Fe(III)-chelate reductase gene LeFRO1 in tomato. Plant Molecular Biology 54(1), 125-136.

Lide, D.R., 1995. CRC handbook of chemistry and physics: a ready-reference book of chemical and physical data. CRC press.

Lindsay, W., Schwab, A., 1982. The chemistry of iron in soils and its availability to plants. Journal of Plant Nutrition 5(4-7), 821-840.

Liu, C., Gao, T., Liu, Y., Liu, J., Li, F., Chen, Z., Li, Y., Lv, Y., Song, Z., Reinfelder, J.R., 2019. Isotopic fingerprints indicate distinct strategies of Fe uptake in rice. Chemical Geology 524, 323-328.

Liu, S.-A., Teng, F.-Z., Li, S., Wei, G.-J., Ma, J.-L., Li, D., 2014. Copper and iron isotope fractionation during weathering and pedogenesis: insights from saprolite profiles. Geochimica et Cosmochimica Acta 146, 59-75.

Liu, W., Zhu, Y., Hu, Y., Williams, P., Gault, A., Meharg, A.A., Charnock, J., Smith, F., 2006. Arsenic sequestration in iron plaque, its accumulation and speciation in mature rice plants (Oryza sativa L.). Environmental Science & Technology 40(18), 5730-5736.

López-Millán, A.F., Duy, D., Philippar, K., 2016. Chloroplast iron transport proteins–function and impact on plant physiology. Frontiers in plant science 7, 178.

Lubkowitz, M., 2011. The oligopeptide transporters: a small gene family with a diverse group of substrates and functions? Molecular plant 4(3), 407-415.

Macholdt, J., Honermeier, B., 2017. Yield stability in winter wheat production: a survey on German farmers' and advisors' views. Agronomy 7(3), 45.

Macías, F., Arbestain, M.C., 2010. Soil carbon sequestration in a changing global environment. Mitigation and Adaptation Strategies for Global Change 15(6), 511-529.

Manthey, J., Crowley, D.E., Luster, D.G., 1994. Biochemistry of metal micronutrients in the rhizosphere. CRC Press.

Marschner, H., 1995. Mineral nutrition of higher plants. Academic Press, London.

Marschner, H., 2011. Marschner's mineral nutrition of higher plants. Academic press, London.

Marschner, H., Römheld, V., Kissel, M., 1986. Different strategies in higher plants in mobilization and uptake of iron. Journal of plant nutrition 9(3-7), 695-713.

Mathers, A.C., 1970. Effect of Ferrous Sulfate and Sulfuric Acid on Grain Sorghum Yields 1. Agronomy journal 62(5), 555-556.

Mendoza-Cózatl, D.G., Xie, Q., Akmakjian, G.Z., Jobe, T.O., Patel, A., Stacey, M.G., Song, L., Demoin, D.W., Jurisson, S.S., Stacey, G., 2014. OPT3 is a component of the iron-signaling network between leaves and roots and misregulation of OPT3 leads to an over-accumulation of cadmium in seeds. Molecular plant 7(9), 1455-1469.

Mengel, K., 1994. Iron availability in plant tissues-iron chlorosis on calcareous soils. Plant and soil 165(2), 275-283.

Mon, J., Bronson, K., Hunsaker, D., Thorp, K., White, J., French, A., 2016. Interactive effects of nitrogen fertilization and irrigation on grain yield, canopy temperature, and nitrogen use efficiency in overhead sprinkler-irrigated durum wheat. Field crops research 191, 54-65.

Moog, P., van der Kooij TA , Brüggemann W, Schiefelbein JW, Kuiper PJ., 1995. Responses to iron deficiency in Arabidopsis thaliana: The Turbo iron reductase does not depend on the formation of root hairs and transfer cells. Planta 195, 505-513.

Mori, S., 1999. Iron acquisition by plants. Current opinion in plant biology 2(3), 250-253.

Mori, S.h., 1998. Iron transport in graminaceous plants. Iron transport and storage in microorganisms, plants, and animals.

Morrissey, J., Baxter, I.R., Lee, J., Li, L., Lahner, B., Grotz, N., Kaplan, J., Salt, D.E., Guerinot, M.L., 2009. The ferroportin metal efflux proteins function in iron and cobalt homeostasis in Arabidopsis. The Plant Cell 21(10), 3326-3338.

Moynier, F., Fujii, T., Wang, K., Foriel, J., 2013. Ab initio calculations of the Fe (II) and Fe (III) isotopic effects in citrates, nicotianamine, and phytosiderophore, and new Fe isotopic measurements in higher plants. Comptes Rendus Geoscience 345(5), 230-240.

Müller, M., Schmidt, W., 2004. Environmentally induced plasticity of root hair development in Arabidopsis. Plant Physiology 134(1), 409-419.

Murad, E., Fischer, W.R., 1988. The geobiochemical cycle of iron, Iron in soils and clay minerals. Springer, pp. 1-18.

Nakanishi, H., Ogawa, I., Ishimaru, Y., Mori, S., Nishizawa, N.K., 2006. Iron deficiency enhances cadmium uptake and translocation mediated by the Fe2+ transporters OsIRT1 and OsIRT2 in rice. Soil Science & Plant Nutrition 52(4), 464-469.

Neilands, J., 1987. Comparative biochemistry of microbial iron assimilation. Iron transport in microbes, plants and animals, 3-34.

Nikolic, M., Römheld, V., 2007. The dynamics of iron in the leaf apoplast, The apoplast of higher plants: compartment of storage, transport and reactions. Springer, pp. 353-371.

Nishiyama, R., Kato, M., Nagata, S., Yanagisawa, S., Yoneyama, T., 2012. Identification of Zn‐nicotianamine and Fe‐2′-deoxymugineic acid in the phloem sap from rice plants (Oryza sativa L.). Plant and cell physiology 53(2), 381-390.

Nogueira Arcanjo, F.P., Santos, P.R., Costa Arcanjo, C.P., Meira Magalhães, S.M., Madeiro Leite, Á.J., 2012. Daily and weekly iron supplementations are effective in increasing hemoglobin and reducing anemia in infants. Journal of tropical pediatrics 59(3), 175-179.

O'Brien, T., Sammut, M., Lee, J., Smart, M., 1985. The vascular system of the wheat spikelet. Functional Plant Biology 12(5), 487-511.

Olson, R., 1950. Effects of acidification, iron oxide addition, and other soil treatments on sorghum chlorosis and iron absorption. Soil Sci. Soc. Am., Proc.;(United States) 15.

Pedas, P., Ytting, C.K., Fuglsang, A.T., Jahn, T.P., Schjoerring, J.K., Husted, S., 2008. Manganese efficiency in barley: identification and characterization of the metal ion transporter HvIRT1. Plant physiology 148(1), 455-466.

Pich, A., Scholz, G., Stephan, U.W., 1994. Iron-dependent changes of heavy metals, nicotianamine, and citrate in different plant organs and in the xylem exudate of two tomato genotypes. Nicotianamine as possible copper translocator. Plant and Soil 165(2), 189-196.

Poitrasson, F., 2006. On the iron isotope homogeneity level of the continental crust. Chemical Geology 235(1-2), 195-200.

Poitrasson, F., Freydier, R., 2005. Heavy iron isotope composition of granites determined by high resolution MC-ICP-MS. Chemical Geology 222(1-2), 132-147.

Ponnamperuma, F., Tianco, E.M., Loy, T., 1967. Redox equilibria in flooded soils: I. The iron hydroxide systems. Soil Science 103(6), 374-382.

Rathore, V.S., Nathawat, N.S., Bhardwaj, S., Sasidharan, R.P., Yadav, B.M., Kumar, M., Santra, P., Yadava, N.D., Yadav, O.P., 2017. Yield, water and nitrogen use efficiencies of sprinkler irrigated wheat grown under different irrigation and nitrogen levels in an arid region. Agricultural Water Management 187, 232-245.

Rellán-Álvarez, R., Giner-Martínez-Sierra, J., Orduna, J., Orera, I., Rodríguez-Castrillón, J.Á., García-Alonso, J.I., Abadía, J., Álvarez-Fernández, A., 2009. Identification of a tri-iron (III), tri-citrate complex in the xylem sap of iron-deficient tomato resupplied with iron: new insights into plant iron long-distance transport. Plant and Cell Physiology 51(1), 91-102.

Robinson, N.J., Procter, C.M., Connolly, E.L., Guerinot, M.L., 1999. A ferric-chelate reductase for iron uptake from soils. Nature 397(6721), 694.

Rodríguez-Celma, J., Lin, W.-D., Fu, G.-M., Abadía, J., López-Míllán, A.-F., Schmidt, W., 2013. Mutually exclusive alterations in secondary metabolism are critical for the uptake of insoluble iron compounds by Arabidopsis and Medicago truncatula. Plant Physiology 162(3), 1473-1485.

Rodríguez, N.P., Langella, F., Rodushkin, I., Engström, E., Kothe, E., Alakangas, L., Öhlander, B., 2014. The role of bacterial consortium and organic amendment in Cu and Fe isotope fractionation in plants on a polluted mine site. Environmental Science and Pollution Research 21(11), 6836-6844.

Rodushkin, I., Stenberg, A., Andrén, H., Malinovsky, D., Baxter, D.C., 2004. Isotopic fractionation during diffusion of transition metal ions in solution. Analytical Chemistry 76(7), 2148-2151.

Römheld, V., 1991. The role of phytosiderophores in acquisition of iron and other micronutrients in graminaceous species: an ecological approach, Iron nutrition and interactions in plants. Springer, pp. 159-166.

Römheld, V., Marschner, H., 1986. Evidence for a specific uptake system for iron phytosiderophores in roots of grasses. Plant Physiology 80(1), 175-180.

Ryan, B.M., Kirby, J.K., Degryse, F., Harris, H., McLaughlin, M.J., Scheiderich, K., 2013. Copper speciation and isotopic fractionation in plants: uptake and translocation mechanisms. New Phytologist 199(2), 367-378.

Sahrawat, K., 2000. Elemental composition of the rice plant as affected by iron toxicity under field conditions. Communications in soil science and plant analysis 31(17-18), 2819-2827.

Sattelmacher, B., 2001. The apoplast and its significance for plant mineral nutrition. New Phytologist 149(2), 167-192.

Schaaf, G., Ludewig, U., Erenoglu, B.E., Mori, S., Kitahara, T., von Wirén, N., 2004. ZmYS1 functions as a proton-coupled symporter for phytosiderophore-and nicotianamine-chelated metals. Journal of Biological Chemistry 279(10), 9091-9096.

Schauble, E.A., 2004. Applying stable isotope fractionation theory to new systems. Reviews in Mineralogy and Geochemistry 55(1), 65-111.

Schirach, F., Wenkel, K.-O., Germar, R., 1988. Sprinkling recommendations for practice in usig the systems IBSB-2 and BEREST. Gartenbau (German DR).

Schmidt, W., Tittel, J., Schikora, A., 2000. Role of hormones in the induction of iron deficiency responses in Arabidopsis roots. Plant Physiology 122(4), 1109-1118.

Schmitt, A.-D., Cobert, F., Bourgeade, P., Ertlen, D., Labolle, F., Gangloff, S., Badot, P.-M., Chabaux, F., Stille, P., 2013. Calcium isotope fractionation during plant growth under a limited nutrient supply. Geochimica et Cosmochimica Acta 110, 70-83.

Schoenberg, R., von Blanckenburg, F., 2005. An assessment of the accuracy of stable Fe isotope ratio measurements on samples with organic and inorganic matrices by high-resolution multicollector ICP-MS. International Journal of Mass Spectrometry 242(2), 257-272.

Schweitzer, K., Hierath, C., 2010. Use of sandy soils in context with regional diversity and soil productivity, Tour Guide of the International Conference on Soil Fertility and Soil Productivity in Berlin, pp. 17-20.

Schwertmann, U., 1958. The effect of pedogenic environments on iron oxide minerals, Advances in soil science. Springer, pp. 171-200.

Schwertmann, U., 1988. Occurrence and formation of iron oxides in various pedoenvironments, Iron in soils and clay minerals. Springer, pp. 267-308.

Senoura, T., Sakashita, E., Kobayashi, T., Takahashi, M., Aung, M.S., Masuda, H., Nakanishi, H., Nishizawa, N.K., 2017. The iron-chelate transporter OsYSL9 plays a role in iron distribution in developing rice grains. Plant molecular biology 95(4-5), 375-387.

Sharma, R., 1992. Duration of the vegetative and reproductive period in relation to yield performance of spring wheat. European Journal of Agronomy 1(3), 133-137.

Shenker, M., Chen, Y., 2005. Increasing iron availability to crops: fertilizers, organo‐fertilizers, and biological approaches. Soil Science & Plant Nutrition 51(1), 1-17.

Silber, A., Yones, L.B., Dori, I., 2004. Rhizosphere pH as a result of nitrogen levels and NH_4/NO_3 ratio and its effect on zinc availability and on growth of rice flower (Ozothamnus diosmifolius). Plant and soil 262(1-2), 205-213.

Skopp, J., Jawson, M., Doran, J., 1990. Steady-state aerobic microbial activity as a function of soil water content. Soil Science Society of America Journal 54(6), 1619-1625.

Stumm, W., 1987. The dissolution of oxides and aluminum silicates: Examples of surface-coordination-controlled kinetics. Aquatic surface chemistry.

Takagi, S.i., Nomoto, K., Takemoto, T., 1984. Physiological aspect of mugineic acid, a possible phytosiderophore of graminaceous plants. Journal of Plant Nutrition 7(1-5), 469-477.

Teutsch, N., Von Gunten, U., Porcelli, D., Cirpka, O.A., Halliday, A.N., 2005. Adsorption as a cause for iron isotope fractionation in reduced groundwater. Geochimica et Cosmochimica Acta 69(17), 4175-4185.

Trost, B., Ellmer, F., Baumecker, M., Meyer‐Aurich, A., Prochnow, A., Drastig, K., 2014. Effects of irrigation and nitrogen fertilizer on yield, carbon inputs from above ground harvest residues and soil organic carbon contents of a sandy soil in Germany. Soil use and management 30(2), 209-218.

Tsukamoto, T., Nakanishi, H., Uchida, H., Watanabe, S., Matsuhashi, S., Mori, S., Nishizawa, N.K., 2008. 52Fe translocation in barley as monitored by a positron-emitting tracer imaging system (PETIS): evidence for the direct translocation of Fe from roots to young leaves via phloem. Plant and Cell Physiology 50(1), 48-57.

Vempati, R., Loeppert, R., 1988. Chemistry and mineralogy of Fe‑containing oxides and layer silicates in relation to plant available iron. Journal of plant nutrition 11(6-11), 1557-1574.

von Blanckenburg, F., von Wirén, N., Guelke, M., Weiss, D.J., Bullen, T.D., 2009. Fractionation of metal stable isotopes by higher plants. Elements 5(6), 375-380.

von Wirén, N., Bennett, M.J., 2016. Crosstalk between gibberellin signaling and iron uptake in plants: an Achilles' heel for modern cereal varieties? Developmental cell 37(2), 110-111.

von Wirén, N., Klair, S., Bansal, S., Briat, J.-F., Khodr, H., Shioiri, T., Leigh, R.A., Hider, R.C., 1999. Nicotianamine chelates both FeIII and FeII. Implications for metal transport in plants. Plant Physiology 119(3), 1107-1114.

Walker, E.L., Waters, B.M., 2011. The role of transition metal homeostasis in plant seed development. Current opinion in plant biology 14(3), 318-324.

Wallace, A., Lunt, O., 1960. Iron chlorosis in horticultural plants, a review, Proceedings. American Society for Horticultural Science.

Wallace, A., Wallace, G., 1992. Some of the problems concerning iron nutrition of plants after four decades of synthetic chelating agents. Journal of Plant Nutrition 15(10), 1487-1508.

Walter, K., Don, A., Tiemeyer, B., Freibauer, A., 2016. Determining soil bulk density for carbon stock calculations: a systematic method comparison. Soil Science Society of America Journal 80(3), 579-591.

Wang, C., Liu, W., Li, Q., Ma, D., Lu, H., Feng, W., Xie, Y., Zhu, Y., Guo, T., 2014. Effects of different irrigation and nitrogen regimes on root growth and its correlation with above-ground plant parts in high-yielding wheat under field conditions. Field Crops Research 165, 138-149.

Waters, B.M., Chu, H.-H., DiDonato, R.J., Roberts, L.A., Eisley, R.B., Lahner, B., Salt, D.E., Walker, E.L., 2006. Mutations in Arabidopsis yellow stripe-like1 and yellow stripe-like3 reveal their roles in metal ion homeostasis and loading of metal ions in seeds. Plant Physiology 141(4), 1446-1458.

Weber, K.A., Achenbach, L.A., Coates, J.D., 2006. Microorganisms pumping iron: anaerobic microbial iron oxidation and reduction. Nature Reviews Microbiology 4(10), 752-764.

Welch, R.M., Shuman, L., 1995. Micronutrient nutrition of plants. Critical Reviews in plant sciences 14(1), 49-82.

Wiederhold, J.G., 2015. Metal stable isotope signatures as tracers in environmental geochemistry. Environmental science & technology 49(5), 2606-2624.

Wiederhold, J.G., Kraemer, S.M., Teutsch, N., Borer, P.M., Halliday, A.N., Kretzschmar, R., 2006. Iron isotope fractionation during proton-promoted, ligand-controlled, and reductive dissolution of goethite. Environmental science & technology 40(12), 3787-3793.

Wiederhold, J.G., Teutsch, N., Kraemer, S.M., Halliday, A.N., Kretzschmar, R., 2007. Iron isotope fractionation in oxic soils by mineral weathering and podzolization. Geochimica et Cosmochimica Acta 71(23), 5821-5833.

Wiggenhauser, M., Bigalke, M., Imseng, M., Keller, A., Archer, C., Wilcke, W., Frossard, E., 2018. Zinc isotope fractionation during grain filling of wheat and a comparison of zinc and cadmium isotope ratios in identical soil–plant systems. New Phytologist 219(1), 195-205.

Wu, B., Amelung, W., Xing, Y., Bol, R., Berns, A.E., 2019. Iron cycling and isotope fractionation in terrestrial ecosystems. Earth-Science Reviews 190, 323-352.

Wu, L., Beard, B.L., Roden, E.E., Kennedy, C.B., Johnson, C.M., 2010. Stable Fe isotope fractionations produced by aqueous Fe (II)-hematite surface interactions. Geochimica et Cosmochimica Acta 74(15), 4249-4265.

Yoneyama, T., Gosho, T., Kato, M., Goto, S., Hayashi, H., 2010. Xylem and phloem transport of Cd, Zn and Fe into the grains of rice plants (Oryza sativa L.) grown in continuously flooded Cd-contaminated soil. Soil Science & Plant Nutrition 56(3), 445-453.

Zhai, Z., Gayomba, S.R., Jung, H.-i., Vimalakumari, N.K., Piñeros, M., Craft, E., Rutzke, M.A., Danku, J., Lahner, B., Punshon, T., 2014. OPT3 is a phloem-specific iron transporter that is essential for systemic iron signaling and redistribution of iron and cadmium in Arabidopsis. The Plant Cell 26(5), 2249-2264.

Zhang, C., Römheld, V., Marschner, H., 1995a. Distribution pattern of root‐supplied 59iron in iron‐sufficient and iron‐deficient bean plants. Journal of plant nutrition 18(10), 2049-2058.

Zhang, C., Römheld, V., Marschner, H., 1995b. Retranslocation of iron from primary leaves of bean plants grown under iron deficiency. Journal of Plant Physiology 146(3), 268-272.

Zhang, X., Zhang, D., Sun, W., Wang, T., 2019. The Adaptive Mechanism of Plants to Iron Deficiency via Iron Uptake, Transport, and Homeostasis. International journal of molecular sciences 20(10), 2424.

Zocchi, G., Cocucci, S., 1990. Fe uptake mechanism in Fe-efficient cucumber roots. Plant Physiology 92(4), 908-911.

Zou, C., Gao, X., Shi, R., Fan, X., Zhang, F., 2008. Micronutrient deficiencies in crop production in China, Micronutrient deficiencies in global crop production. Springer, pp. 127-148.

Zuo, Y., Zhang, F., 2011. Soil and crop management strategies to prevent iron deficiency in crops. Plant and Soil 339(1-2), 83-95.

VII

APPENDIX A

Supporting information for chapter III

Table A1: Chemical compositions of nutrient solutions for Fe-deficient and control treatments.

Treatments / Compositions	Fe-deficient mmol L^{-1}	Control mmol L^{-1}
KNO$_3$	2.5	2.5
Ca(NO$_3$)$_2$*4H$_2$O	2.5	2.5
MgSO$_4$	1	1
KH$_2$PO$_4$	0.5	0.5
Fe-EDTA	**0.0022**	**0.0896**
MnCl$_2$*4H$_2$O	0.01	0.01
CuSO$_4$*5H$_2$O	0.001	0.001
ZnSO$_4$*7H$_2$O	0.001	0.001
H$_3$BO$_3$	0.05	0.05
Na$_2$MoO$_4$*2H$_2$O	0.0005	0.0005

The Fe concentrations of above-ground (shoot) and whole plant were calculated with the following equation:

$$Fe_{Shoot\ or\ Plant} = \frac{\sum_i m_i c_i}{\sum_i m_i} \quad (Eq.\,A1)$$

i symbolizes the different plant organs (root, stem, leaves, spike/husk and grain), m the plant dry weight (g), c the Fe concentration ($\mu g\ kg^{-1}$).

Table A2: Fe concentrations and stable Fe isotope compositions of different plant organs and total wheat plants during three growth stages (data are given as mean ± standard error of replicates).

| Harvest time	Plant organ	Dry weight (g)		Fe concentration (µg g^{-1})		δ^{56}Fe (‰)		Δ^{56}Fe $_{plant-nutrient\ solution}$ (‰)	
		Fe-deficient	control	Fe-deficient	control	Fe-deficient	control	Fe-deficient	control
anthesis	root	1.50 ± 0.19	2.15 ± 0.27	216 ± 47	463 ± 42	0.13 ± 0.07	0.23 ± 0.02	-0.25	-0.15
	stem	3.74 ± 0.16	5.24 ± 0.20	27 ± 2	39 ± 3	0.26 ± 0.05	0.10 ± 0.08	-0.12	-0.28
	leaf	1.89 ± 0.09	2.63 ± 0.20	63 ± 10	102 ± 3	0.36 ± 0.10	0.39 ± 0.10	-0.02	0.01
	spike	1.95 ± 0.21	2.54 ± 0.26	50 ± 5	41 ± 3	-0.12 ± 0.02	-0.33 ± 0.10	-0.50	-0.71
	above-ground organs	7.57 ± 0.41*	10.41 ± 0.16*	42 ± 4**	56 ± 1**	0.18 ± 0.02$^{#}$	0.16 ± 0.06$^{#}$	-0.20	-0.22
	whole plant	9.07 ± 0.46*	12.57 ± 0.41*	71 ± 5**	125 ± 8**	0.16 ± 0.05$^{#}$	0.20 ± 0.03$^{#}$	-0.22	-0.18
post-anthesis	root	2.95 ± 0.31	1.67 ± 0.17	104 ± 18	262 ± 14	0.28 ± 0.06	0.30 ± 0.02	-0.10	-0.08
	stem	5.34 ± 0.33	5.25 ± 0.22	21 ± 2	23 ± 2	0.21 ± 0.06	0.30 ± 0.10	-0.17	-0.08
	leaf	2.73 ± 0.22	2.57 ± 0.14	64 ± 3	92 ± 5	0.14 ± 0.19	0.76 ± 0.11	-0.24	0.38
	spike	6.42 ± 0.78	6.86 ± 0.45	49 ± 5	51 ± 2	0.11 ± 0.08	-0.45 ± 0.37	-0.27	-0.83
	above-ground organs	14.49 ± 0.70*	14.69 ± 0.73*	42 ± 3**	48 ± 1**	0.14 ± 0.02$^{#}$	0.08 ± 0.13$^{#}$	-0.24	-0.30
	whole plant	17.43 ± 1.00*	16.36 ± 0.86*	52 ± 5**	70 ± 1**	0.19 ± 0.02$^{#}$	0.17 ± 0.09$^{#}$	-0.19	-0.21
maturity	root	0.80 ± 0.11	1.00 ± 0.04	237 ± 71	174 ± 30	0.45 ± 0.10	0.24 ± 0.16	0.07	-0.14
	stem	3.10 ± 0.46	3.95 ± 0.12	26 ± 2	31 ± 5	0.30 ± 0.19	0.26 ± 0.06	-0.08	-0.12
	leaf	1.50 ± 0.19	2.08 ± 0.08	66 ± 5	178 ± 16	0.47 ± 0.15	0.80 ± 0.08	0.09	0.42
	husk	1.40 ± 0.28	2.40 ± 0.27	41 ± 7	57 ± 8	-0.16 ± 0.44	0.10 ± 0.08	-0.54	-0.28
	grain	4.45 ± 0.76	5.18 ± 0.42	53 ± 4	67 ± 4	0.14 ± 0.05	-0.63 ± 0.32	-0.24	-1.01
	spike	5.85 ± 0.97*	7.58 ± 0.69*	50 ± 4**	64 ± 5**	0.08 ± 0.10$^{#}$	-0.42 ± 0.23$^{#}$	-0.30	-0.80
	above-ground organs	10.45 ± 1.60*	13.60 ± 0.83*	45 ± 2**	72 ± 4**	0.20 ± 0.07$^{#}$	0.13 ± 0.11$^{#}$	-0.18	-0.25
	whole plant	11.25 ± 1.39*	14.6 ± 0.87*	59 ± 4**	79 ± 5**	0.27 ± 0.08$^{#}$	0.14 ± 0.11$^{#}$	-0.11	-0.24
nutrient solution		–	–	–	–	0.38 ± 0.09		–	

* Sum of organs; **calculated from Eq.S1; $^{#}$ calculated from Eq. 2
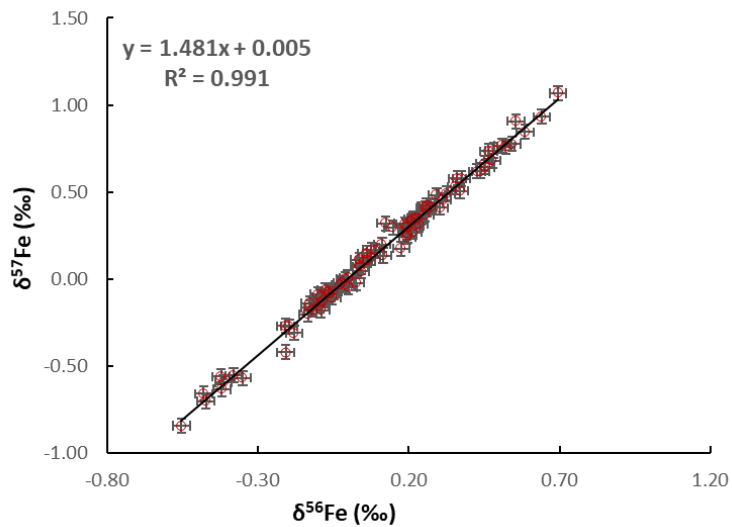
Fig. A1: Three-isotope plot for measured values of $\delta^{56}Fe$ and $\delta^{57}Fe$ in this study. The fitting equation with a slope of 1.481 ($R^2 = 0.991$) indicates the absence of mass-independent isotope fractionation during analytical sessions.
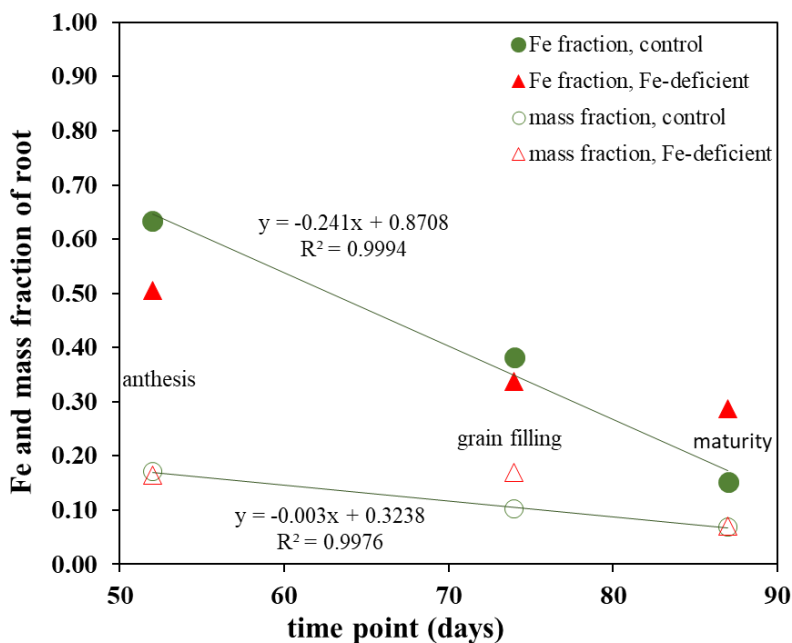
Fig. A2: Relative Fe fractions and mass fractions of roots (expressed relative to the total plant Fe stock and biomass, respectively) along the growth cycle of wheat (anthesis, post-anthesis and maturity stages). Full symbols represent root the Fe fraction under control (green circle) and Fe-deficient (red triangle) supply. Hollow symbols represent root mass fraction under control (green circle) and Fe-deficient (red triangle) supply. The relationships for the Fe deficient treatments were not significant at the $p < 0.05$ level of probability.

VIII

APPENDIX B

Supporting information for chapter IV

The investigated trails had been set up in 1969 as a non-randomized design. All three field replicates are in the box with same color. Each trail is 5 meters long and 4 meters wide.
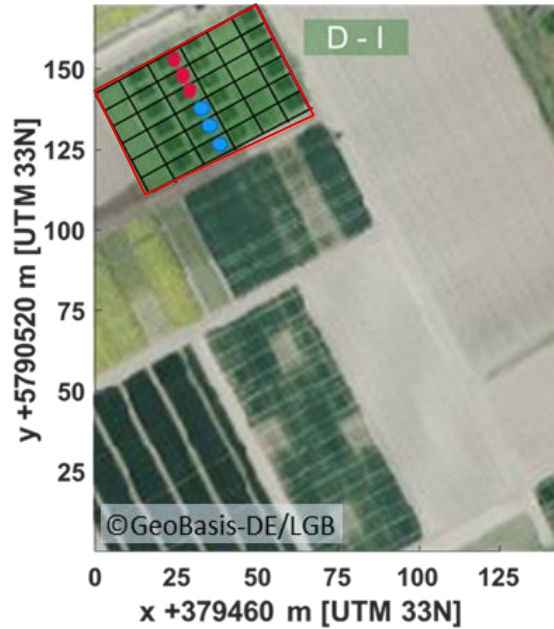
Fig. B1: Overview of the sampled plots in the Thy_D1 experiment. The red frame mark the field where winter wheat was grown in the year of the investigations. The circles show the soil sample locations in the field. The blue circles represent monitoring plots with irrigation, the red circles the plots without irrigation on the strip of the "Medium mineral N + straw" treatment. The monitoring plots are considered as three field replicates.
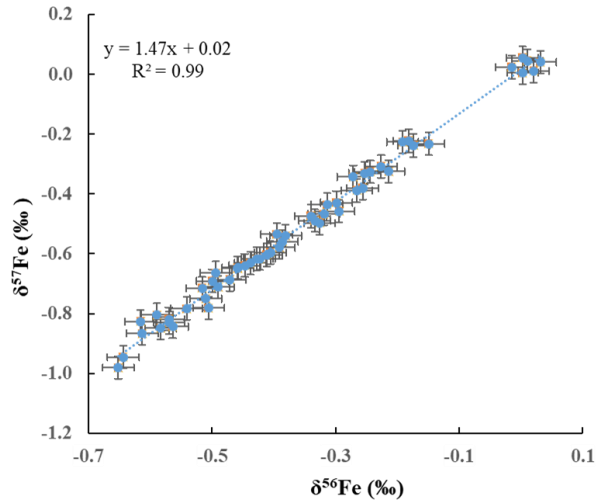
Fig. B2: Three-isotope plot for measured values of δ^{56}Fe and δ^{57}Fe in this study.

Fig. B3: (a) Iron concentrations in bulk soil and (b) cumulative iron stocks in plots with and without irrigation in Thyrow. The dotted lines visualize the sampled soil layers. Each data point represents three field replicates and their standard error.

Table B1: Crop yields and straw weight under different irrigation treatments (mean $\pm$ *SE*, n=3).

Soil managements	Crop yields t ha^{-1}	Straw weight t ha^{-1}
with irrigation	4.51[*]	4.99[#]
without irrigation	3.27	3.64

* indicates significant difference ($p < 0.05$) of crop yields between different irrigation treatments.

[#] indicates significant difference ($p < 0.05$) of straw weight between different irrigation treatments.

Table B2: Fe concentrations and δ^{56}Fe values in plant tissues.

Soil managements	Plant tissue	Fe conc. [mg kg^{-1}]	Error[a] [mg kg^{-1}]	δ^{56}Fe ‰	Error[a] [‰]
with irrigation	root	1561	188	-0.05	0.01
	stem	21	2	-0.31	0.06
	leaves	101	11	-0.53	0.09
	spike	42	4	-0.38	0.09
without irrigation	root	1340	69	-0.05	0.01
	stem	26	3	-0.22	0.14
	leaves	106	6	-0.37	0.07
	spike	41	2	-0.46	0.07

[a] Errors refer to the standard error for the field replicates.

Table B3: Fe concentrations and δ^{56}Fe values in plant available pool.

Soil managements	Depth cm	Fe conc. [mg kg^{-1}]	Error[a] [mg kg^{-1}]	δ^{56}Fe ‰	Error[a] [‰]
with irrigation	0-24	771	35	-0.06	0.05
	24-30	668	13	-0.04	0.07
	30-40	553	20	-0.02	0.07
	40-50	432	32	0.03	0.07
	50-59	415	38	-0.07	0.04
	59-70	647	113	-0.12	0.09
	70-100	1504	145	-0.16	0.03
without irrigation	0-24	701	15	-0.11	0.04
	24-30	583	8	-0.03	0.01
	30-40	507	26	0.01	0.01
	40-50	395	39	-0.03	0.04
	50-59	430	18	-0.14	0.04
	59-70	834	37	-0.14	0.08
	70-100	1473	207	-0.09	0.03
irrigation water	0.023[b]				

[a] Errors refer to the standard error for the field replicates. [b] the unit of the concentration in irrigation water is µg L^{-1}.

ACKNOWLEDGEMENT

Band / Volume 503
Lagrangian Simulation of Stratospheric Water Vapour: Impact of Large-Scale Circulation and Small-Scale Transport Processes
L. Poshyvailo (2020), 124 pp
ISBN: 978-3-95806-488-1

Band / Volume 504
Water Management in Automotive Polymer-Electrolyte-Membrane Fuel Cell Stacks
S. Asanin (2020), XVIII, 172 pp
ISBN: 978-3-95806-491-1

Band / Volume 505
Towards a new real-time irrigation scheduling method: observation, modelling and their integration by data assimilation
D. Li (2020), viii, 94 pp
ISBN: 978-3-95806-492-8

Band / Volume 506
Modellgestützte Analyse kosteneffizienter CO_2-Reduktionsstrategien
P. M. Lopion (2020), XIV, 269 pp
ISBN: 978-3-95806-493-5

Band / Volume 507
Integration of Renewable Energy Sources into the Future European Power System Using a Verified Dispatch Model with High Spatiotemporal Resolution
C. Syranidou (2020), VIII, 242 pp
ISBN: 978-3-95806-494-2

Band / Volume 508
Solar driven water electrolysis based on silicon solar cells and earth-abundant catalysts
K. Welter (2020), iv, 165 pp
ISBN: 978-3-95806-495-9

Band / Volume 509
Electric Field Assisted Sintering of Gadolinium-doped Ceria
T. P. Mishra (2020), x, 195 pp
ISBN: 978-3-95806-496-6

Band / Volume 510
Effect of electric field on the sintering of ceria
C. Cao (2020), xix, 143 pp
ISBN: 978-3-95806-497-3

Schriften des Forschungszentrums Jülich
Reihe Energie & Umwelt / Energy & Environment

JÜLICH
Forschungszentrum